The emergence of plant community dynamics and functional traits in response to the hydrological regime – a modelling approach

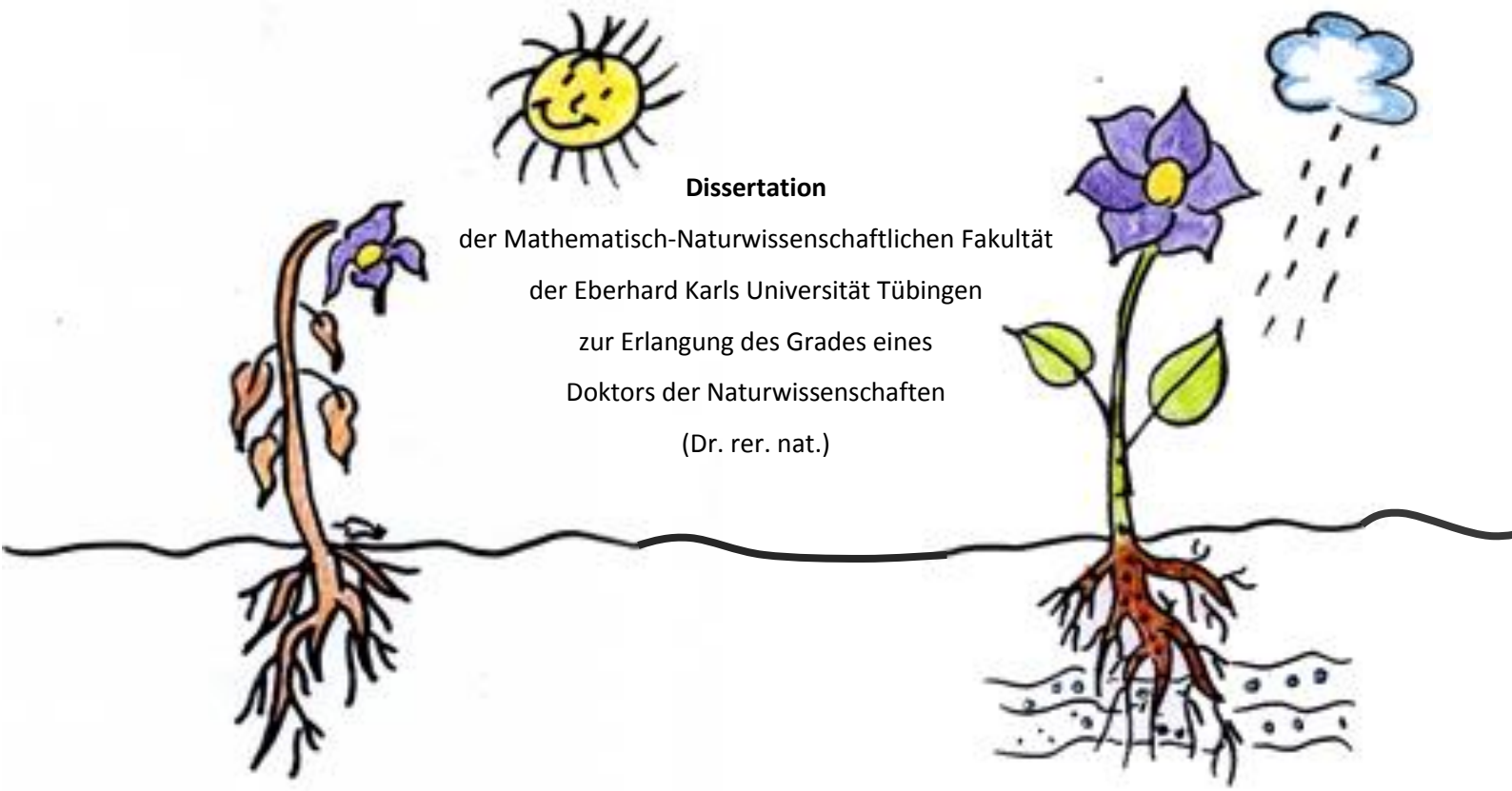

Dissertation

der Mathematisch-Naturwissenschaftlichen Fakultät

der Eberhard Karls Universität Tübingen

zur Erlangung des Grades eines

Doktors der Naturwissenschaften

(Dr. rer. nat.)

vorgelegt von

Msc. Maximiliane Marion Herberich

aus Miltenberg

Tübingen

2017

The emergence of plant community dynamics and functional traits in response to the hydrological regime – a modelling approach

Dissertation

der Mathematisch-Naturwissenschaftlichen Fakultät

der Eberhard Karls Universität Tübingen

zur Erlangung des Grades eines

Doktors der Naturwissenschaften

(Dr. rer. nat.)

vorgelegt von

Msc. Maximiliane Marion Herberich

aus Miltenberg

Tübingen

2017

Gedruckt mit Genehmigung der Mathematisch-Naturwissenschaftlichen Fakultät der Eberhard Karls Universität Tübingen.

Tag der mündlichen Qualifikation:	27.03.2018
Dekan:	Prof. Dr. Wolfgang Rosenstiel
1. Berichterstatter:	Prof. Dr. Katja Tielbörger
2. Berichterstatter:	Dr. Sebastian Gayler

Abstract

To predict vegetation response to today's rapid changes in the hydrological regime due to climate change and other anthropogenic alterations calls for a truly dynamic representation of vegetation in a coupled vegetation-hydrology model. However, existing models are deficient to capture the complex, spatiotemporal dynamics of multi-species natural ecosystems because they model few plant functional types or life forms defined *a priori* by a small set of postulated characteristics.

This dissertation aims to surpass this deficiency and refine the prediction of plant community dynamics and functional trait composition in response to the hydrological regime. Therefore, I developed a novel, highly dynamic, spatially-explicit, individual-based model that simulates plant functional trait abundance solely as a function of soil water potentials and individual behavior. An important innovation is that the model is devoid of *a priori* defined functional trait trade-offs but instead is able to represent continuous variation of functional traits. The model is used for simulation experiments to investigate possible changes in the function and structure of plant communities subjected to gradients of soil water availability.

I show that plant functional traits and their combinations (plant functional types) segregate in a predictable manner across the full range of soil water availability confirming accumulating evidence of hydrological niche segregation from field experiments. Interestingly, this segregation was not a consequence of universal functional trait trade-offs and trait correlations. Instead the correlation intensities, including the classical competition-colonization trade-off, were a function of the soil water availability. Furthermore, the entire biomass-density relationship of the plant communities, among this the value of the slope of the classical self-thinning line, was strongly and consistently modified by water stress. Specifically, the growth reduction in water stressed communities decreased the potential for density-dependent mortality which consequently steepened the thinning slope in communities with high density and levelled the thinning slope in communities with low density. Remarkably, temporally-varying soil water promoted diversity even in humid climates. This suggests that the

temporal-storage effect can act globally as a coexistence mechanism driving hydrological niche segregation. Functional diversity of plant communities boosted coexistence under temporally-varying soil water through a change in the functional traits which buffered the population growth rate against increasing temporal variability of soil water from seed dispersal distance to water stress tolerance and life form.

Interestingly, many of the predicted patterns of the plant community dynamics and functional traits changed similarly at both ends of the soil water range, i.e. excessive and insufficient water availability selected for a comparable vegetation response. This implies that species' specific water stress intensity and the corresponding spatiotemporal variation of this water stress intensity, rather than climatic means, might determine vegetation response and thus, species distribution and abundance.

In general, the model design allowed for the addition of few key characteristics of natural plant communities such as variation within functional traits, local interactions as well as complete lifecycle including recruitment, and thus allowed for a better understanding of the mechanisms underlying the response of these communities to changes in the hydrological regime.

Kurzfassung

Um die Reaktion der Vegetation auf die durch Klimawandel und andere anthropogene Eingriffe hervorgerufenen gegenwärtigen schnellen Veränderungen des Wasserhaushaltes vorhersagen zu können, sollte die Vegetationsdynamik in einem gekoppelten Vegetations-Hydrologie Modell wirklichkeitsgetreu repräsentiert werden. Existierende dynamische Vegetationsmodelle erfassen die Komplexität und raumzeitliche Dynamik von natürlichen, diversen Ökosystemen allerdings nur unzureichend, da sie sich auf die Modellierung weniger Pflanzenfunktionstypen oder Lebensformen beschränken, die *a priori,* basierend auf einer kleinen Auswahl postulierter Merkmale, definiert werden.

Diese Dissertation beabsichtigt diese Einschränkungen aufzuheben und die Vorhersage der Dynamik und der Zusammensetzung der Funktionsmerkmale von Pflanzengesellschaften in Reaktion auf das hydrologische Regime zu verbessern. Darum habe ich ein neuartiges, dynamisches, räumlich explizites, Individuen-basiertes Modell entwickelt, das die Abundanz von Pflanzenfunktionsmerkmalen ausschließlich als Reaktion aufs Bodenwasserpotentialen und dem Verhalten der Individuen simuliert. Eine wichtige Innovation des Modells ist, dass es frei von *a priori* definierten Trade-offs zwischen Pflanzenfunktionsmerkmalen ist, sondern eine stetige Variation der Pflanzenfunktionsmerkmale repräsentieren kann. Mithilfe dieses Modells wurden mehrere Simulationsstudien durchgeführt, um mögliche Änderung in der Zusammensetzung der Funktionsmerkmale und der Struktur von Pflanzengesellschaften entlang von hydrologischen Gradienten zu untersuchen.

Es zeigte sich, dass Pflanzenfunktionsmerkmale und ihre Kombinationen (Pflanzenfunktionstypen) in einer vorhersehbaren Weise entlang des gesamten hydrologischen Gradienten segregiert sind. Dieses Resultat bestätigt zunehmende Nachweise hydrologischer Nischensegregation in Feldexperimenten. Interessanterweise war diese Segregation keine Konsequenz aus universellen Trade-offs zwischen den Pflanzenfunktionsmerkmalen. Stattdessen war die Intensität der simulierten Korrelationen, darunter der klassische competition-colonization Trade-off, eine Reaktion auf die Verfügbarkeit des

Bodenwassers. Weiterhin hat sich das gesamte Biomasse-Dichte Verhältnis der Pflanzengesellschaften, einschließlich des Wertes der Steigung der klassischen Selbstausdünnungslinie, je nach Wasserstressintensität gleichermaßen geändert. Im Einzelnen hat die Wachstumsreduktion in wassergestressten Gesellschaften das Potential für dichteabhängige Mortalität erniedrigt, was eine Erniedrigung der Steigung der Selbstausdünnungslinie in Gesellschaften mit hoher Dichte beziehungsweise eine Erhöhung der Steigung der Selbstausdünnungslinie in Gesellschaften mit niedriger Dichte zur Folge hatte. Zeitlich variierende Wasserverfügbarkeit förderte Koexistenz sogar in humiden Umgebungen. Das deutet darauf hin, dass der temporal-storage Effekt global unter verschiedenen Klimabedingungen ein Mechanismus für Koexistenz sein kann. Funktionelle Diversität der Pflanzengesellschaften erhöhte Koexistenz zusätzlich bei zeitlich variierender Wasserverfügbarkeit und zwar durch einen Wechsel der Pflanzenfunktionsmerkmale, die die Population gegen zunehmende zeitliche Varianz im Bodenwasser stärken. Der Wechsel erfolgte hinsichtlich Samenausbreitungsdistanz, Wassertoleranz und Lebensform.

Interessanterweise änderten sich viele der beobachteten Muster in der Dynamik und bezüglich Pflanzenfunktionsmerkmale der Pflanzengesellschaften konsistent an beiden Enden der gesamten Bodenwasserskala, sprich exzessive und unzureichende Wasserverfügbarkeit riefen eine ähnliche Reaktion in der Vegetation hervor. Das impliziert, dass die artenspezifische Wasserstressintensität und die entsprechende raumzeitliche Variation dieser Stressintensität, im Gegensatz zu klimatischen Mittelwerten, die Reaktion der Vegetation und damit Artenverteilung und Abundanz bestimmen.

Im Allgemeinen erlaubt das Modelldesign die Ergänzung wichtiger Schlüsselcharakteristika natürlicher Pflanzengesellschaften, wie die Variation der Pflanzenfunktionsmerkmale, lokale Interaktionen sowie vollständige Lebenszyklen inklusive Reproduktion. Dies führte zu einem weit tieferen Verständnis der Mechanismen, die der Reaktion natürlicher Pflanzengesellschaften auf Änderungen im Wasserhaushalt zugrunde liegen.

Acknowledgments

This dissertation would not have been the same without the support and encouragement of many people. I sincerely thank my supervisors Katja Tielbörger, Sebastian Gayler and Madhur Anand who supported me throughout this thesis scientifically and in every other way. Thank you for all your encouragement and your belief in my research. Further thanks goes to the vegetation ecology working group for their interesting discussions concerning result interpretation as well as for stimulating insights into other fields of vegetation ecology and last but not least for many tasty picnics! Special thanks to Michal Gruntman for being available for discussion and reassuring me in my research progress when Katja was in sabbatical. Many thanks go to my doctoral colleagues and Monika from the IRTG for the many small things which made the last years more pleasant. I am grateful to the Anand lab who hosted me for several months in Guelph, Canada. I am particularly grateful to Virginia Capmourteres and her unlimited motivation and energy to make me feel at home in Guelph. I further acknowledge Virginia Herrmann, Florian Schneider, Maria Georgi and Carla Herth for their constructive comments to improve the language quality. I would like to thank the German Research Foundation (DFG) for financial support of the project within the International Research Training Group ‘‘Integrated Hydrosystem Modelling’’ (IRTG 1829) at the University of Tübingen.

Finally, I am grateful for the people who kept me going in the last years and who believed that I would finish even when I didn’t: Mama, Doga and Samu!

Contents

Declaration of own contribution

During my work on the here presented dissertation, I was supervised by Prof. Dr. Katja Tielbörger, Dr. Sebastian Gayler and Prof. Dr. Madhur Anand. Together with my supervisors, I developed the general study design and the conceptual idea of the model used for the simulation experiments. The model was implemented, tested and verified by myself. I further designed the simulation experiments for each chapter and performed the simulation experiments. I analyzed the model output including all statistical tests and designed the graphs. I further wrote the first draft of the dissertation. The here presented versions of chapter 2 and 3 received several revisions concerning the storyline and language by all my supervisors and two anonymous external reviewers. Dr. Sebastian Gayler helped with Fig. 3.4 in chapter 3. The storyline and language of chapter 4 was improved by Prof. Dr. Katja Tielbörger, Dr. Sebastian Gayler and Prof. Dr. Madhur Anand. Chapter 1, 5 and 6 received comments on the language and storyline by Prof. Dr. Katja Tielbörger and Dr. Sebastian Gayler. The cover picture was adapted from www.hiba.de

List of Figures

List of Tables

Chapter 1

Introduction

Coupled modelling of vegetation and hydrology dynamics. The dynamics of vegetation and hydrology are strongly interrelated and coupled by a set of complex feedbacks (e.g. Mauchamp et al. 1994; Orellana et al. 2011). Vegetation influences several hydrological processes such as interception, infiltration, evapotranspiration and runoff (Manfreda et al. 2010). In turn, water is a key resource for plants (Silvertown et al. 2015) which influences other soil conditions such as oxygen concentration and nutrient availability (Mustroph et al. 2016). Simultaneously, water can act as a disturbance agent (flooding and drought) (Grime 1977). Thus, the hydrological regime is one of the major drivers for plant individual performance and consequently determines the distribution and abundance of plant species in time and space across various scales (Silvertown et al. 2015). Anthropogenic climate change and the associated global changes in temperature and precipitation inevitably modify this interrelation (Field et al. 2014). Accordingly, there has been a steady rise in the number of climate impact studies on vegetation dynamics as a function of the hydrological regime and vice-versa. For example, it is expected that climate change induced alterations of hydrological measures will have a greater impact on the composition and distribution of plant communities than the change in temperature means itself (Reyer 2013; Silvertown et al. 2015).

Process-based dynamic models are able to address complex interrelationships, and thus can enhance our understanding of the feedbacks between vegetation and hydrology dynamics in a changing climate. However, state-of-the-art vegetation models typically assume static hydrological conditions, which fail in accurately representing the effects of climate change on spatiotemporal soil water availability (e.g. Esther et al. 2008; Fischer et al. 2014). *Vice-versa*, current hydrological models usually consider vegetation as an entity and reduce it to a single variable, e.g. the total plant cover or the leaf area index, treating vegetation as a static homogenous 'green layer' (e.g. Therrien et al. 2006).

In recent decades, dynamic global vegetation models have emerged as a powerful tool for quantifying vegetation response to changes in the hydrological regime. These models account for both detailed hydrogeological cycles as well as vegetation demography, including reproduction, growth, recruitment and mortality (Snell et al. 2014). However, existing dynamic global vegetation models tried to capture the essential vegetation dynamics of an ecosystem by modelling few plant functional types or life forms only, which were defined *a priori* by a small set of postulated characteristics limiting their explanatory power (e.g. Bonan et al. 2002; Verant et al. 2004; Lapola et al. 2008).

Plant functional types. A major challenge of vegetation modelling is how to represent the complexity and spatiotemporal variability of multi-species natural ecosystems. An efficient approach to reduce this complexity is to group plant species based on their response to an environmental factor. Non-phylogenetic groups, which respond in a similar way based on a shared response mechanism to a syndrome of environmental factors, are called plant functional types (PFTs, Gitay & Noble 1997). Plant functional types are a comprehensive simplification of natural ecosystems and provide a solid base for predicting the dynamics of ecosystems or any of their components (Gitay & Noble 1997). Plant functional types can enable highly explorative modelling studies if the simulated PFTs are not only restricted to groups which respond similarly to the present state of the studied environmental factor but already include PFTs which respond similarly to a possible future state (Gitay & Noble 1997). Plant species can be grouped into subjective PFTs based on the observation of one or more ecosystems (Gitay & Noble 1997). Most existing dynamic global vegetation models classify PFTs subjectively (e.g. Bonan et al. 2002; Verant et al. 2004; Lapola et al. 2008). Classical examples of subjective PFTs are differentiations of species into trees, grasses and shrubs. However, the intuitive identification of PFTs based on visual observation runs the risk of grouping species which share a set of morphological characters but do not necessarily respond similarly to an environmental factor (Gitay & Noble 1997). Alternatively, PFTs can be classified inductively based on the importance of an environmental factor for the functioning of an ecosystem. One approach to derive inductive PFTs is through species' characteristics which may define the response of species to the given environmental factor (Gitay & Noble 1997).

Functional traits can be a direct link between species response and environmental factors (Cornelissen et al. 2003). These traits relate environmental factors to individual fitness via their effects on growth, reproduction, and survival (Laughlin & Laughlin 2013). Thus, functional traits enable us to understand how changing environmental conditions affect vegetation composition and structure across different scales of ecological organization (Cornelissen et al. 2003). This makes the integration of functional traits into dynamic vegetation models highly desirable.

A novel modelling approach that identifies inductive PFTs based on the combination of functional traits has yielded highly unexpected, yet plausible, functional compositions of plant communities adapting to disturbance (Seifan et al. 2012). In difference to previous models, this modelling approach relaxes assumptions about dichotomous trade-offs so that the emerging trait combinations, i.e. PFTs, reflect the best adaptation to the specific disturbance regime (Seifan et al. 2012). Seifan et al. (2012) indicated that an unrestricted modeling approach that does not define trade-offs among plant traits *a priori* is very useful for identifying the relationship between traits and environmental factors. In contrast to existing dynamic vegetation models, this trade-off unrestricted approach does not rely on plant functional types with fixed trait values, but is sufficiently flexible to represent continuous variation in functional traits. Thus, this modelling approach can exploit the huge advances in the availability of trait data (e.g. Wright et al. 2004; Kattge et al. 2011).

Individual-based modelling. Predicting the response of vegetation to today's rapid changes in the environment calls for a truly dynamic representation of vegetation. Existing dynamic vegetation models include only simplistic representations of biotic interactions ignoring individual variation within plant functional types or life forms (Scheiter et al. 2013). Individual-based models include variability, local interactions, and complete life cycles of individuals as well as heterogeneous distributions of environmental factors (Grimm 1999). As opposed to existing dynamic vegetation models, individual-based models thus provide direct insights into whether the emergent community patterns are driven by the studied environmental factor or by internal processes such as demography or competition (Kaiser 1979; Grimm 1999).

Hydrological niche segregation. The influence of soil water on the composition and distribution of plant communities is especially evident in the increasing number of field observations related to the so-called hydrological niche segregation (Silvertown et al. 2015). Plant species can be defined by species-specific ranges of soil water conditions, i.e. their hydrological niche, such that the species' presence and location in the landscape can be described using functions of soil water (Silvertown et al. 1999). However, the mere description of distribution patterns is not sufficient to predict species' response to changes in soil water; we also need to know the mechanisms which underlie these patterns.

Classical niche theories emphasize trait trade-offs as a mechanism underlying species segregation along environmental gradients (Chesson 2000; Tilman 2004). At present, there is little field evidence of the trade-offs associated with hydrological niche segregation (Silvertown et al. 2015). For example, species segregation along soil water gradients in English meadows was caused by a trade-off between species' tolerances to aeration stress and soil-drying stress (Silvertown et al. 1999). Another trade-off possibly associated with hydrological niche segregation exists between water-use efficiency and relative growth rate (Angert et al. 2009). However, given the ubiquity of trade-offs in natural plant communities, it is likely that further trait correlations will have consequences for species segregation along hydrological gradients (Silvertown 2004; Silvertown et al. 2015). Further, it has been shown that the predictive power of a given trait for a species response pattern may change across different abiotic and biotic conditions (de Bello et al. 2005). Thus, a study investigating the trait correlations associated with hydrological niche segregation needs to include an analysis whether these correlations remain stable in different environments.

Even less is known about the consequences of hydrological niche segregation on the community structure (Silvertown et al 2015) such as on density-dependent effects. A prominent ecological principle, which relates changes in biomass and density over time, is the self-thinning rule (Yoda et al. 1963; Weiner & Freckleton 2010). The rule predicts that this relationship forms a straight self-thinning line with a slope of - 3/2 in even-aged monospecific plant populations undergoing density-dependent mortality when the logarithm of mean surviving plant biomass is plotted against the logarithm of plant

density. A previous experiment indicated that there was no significant change in the slope of the self-thinning line under moderate water deficit in comparison to well-watered conditions (Liu et al 2006). However, to the best of my knowledge, there is no study which examines changes in the self-thinning line along a complete stress gradient, e.g. from excessive to insufficient water availability. This is especially regrettable since experiments on how the slope of the self-thinning line changes with serious deficit of other resources such as nitrogen are abundant and could provide testable predictions (Morris 2003).

Few studies showed that hydrological niche segregation is responsible for coexistence (e.g. Verhulst et al. 2008; Adler et al. 2006; for a review see Silvertown et al. 2015). However, little is known about the coexistence mechanisms associated with hydrological niche segregation. One mechanism which promotes plant species coexistence under temporally-varying environments is the temporal storage effect (Chesson 2000; Silvertown et al. 2015). The temporal storage effect results from the interaction of three main contributing elements: (1) species-specific responses to the environment, (2) covariance between the environment and competition, and (3) buffered population growth rate (Chesson 1994; Chesson 2000a; Chesson 2000b). Thereby, population growth may be buffered against temporal variation by various plant traits which decrease the sensitivity of specific life-history stages to temporal environmental variation (Chesson 2000a; Májeková et al. 2014). Few studies indicated that temporally-varying soil water can promote coexistence via the temporal storage effect in arid environments (Adler et al. 2006; Cheng et al. 2006; Verhulst et al. 2008; Angert et al. 2009; Kowaljow & Fernandez 2011; for a review see Silvertown et al. 2015). However, also in relatively wet environments soil water is highly variable in both time and space (Dawson 1993; Oddershede et al. 2015), so that hydrologically heterogeneous habitats such as wet heathlands or temporarily flooded meadows may possibly promote coexistence through the temporal storage effect (Silvertown et al 2015). Still, this assumption remains untested to date.

Objectives and structure. This dissertation is a comprehensive attempt to deduce the emergence of community dynamics as well as the abundance of plant functional traits and their specific combinations (PFTs) in response to the hydrological regime. By extending the trade-off

unrestricted modelling approach to the complex interrelation of vegetation and hydrology, I aim to broaden the applicability of dynamic vegetation models and tackle the short-comings of present dynamic vegetation models described above. I therefore designed a spatially-explicit individual-based model PLANTHeR (PLAnt fuNctional Traits Hydrological Regimes) which describes plant functional trait abundance solely as a function of soil water potentials and individual behavior. An important innovation is that there are no *a priori* defined trade-offs but instead a potentially continuous variation of functional traits so that the model is neither restricted to a certain set of species nor scaled to a specific ecosystem. A complete model description of PLANTHeR following the ODD (Overview, Design concepts, Details (Grimm et al. 2006, 2010)) protocol is presented in the following chapter 2. In chapter 3 to 5, PLANTHeR is used to perform three sets of simulation experiments to increase our present knowledge of the mechanisms underlying hydrological niche segregation. First, I examined (1) whether plant functional traits and plant functional types segregate in a predictable manner along gradients of soil water potentials and (2) whether consistent functional trait correlations underlie a possible segregation (chapter 3). Second, I investigated changes in the structure of plant communities across the full range of soil water availability with special regards to density-dependent effects such as self-thinning (chapter 4). Third, I tested whether temporally-varying soil water potentials can promote coexistence via the temporal storage effect in humid climates (chapter 5). This chapter also highlights the functional traits which are key to explaining the response of plant individuals to temporal variation of soil water potentials. Finally, I draw conclusions from this dissertation and give an outlook towards potential future research (chapter 6).

Chapter 2

The individual-based model PLANTHeR

The content presented in this chapter is modified from Herberich, M. M., Gayler, S., Anand, M., Tielbörger, K., 2017. Hydrological niche segregation of plant functional traits in an individual-based model. Ecol. Model. 356, 14-24.

PLANTHeR was designed as an individual-based model. Individual-based models are powerful tools to explain functional composition and distribution of vegetation along environmental gradients because they include variability, local interactions, and complete life cycles of individuals as well as heterogeneous distributions of environmental factors (Grimm 1999). Thus, as opposed to existing state-variable models, individual-based models provide direct insights into whether the observed community patterns are driven by the studied environmental factor or by internal processes such as demography or competition (Kaiser 1979; Grimm 1999).

PLANTHeR was implemented in Netlogo 5.2.0 (Wilensky 1999).

The model description follows the ODD (Overview, Design concepts, Details, (Grimm et al. 2006, 2010)) protocol for describing individual- and agent-based models.

2.1. Purpose

PLANTHeR is intended to provide a scientific basis for an integrated vegetation-hydrology management. Its purpose is to predict functional trait abundance and plant community patterns under given soil water potentials. For example, PLANTHeR can use simulation results of a physics-based hydrological model as an input to predict the effects of climate change scenarios on a given plant community. PLANTHeR uses functional traits instead of species so that it can be applied globally to different hydrological regimes and vegetation types. Functional traits and other parameters are chosen so that they have a direct biological correlation. The advantages are that 1. Parameters are easily measurable in the field, and 2. Stakeholders such as conservation agencies can interpret the simulation results readily.

2.2. Entities, State Variables, and Scales

The model comprises three entities: grid cells and two types of agents, i.e. adult plants and viable seeds. All agents are immobile but have a state variable habitat cell. Furthermore, each agent is classified by its age and plant functional type (PFT) which is based on the parametrization of six functional traits (Sect. 2.3; Appendix A Table A1). Adult plants have the additional state variable biomass [mg].

Grid cells have only one state variable: soil water potential Ψ [mm]. Each cell represents a site in which a single individual can establish, grow, reproduce and die, and from which neighboring plants can extract nutrients (Crawley & May 1987). Thus, translation of the cell size into real-life communities depends on the modelled system, and may represent an area between a few square centimeters to a few square meters (Caplat et al. 2008; Schippers et al. 2001). The ideal cell size corresponds to the smallest scale of plant interactions. Here, I choose a cell size of 5 x 5 cm, which corresponds to the size of an average adult plant typical for much of the temperate herbaceous vegetation (Schippers et al. 2001).

One time step equals one growing season in which the individuals could potentially run through a complete life cycle.

2.3. Functional traits and PFT parameterization

PLANTHeR models diverse communities based on a set of PFTs. These PFTs result from the parametrization of six functional traits (Seifan et al. 2012, 2013; Herberich et al. 2017). I selected general, composite functional traits that can represent several alternative functional traits depending on the specific ecosystem. These traits were chosen to represent individual response to different soil water potentials in time and space. Two traits were related to the individual's competitive ability (seedling competitive ability and maximum adult growth rate). Two traits represented colonization abilities in time and space (seed dormancy and seed dispersal distance), and two traits affected the individual's longevity (life form and water stress tolerance).

An important innovation PLANTHeR is that it does not rely on plant functional types with fixed properties, but is sufficiently flexible to represent continuous variation in functional traits. Thus,

PLANTHeR can exploit the huge advances in the availability of trait data (e.g. Wright et al. 2004; Kattge et al. 2011). The parametrization of each functional trait depends on the specific study question and/ or ecosystem. Parametrization chosen for the simulation experiments presented in this thesis can be found in chapters 3 to 5.

2.4. Process Overview and Scheduling

The model executes the following actions once per time step (Fig. 2.1). The model assumes no hierarchies among individuals; thus, the order in which individuals execute these actions is randomized each time step.

1) All annuals die by default (Sect. 2.17.6).
2) Seed survival for each individual seed is determined following section 2.17.1.
3) Individuals check the water availability in their zone of influence (ZOI), which depends on the number and size of their neighbors as well as the soil water potential (Sect. 2.17.7).
4) Seed germination for each individual seed is determined by the seed's water availability and dormancy strategy (Sect. 2.17.2).
5) One seed per cell is chosen to establish out of all present germinating seeds (Sect. 2.17.3).
6) Individuals check the water availability in their zone of influence (ZOI), which depends on the number and size of their neighbors as well as the soil water potential (Sect. 2.17.7).
7) Adult plants grow (Sect. 2.17.4).
8) Individuals check the water availability in their zone of influence (ZOI), which depends on the number and size of their neighbors as well as the soil water potential (Sect. 2.17.7).
9) Adult plants produce seeds depending on the annual increment of their ZOI and water availability. Seeds disperse from their parental plant based on their functional trait value maximum dispersal distance (Sect. 2.17.5).
10) Individuals check the water availability in their zone of influence (ZOI), which depends on the number and size of their neighbors as well as the soil water potential (Sect. 2.17.7).
11) The mortality probability due to natural senescence of perennial adults is calculated. For all adults, mortality due to long-term water stress is determined (Sect. 2.17.6).

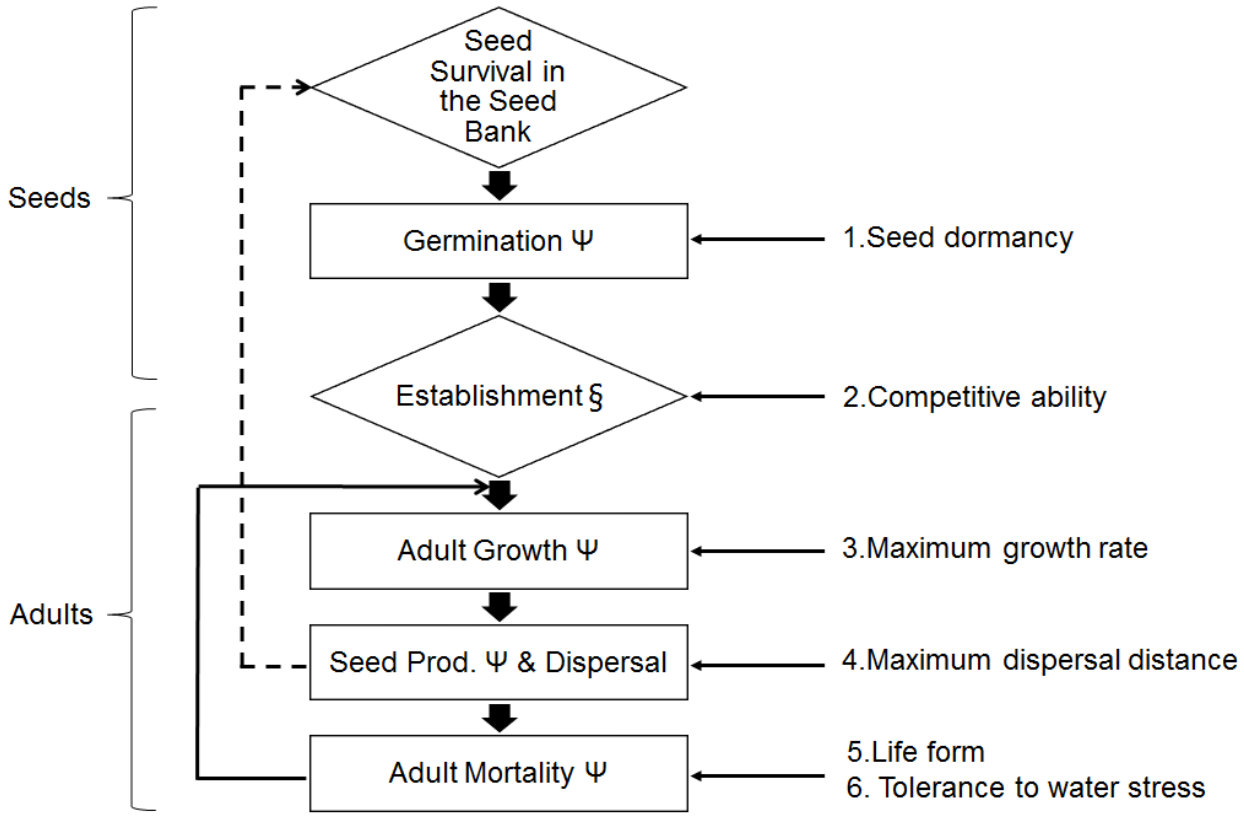

Fig. 2.1. Yearly life cycle of individual plants in the model. Dashed line – seed production; § – stages in which the individual outcome is affected by its interaction with neighbors; Ψ – stages in which the individual outcome is affected by the individual's water availability F_Ψ (Sect. 2.17.7).

2.5. Basic principles

Seeds do not compete with adult plants for water since (1) viable dormant seeds generally have a low water content and do not absorb water actively during the growing season, and (2) only the micro-climatic conditions in the intermediate vicinity of the seed are determining the seed fate (Mayer & Poljakoff-Mayber 1982). The system includes a carrying capacity as only one individual can grow per cell. The model was designed by pattern-oriented modelling at both the individual level (sigmoidal plant growth, growth dependent mortality, etc.), and the system level (changes in the size structure of the population or community) (Grimm et al. 2005).

2.6. Emergence

All results observed at the community level such as functional trait composition and density effects (self-thinning) emerged from local interactions, and complete life cycles of individuals as well as the soil water potentials.

2.7. Adaptation

None of agents has adaptive behavior.

2.8. Objectives

None of agents has objectives.

2.9. Learning

No learning is represented.

2.10. Prediction

No prediction is represented.

2.11. Sensing

Individuals are assumed to sense the soil water potentials in their Zone of Influence. When competing for water, individuals are assumed to sense other individuals and their biomass which overlap with their own ZOI.

2.12. Interactions

Individuals interact directly by means of 1. competition for vacant positions (Sect. 2.17.3) and 2. competition for available water (Sect. 2.17.6).

2.13. Stochasticity

Stochasticity is included in several processes:

1. Initialization of the plant community (Sect. 2.16): 1. Each grid cell has a 50% chance of being occupied by an adult plant. 2. The individual functional trait combination is determined randomly.
2. Viability of each seed is drawn from a normal distribution (Sect. 2.17.1).
3. Germination is simulated as a stochastic event with a probability that is a function of the functional trait seed dormancy and the reduction function $f(\Psi)$ (Sect. 2.17.2).
4. Seedling establishment is modelled as a weighted lottery in which the probability that a seed establishes is determined by its competitive ability and life form with 2:1 chances for annual individuals (Sect. 2.17.3).

5. The seed dispersal distance is determined from a log-normal dispersal kernel and dispersal direction was chosen from a uniform distribution (Sect. 2.17.5).
6. Perennial mortality due to senescence is simulated as a stochastic event with a probability that is a function of the annual ZOI increment. (Sect. 2.17.6)

2.14. Collectives

Collectives are not represented.

2.15. Observation

A summary output file reports population status at the end of each time step. The summary includes the total population size, the total number of seeds, mean adult age, mean seed age, the number and summed ZOI of individuals per PFT, the number of seeds per PFT, PFT richness, Shannon diversity index, the relative density of traits among all coexisting individuals i.e. seeds, and total number of dead individuals due to water stress and senescence.

Spatial information is also provided by the model's animation display, which shows the location of adults, and seeds. The size of an adult individual represents the size of its ZOI.

For model testing an additional file with output per individual recorded at the end of each time step the individual's identity, spatial location, age, PFT, functional trait values, biomass [mg], and total water availability F_{ψ}.

2.16. Initialization

The model is initialized with a random spatial distribution of the plant functional types whereby each grid cell has a 50% chance of being occupied by an adult plant. The specific individual identity is determined randomly so that each of the modelled PFTs (Sect. 2.3) has an equal probability of occupying the cell (Seifan et al. 2012, 2013). Initial biomass is set to 125 mg.

PLANTHeR is able to simulate spatiotemporal heterogeneous soil water potentials Ψ via input files or based on hypothetical soil water scenarios with various stress gradients and return intervals. The specific soil water scenarios chosen for the simulation experiments to test the proposed research questions stated in chapter 1 can be found in chapter 3 to 5 respectively.

2.17. Submodels

2.17.1. Seed Survival in the Seed Bank

Many plant species regularly found in seed banks have a long-term persistent seed bank with seeds which persist in the soil for at least five years (Bakker et al. 1996). Under constant environmental conditions, seed viability of a species has the shape of a normal distribution around a mean value (Roberts 1972). Here, mean seed viability was set as 10 years with 5 years standard deviation for all seeds regardless of their PFT, which results in a long-term persistent seed bank.

2.17.2. Germination

In each year, germination probability is individually calculated for each seed based on its functional trait value for seed dormancy multiplied by its reduction function $f(\Psi)$ (Levitt 1980).

All seeds remain in the seed bank until they either die (Sect. 2.17.1) or germinate.

2.17.3. Seedling Establishment

After initial germination of all potential seeds, only a single individual in each cell is allowed to establish. Seedling establishment is modelled as a weighted lottery in which the probability for a seed to establish is determined by its competitive ability and life form, with 2:1 chances for annual individuals to establish, following the general assumption that annuals are better colonizers (Schippers et al. 2001; DiVittorio et al. 2007; Watts 2010).

2.17.4. Adult Growth

Adult growth is modeled as the annual increase of the radius of an individual's zone of influence (ZOI). ZOI is a circular area from which individuals could potentially acquire water (Sect. 2.16.7) and is allometrically related to the plant's aboveground biomass ZOI [cm] ~ $B^{2/3}$ [mg] (Weiner et al. 2001; West et al. 1999). I used a modification of the logistic growth function to model the annual increase in ZOI radius, r:

$$r_{(t+1)} = r_t + G \times F_\Psi \times \left(1 - \frac{r_t}{r_{max}}\right) \quad (1)$$

where F_Ψ is the total water availability of an individual (Sect. 2.16.7), t is the individual's age, and G is the PFT's specific maximum growth rate.

The choice of maximum ZOI radius, r_{max}, depends on the studied ecosystem. In this thesis, I fixed it at 5 m, which is the radius that is approximately influenced by a large tree canopy (Caplat & Anand 2009). Note that this growth function can potentially produce aboveground biomass values representative for both grasslands and forest systems. For example, maximum aboveground biomass values reach approximately 8.8 kg/m² in a scenario in which the grid is occupied by individuals at maximum ZOI radius. This is similar to values found for pinyon–juniper woodlands in Arizona by Huffman et al. (2012) (6.5 kg/m²) and by Grier et al. (1992) (5.3 kg/m²). At maximum density, the minimum biomass equals 50 g/m² and maximum biomass equals 278.4 g/m² which is in the range of mean aboveground biomass of grasslands (Tilman et al. 2006).

2.17.5. Seed Production and Dispersal

Minimum and maximum seed numbers are equal for all PFTs [1; 20] (Bauer et al. 2002; Snyder 2011). The actual number of produced seeds, S, is calculated using the Gompertz function:

$$S = 20 \times e^{\left(\ln\frac{1}{20}\right)e^{-I}} \times F_{\Psi} \quad (2)$$

where I is the annual ZOI increment.

Seeds inherit the PFT from their parent plant but differ in the exact values of their functional traits, which are drawn separately for each individual.

For each produced seed, the dispersal distance is determined from a log-normal dispersal kernel with the PFT's specific value for seed dispersal distance as a mean (Stoyan & Wagner 2001). I assume no directed dispersal, so that the direction in which the seed was dispersed was chosen from a uniform distribution [0, 2π]. The cell to which the seed arrives is the individual's habitat cell.

The number of seeds in the system strongly influences the rate of seedling establishment in empty patches. After an initial phase of 20 years, the base model had at most 7% empty cells which is similar to Splechtna & Gratzer (2005) who found 3% to 13% open gaps on average in a virgin forest in Austria.

2.17.6. Adult Mortality

Mortality probability due to long-term water stress was calculated for both annuals and perennials based on mean total water availability for an individual F_{Ψ} (Sect. 2.16.7) over the growing season.

Most higher plants are killed by a loss of 60% to 90% of their water content (Levitt 1980), therefore individuals were assigned dead when their mean F_Ψ fell below 0.1.

Perennial survival probability, m, is a function of natural senescence, which is calculated based on the general assumption that mortality decreases with increasing annual size increment. Individuals with a low size increment are either large in size and have an intrinsic disadvantage due to the sigmoidal growth of plants, or grow under poor conditions and do not have enough resources to sustain a large increment (Schwinning & Weiner 1998; Caplat et al. 2008):

$$m = M_0 \times \mathrm{e}^{-M_d \times I} \quad (3)$$

where M_0 = 0.8 is the probability of mortality at zero growth, and M_d = 0.08 is the decay of growth-dependent mortality.

M_0 and M_d were chosen so that the distribution of individual ages within the base model resembles the negative exponential distribution of forests that predominately regenerate through small gaps (Fig. 2.2; Van Wagner 1978; Splechtna & Gratzer 2005). At the end of each time step all annuals die by default.

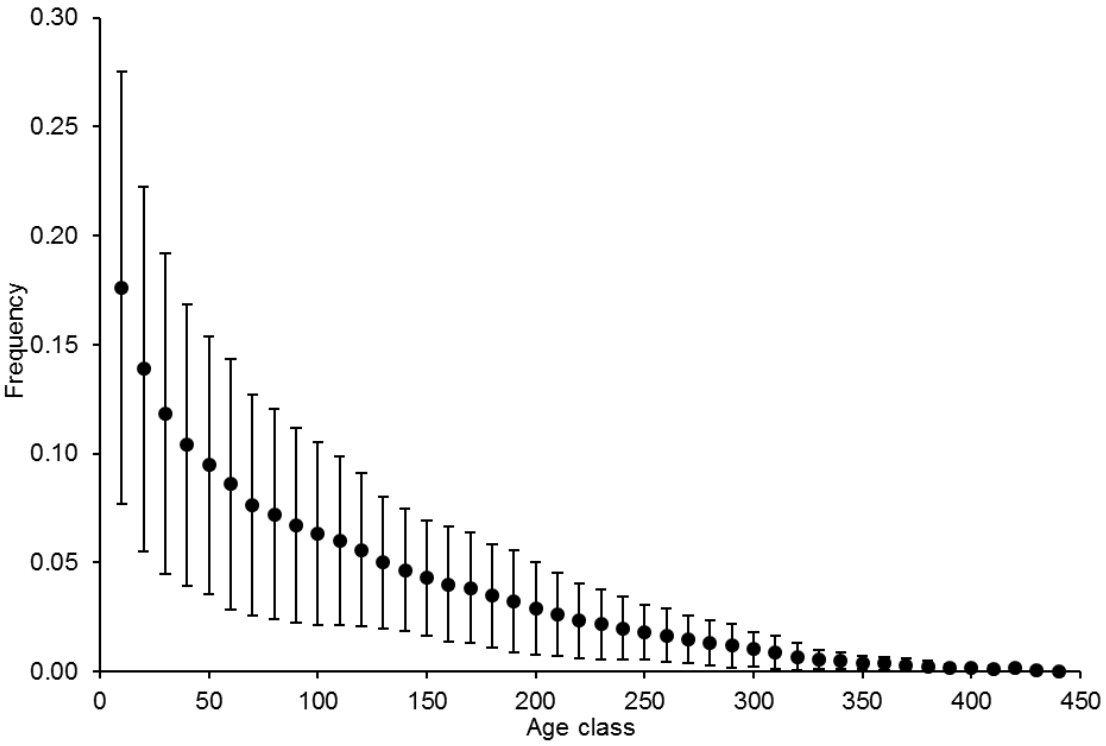

Fig. 2.2. Mean age frequency ± SD across ten replicates for 10-year age classes of a community under optimal soil water availability (Ψ = -1900 mm) after 2000 years.

2.17.7. Competition for water

Non-optimal water conditions limit water extraction by roots. This is simulated by the means of a reduction function $f(\Psi)$, a dimensionless prescribed function of the soil water potential Ψ based on four critical values Ψ_1 - Ψ_{PWP} (Feddes et al. 1978). Water uptake below $|\Psi_1|$ (oxygen deficiency, Yang & Jong (1971)) and above $|\Psi_{PWP}|$ (permanent wilting point) is set equal to zero (equation 4). Between $|\Psi_2|$ and $|\Psi_3|$ water conditions are optimal. Between $|\Psi_1|$ and $|\Psi_2|$ and between $|\Psi_3|$ and $|\Psi_{PWP}|$ a linear relationship is assumed:

$$f(\Psi) = \begin{cases} 0 & \text{if } \Psi < \Psi_{PWP} \\ \frac{\Psi - \Psi_{PWP}}{\Psi_3 - \Psi_{PWP}} & \text{if } \Psi_{PWP} \leq \Psi < \Psi_3 \\ 1 & \text{if } \Psi_3 \leq \Psi < \Psi_2 \\ \frac{\Psi_1 - \Psi}{\Psi_1 - \Psi_2} & \text{if } \Psi_2 \leq \Psi < \Psi_1 \\ 0 & \text{if } \Psi_1 \leq \Psi \end{cases} \quad (4)$$

Values of Ψ_1 - Ψ_{PWP} are available from a number of previous studies (e.g., Wesseling 1991; Bittner et al. 2010). The choice of critical potentials Ψ_i depends on the parametrization of the functional trait water stress tolerance. The critical potentials chosen for the simulation experiments presented in chapter 3 to 5 are given in the respective chapters.

Individuals can acquire water within and beyond their habitat cell according to the distance-dependent zone-of-influence approach (Czárán 1998). The ZOI approach implicitly includes the effect of plants on resource availability for other plants. Namely, according to Lehsten & Kleyer (2007), the ZOI of one plant represents an area of depleted resources for other individuals.

The number of individuals that can overlap with their ZOI is theoretically unlimited. Individuals compete with adjacent individuals for water solely in areas of ZOI overlap. The size symmetry of competition in overlapping areas has been subject to many debates (Weiner et al. 2001). Due to its non-pre-emptable characteristics, competition for water is presumably size-symmetric (Schwinning & Weiner 1998; Schulte et al. 2013). Therefore, resources in areas of ZOI overlap are divided size-symmetric (equation 5) (Weiner et al. 2001).

$$E(\Psi)_{i,(x,y)} = \frac{f_i(\Psi)_{(x,y)}}{N_{(x,y)}} \quad (5)$$

where $E(\Psi)_{i,(x,y)}$ represents the effective amount of water available to individual i of cell (x,y), $f_i(\Psi)$ is the reduction function of individual i in cell (x,y), and $N_{(x,y)}$ is the total number of individuals with cell (x, y) in their ZOI.

The total water availability of an individual i, F_Ψ, is calculated as the average value of $E(\Psi)_i$ over the number of cells within the individual's ZOI C:

$$F_\Psi = \sum_{(x,y)\in ZOI,i} \frac{E(\Psi)_{i,(x,y)}}{C} \quad (6)$$

By summing $E(\Psi)_i$ instead of soil water potentials, non-viable scenarios where $\Psi_1 \leq \Psi$ or $\Psi < \Psi_{PWP}$ are excluded. I assume that when $F_\Psi = 0$ water availability can immediately increase above 0 as soon as $\Psi_{PWP} < \Psi < \Psi_1$ regardless of the duration of periods in which F_Ψ equals zero. In other words, I assume that vegetation shows an elastic response to short-term water stress (Levitt 1980; Borgogno et al. 2010).

Chapter 3

Hydrological Niche Segregation of Plant Functional Traits in an Individual-based Model

The content presented in this chapter is modified from Herberich, M. M., Gayler, S., Anand, M., Tielbörger, K., 2017. Hydrological niche segregation of plant functional traits in an individual-based model. Ecol. Model. 356, 14-24.

Water is one of the major drivers determining distribution and abundance of plant species. Namely, plant species' presence and location in the landscape can be explained using metrics of soil water because plant species are restricted to a species-specific range of soil water conditions, i.e. their hydrological niche. However, little is known about the specific traits that determine the hydrological niche of a plant species. To investigate the relationship between plant functional traits, community structure and hydrological niche segregation, I developed a new generic individual-based model PLANTHeR which describes plant functional trait abundance as a function solely of soil water potentials and individual behavior. An important innovation is that there are no *a priori* defined trade-offs so that the model is neither restricted to a certain set of species nor scaled to a specific ecosystem.

I show that PLANTHeR is able to reproduce well-known ecological rules such as the self-thinning law. I found that plant functional traits and their combinations (plant functional types - PFTs) were restricted to specific ranges of soil water potentials. Furthermore, the existence of functional trait trade-offs and correlations was determined by environmental conditions. Most interestingly, the correlation intensity between traits representing competitive ability and traits promoting colonization ability changed with water stress intensities in a unimodal fashion.

My results suggest that soil water largely governs the functional composition, diversity and structure of plant communities. This has consequences for predicting plant species' response to changes in the hydrological cycle due to global change. I suggest that PLANTHeR is a flexible tool that can be easily adapted for further ecological-modelling studies.

3.1. Introduction

Water is one of the major forces governing vegetation patterns in time and space across a wide range of scales (Manfreda et al. 2010). In contrast to other abiotic factors such as nutrients, water is particularly interesting due to its dual effect on plant performances such as growth, survival or fecundity. On the one hand, water is a key resource, and a shortage in supply limits plant performance (Silvertown et al. 2015). On the other hand, water acts as a disturbance agent (flooding and drought) and can drastically damage individual plants. Furthermore, water also mediates other soil conditions, e.g., oxygen concentration and nutrient availability (Yang & Jong 1971; Mustroph et al. 2016). Thus, both excessive and insufficient water availability impedes individual plant performances and may consequently determine the distribution and abundance of plant species (Feddes et al. 1978; Moeslund et al. 2013).

The influence of water availability on the composition and distribution of local vegetation is especially evident in the increasing number of field observations related to so-called hydrological niche segregation (Silvertown et al. 2015). Plant species can be defined by species-specific ranges of soil water conditions, i.e. their hydrological niche, such that the species' presence and location in the landscape can be described using functions of soil water (Silvertown et al. 1999). However, the mere description of distribution patterns is not sufficient to predict species' response to changes in soil water; we also need to know the specific plant characteristics which underlie these patterns.

Functional traits can be a direct link between species response and environmental factors (Cornelissen et al. 2003). These relate environmental factors to individual fitness via their effects on growth, reproduction, and survival (Laughlin & Laughlin 2013). Thus, functional traits enable us to understand how changing environmental conditions affect vegetation composition and structure across different scales of ecological organization (Cornelissen et al. 2003). Non-phylogenetic groups that share a set of key functional traits, i.e. respond in a similar way based on a shared response mechanism to a syndrome of environmental factors, are called plant functional types (PFTs, Gitay & Noble 1997; Cornelissen et al. 2003).

For a large number of species, the functional traits which accurately indicate how species respond to changing environmental conditions are difficult to quantify (Cornelissen et al. 2003). Instead 'soft functional traits' are frequently used which are only indirect measures of the actual plant function but which are relatively quick and easy to quantify (Hodgson et al. 1999). Several soft functional traits have been associated with species response to water as a resource (e.g., spinescence, leaf size, leaf phenology, bark thickness, seed mass) or as a disturbance agent (e.g., resprouting ability, plant height) (Cornelissen et al. 2003; Violle et al. 2011; Kukowski et al. 2013). However, little is known about the specific traits that may explain the hydrological niche of a plant species (Silvertown et al. 2015). One reason may be the above-mentioned function of water simultaneously as a resource, a disturbance agent and a measure of other soil conditions, each of which selects for partly conflicting adaptations. To make it even more complicated, water is highly dynamic in time and space on a fine scale, so that hydrologically heterogeneous habitats such as wet heathlands or temporarily flooded meadows may even exhibit opposing types of water stress, i.e. seasonal alternation between waterlogging and drought in the same location in the course of a growing season (Oddershede et al. 2015).

Classical niche theories emphasize trait trade-offs as a mechanism underlying species segregation along environmental gradients (Chesson 2000; Tilman 2004). For example, species segregation along soil water gradients in English meadows was caused by a trade-off between species' tolerances to aeration stress and soil-drying stress (Silvertown et al. 1999). Another trade-off possibly associated with hydrological niche segregation exists between water-use efficiency and relative growth rate, i.e. fast-growing species are rarely drought resistant and *vice-versa* (Angert et al. 2009).

However, trade-off-based niche theories fail to provide a general explanation for species' relative abundance and vegetation structure because they assume *a priori* that species that are better at dealing with one environmental constraint are necessarily worse at dealing with another (Tilman 2004). Also, while trade-offs cause species to segregate along environmental gradients, the environmental factor itself could affect postulated classical trade-offs such as the competition–colonization trade-off (Tilman 1994). Besides, a dichotomous trait-space with a singular pre-defined trade-off is insufficient to approximate the complexity and spatiotemporal variability of multi-species

natural ecosystems, especially when it comes to hydrological niches (Kukowski et al. 2013; Silvertown et al. 2015). Therefore, a multi-trait modelling approach should be favored over a dichotomous one when trying to theorize the role of water availability in structuring natural plant communities.

A novel modelling approach that has relaxed classical assumptions about dichotomous trade-offs has yielded highly unexpected, yet plausible, trait combinations for plants adapting to disturbance (Seifan et al. 2012). These authors showed that disturbance promoted trade-offs between different colonization modes and between dormancy and disturbance-tolerance, while surprisingly, the classical competition-colonization trade-off was not generated. Instead, competition strength varied in a consistent manner with changes in disturbance intensity, while dispersal distance varied in a consistent manner with changes in disturbance predictability. These results indicate that an unrestricted modelling approach that does not define *a priori* trade-offs among plant traits is very useful for identifying the relationship between traits and environmental gradients. Also, a trade-off unrestricted approach is sufficiently flexible to include different types of ecosystems and plant strategies ranging from short-lived herbaceous plants to long-lived trees. This represents important progress compared to classical geo-biosphere models. These models tried to capture the essential dynamics of an ecosystem by modelling few plant functional types or life forms defined *a priori* by a small set of postulated characteristics with limited explanatory power (Bonan et al. 2002; Verant et al. 2004; Lapola et al. 2008).

The trade-off unrestricted approach is still underexplored and has never been applied to the complex issue of soil water. I therefore developed a novel generic model named PLANTHeR (PLAnt fuNctional Traits Hydrological Regimes) for explaining the relationship between functional traits, trade-offs and soil water potentials. PLANTHeR does not assume any *a priori* trade-offs and describes plant functional trait abundance as a function solely of the soil water potentials and individual behavior. I selected general, composite functional traits that can represent several alternative soft functional traits depending on the specific ecosystem. Therefore, PLANTHeR is neither restricted to a certain set of species nor scaled to a specific ecosystem, but instead is globally applicable to both forests and grasslands and can be applied readily to different kinds of data sets.

The overall goal of this study was to use PLANTHeR to quantify the importance of water availability for plant community structure and diversity. Specifically, I tested: (1) whether functional traits and plant functional types segregate in a predictable manner along gradients of soil water potentials and (2) whether consistent trait correlations emerge independent of the soil-water potential.

3.2. Materials and methods

To answer the above research question I performed a set of simulation experiment with the individual-based model PLANTHeR. A complete model description following the ODD (Overview, Design concepts, Details, (Grimm et al. 2006, 2010)) protocol can be found in chapter 2. Here, I only specify the ´Functional traits and PFT parameterization`, ´Soil water potentials` and 'Spatial and temporal scales' used in this chapter.

3.2.1. Functional traits and PFT parameterization

Many trade-off based niche models focus on a two- or three-fold trade-off between competitive ability, colonization ability and longevity, i.e. local extinction probability, to explain species coexistence (Tilman 1994). To study functional traits and their correlation, which may explain the hydrological niche of a plant species, I chose six rather general, composite functional traits that can represent several substitutional traits depending on the specific ecosystem. Full factorial combinations representing all potential combinations of these six traits resulted in 64 modelled PFTs (Appendix A Table A1) (Seifan et al. 2012, 2013).

Two traits were related to the individual's competitive ability (seedling competitive ability and maximum adult growth rate). Two traits represented colonization abilities in time and space (seed dormancy and seed dispersal distance), and two traits affected the individual's longevity (life form and water stress tolerance). Each functional trait is represented by two opposing strategies: perennial(P)/annual(a) life form, high(T)/low(t) water stress tolerance, long(D)/short(d) seed dispersal distance, long-(S)/short-term(s) seed dormancy, strong(C)/weak(c) seedling competitive ability, and high(G)/low(g) maximum adult growth rate (Seifan et al. 2012, 2013). Except for the functional trait life form and water stress tolerance (Sect. 2.1.4.7), the functional trait strategy indicated by the capital letter stands for 80% of the maximum trait value whereas the strategy indicated by the lowercase

letter stands for 20%. Seed dormancy, seedling competitive ability, and maximum adult growth rate are probabilistic traits a maximum of 100%. Maximum seed dispersal distance is 40 m. The exact functional trait values are drawn separately for each individual from a normal distribution with the PFT strategy as mean and 10% of the maximum trait value as standard deviation.

Differences between PFT strategies for high(T)/low(t) water stress tolerance are simulated by means of a reduction function f(Ψ), a dimensionless prescribed function of the soil water potential Ψ [mm] based on four critical values Ψ_1 - Ψ_{PWP} (Feddes et al. 1978). The critical potentials Ψ_i [mm] were chosen in a manner to ensure that the two opposing PFT strategies high and low water stress tolerance would be maximally different (Table 3.1). Thereby, high water stress tolerance indicates high tolerance to dry conditions but low tolerance to wet conditions and *vice-versa* for low water stress tolerance. This trade-off between soil drying and waterlogging tolerance has been reported for various environments and phylogenetic groups (Silvertown et al. 1999).

Table 3.1
Critical potentials Ψ_i [mm] of water uptake governing the reduction function $f(\Psi)$ for plant functional types with high water stress tolerance (T) and low water stress tolerance (t).

Ψ_i	Water stress tolerance high (T)	Water stress tolerance low (t)
Ψ_1	-150	-1
Ψ_2	-300	-10
Ψ_3	-10000	-2000
Ψ_{PWP}	-240000	-80000

3.2.2. Soil water potentials

In this study, only cases with negligible seasonal and inter-annual soil water potential variability are considered. The growing season is thus assumed to be statistically homogenous and modelled in 17 soil water potential Ψ [mm] scenarios (Table 3.2). Soil water potentials were chosen based on the shape of reduction functions $f(\Psi)$ to represent gradients of water stress intensities for high water stress tolerant (T) and low water stress tolerant (t) PFTs (Sect. 3.2.1). At soil water potentials between -300 and -2000 mm, the values of both reduction functions, $f_T(\Psi)$ for high water stress tolerance (T) and $f_t(\Psi)$ for low water stress tolerance (t), are equal to one, i.e. no PFT experiences any stress. Therefore, Ψ = -1900 mm was chosen to represent a 'base model'.

Table 3.2
17 simulated soil water potentials Ψ [mm] representing different stress intensities f(Ψ) for high water stress tolerant (T) and low water stress tolerant (t) PFTs.

Stress	Excessive water availability	Excessive water availability	Insufficient water availability	Insufficient water availability
Baseline	Water stress tolerance low (t)	Water stress tolerance high (T)	Water stress tolerance low (t)	Water stress tolerance high (T)
f(Ψ)	Ψ	Ψ	Ψ	Ψ
1	-1900	-1900	-1900	-1900
0.7	-7.3	-255	-25400	-79000
0.5	-5.5	-225	-41000	-125000
0.3	-3.7	-195	-56000	-171000
0	0	-150	-80001	-300000

3.2.3. Spatial and temporal scales

The goal of this study was to explain the relationship between functional traits, trade-offs and soil water potentials. To ensure that the resulting functional traits, PFTs and trait correlations were not just a representation of a single moment in time, I compared PFT richness and Shannon diversity index every 100 years along the simulation runs (Seifan et al. 2012) (Fig. 3.1). PFT richness and Shannon diversity index were generally consistent in their trend in time, however, these two measures did not stabilize at the exact point in time for all soil water potentials. PFT richness stabilized latest after 1500 years, i.e. no significant differences ($p > 0.05$) in PFT richness for all soil water potentials after 1500 years. On the other hand, the values of the Shannon diversity index stabilized latest after 1100 years for all soil water potentials. I therefore chose 2000 years as the simulation time. Each of the 17 soil water potential scenarios was repeated ten times. The model landscape consisted of a grid of 800 × 800 cells with periodic boundaries to avoid boundary effects.

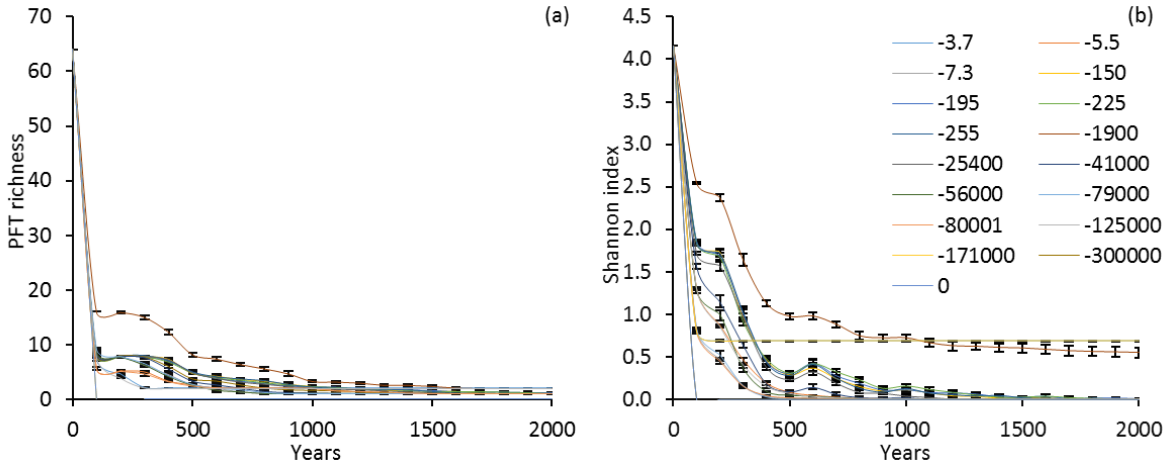

Fig. 3.1. Change in mean ± SD PFT richness (a) and Shannon diversity index (b) of ten repetitions over time for 17 soil water potentials.

3.2.4. Model plausibility

To check the plausibility of the model behavior, I tested whether PLANTHeR is able to reproduce some well-established ecological patterns. Competition is a key trait to predict patterns of species segregation along environmental gradients both in classical trade-off based niche models as well as in the trade-off unrestricted approach (Tilman 1994; Seifan et al. 2012). I therefore focused on testing the ability of PLANTHeR to reproduce the self-thinning rule, which describes the effects of competition on plant populations by relating changes in mean plant biomass to density over time (Westoby 1984). The rule predicts that even-aged monospecific plant populations undergoing density-dependent mortality form a straight self-thinning line with a slope of - 3/2 when the logarithm of mean surviving plant biomass is plotted against the logarithm of plant density (Yoda et al. 1963; Westoby 1984).

3.2.5. Statistical analysis

Pearson correlation tests were used to study which trade-offs and correlations between traits emerge depending on soil water potential. The value of the correlation coefficient and its significance were interpreted as the relative strength of the trade-off/co-occurrence in a particular scenario (Seifan et al. 2012, 2013).

To test the model plausibility, I analyzed the thinning slope for the ten replicates of the base model. I therefore selected *a posteriori* the data points during which the population was undergoing density-dependent mortality, indicated by a characteristic decay of positive skewness of the biomass distribution (Berger et al. 2002). Regression lines were fitted to the $\log_{10}$-transformed mean plant biomass w and plant density N using a reduced major axis analysis (RMA) (sensu Warton et al. 2006). I tested with a two-sided one-sample t-test whether the slopes were equal to -3/2.

All statistical analyses were performed in R 3.1.2.

3.3. Results

3.3.1. Functional trait and plant functional type segregation

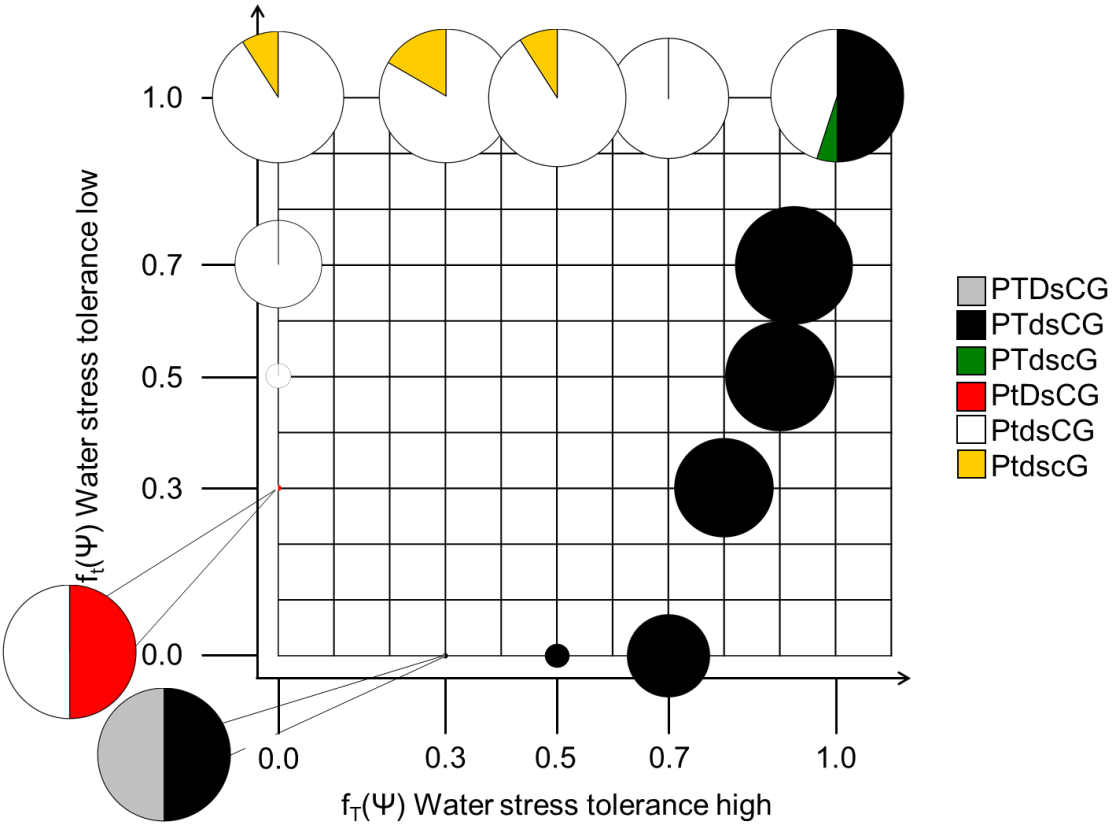

Fig. 3.2. PFTs successful under seventeen different soil water potentials after 2000 years. The axes depict the dimensionless reduction function f(Ψ) for high (T)/low(t) water stress tolerant PFTs. The pie diameter is proportional to the community yield weighted by the yield of the base model (upper right pie). perennial(P)/annual(a) life form, high(T)/low(t) water stress tolerance, long(D)/short(d) seed dispersal distance, long-(S)/short-term(s) seed dormancy, strong(C)/weak(c) seedling competitive ability, and high(G)/low(g) maximum adult growth rate.

Functional trait strategies and PFTs segregated in a predictable manner along gradients of soil water potential (Fig. 3.2, Fig. 3.3). PFTs that were successful after 2000 years differed only in their water stress tolerance, seed dispersal distance and seedling competitive ability (Fig. 3.2). Irrespective of soil water potential, perennials with a short-term seed dormancy, strong competitive ability, and high maximum growth rate dominated the model landscape (Fig. 3.3). When the soil water potential Ψ was within the range where both reduction functions, $f_T(\Psi)$ for high water stress tolerance (T) and $f_t(\Psi)$ for low water stress tolerance (t), were equal, individuals with high (T) and low (t) water stress tolerance coexisted. In all other cases, the strategy with the higher value of the reduction function dominated. In both scenarios with the lowest value of the reduction functions, either caused by excessive (soil water potential Ψ = -3.7 mm) or by insufficient water availability (Ψ = -171000 mm), individuals with

long (D) and short (d) maximum seed dispersal distance coexisted. In all other scenarios, individuals with short (d) maximum seed dispersal distance dominated.

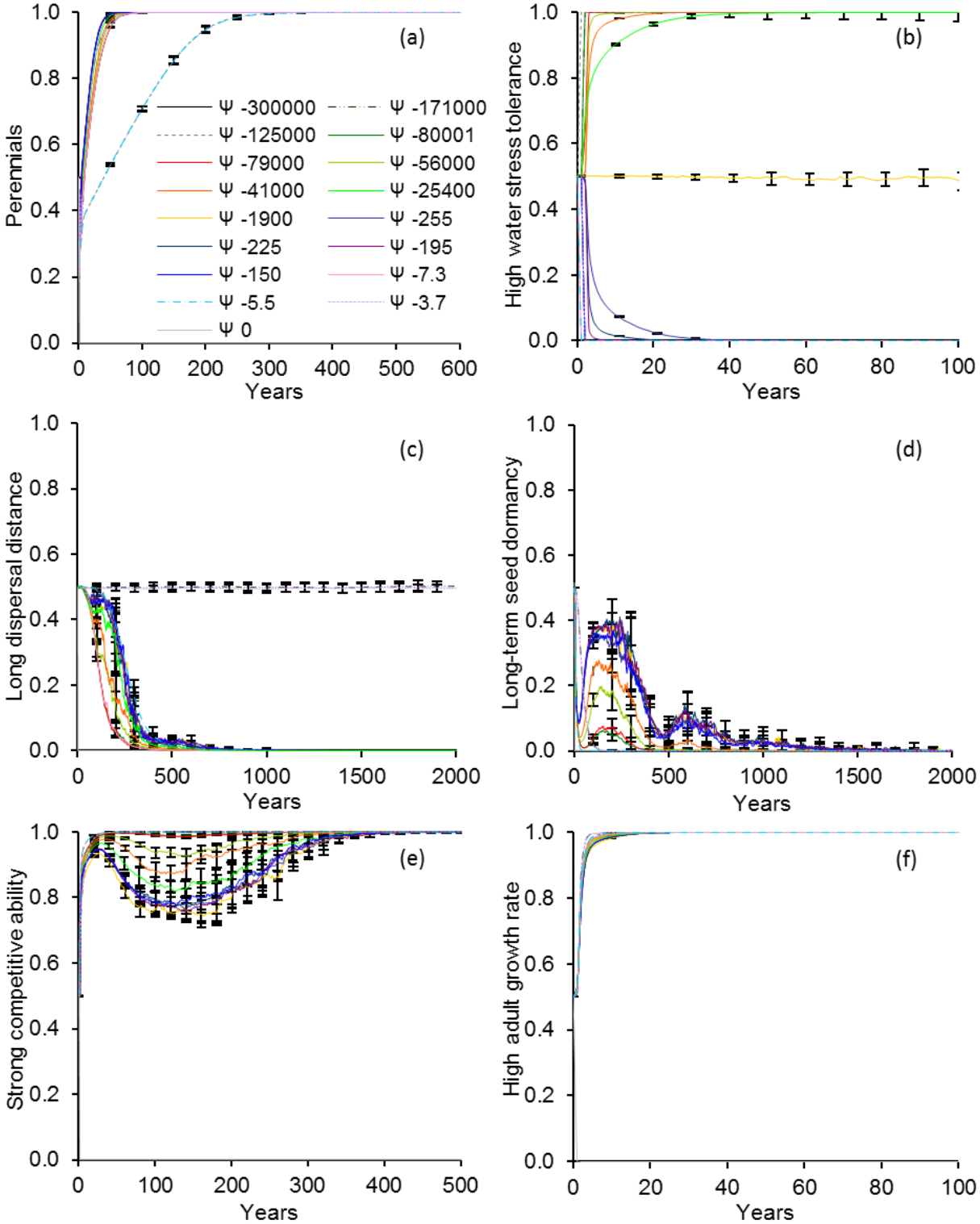

Fig. 3.3. Change in mean ± SD relative densities of the capital letter PFT strategy (fraction of PFT strategy among all coexisting individuals) over time under seventeen soil water potentials [mm]. (a) Fraction of perennials. (b) Fraction of high water stress tolerance: high tolerance to dry conditions but low tolerance to wet conditions. (c) Fraction of long maximum dispersal distance. (d) Fraction of long-term seed dormancy: 20% ± 10 germination per year. (e) Fraction of strong competitive ability: seedlings' ability to establish in a cell when competing with others. (f) Fraction of high maximum adult growth rate.

3.3.2. Trade-offs and positive correlations

All six studied functional traits were correlated with each other. However, strength and significance varied depending on the soil water potential Ψ (Fig. 3.4). When Ψ was within the range where either $f_T(\Psi) = 0$ or $f_t(\Psi) = 0$ (i.e. no variance in the functional trait water stress tolerance), the correlation coefficients including water stress tolerance could not be computed. Among others, I tested how differences in soil water potential affected trait correlations between traits representing competitive ability (seedling competitive ability and maximum adult growth rate) and traits representing colonization abilities in time and space (seed dormancy and seed dispersal distance) (Fig. 3.4a). I found significant negative correlations for all trait combinations representing a competition colonization trade-off. However, these correlations were not constant but changed in a unimodal fashion with water stress intensities (Fig. 3.4a). The correlation between traits representing competitive ability and seed dispersal distance became less negative with increasing water stress intensity. On the contrary, the correlation between traits representing competitive ability and seed dormancy more negative with increasing water stress intensity. Furthermore, I detected a significant positive correlation between seed dormancy and seed dispersal distance, which weakened consistently with increasing water stress intensity. Moreover, I found a significant positive correlation between seedling competitive ability and adult growth rate, which strengthened consistently with increasing water stress intensity. Regarding a possible competition-longevity trade-off (Fig. 3.4b), all traits related to competitive ability were significantly positively correlated with life form. Again, these trait correlations were not constant but changed consistently along water stress intensities in a unimodal fashion. The correlation coefficients between water stress tolerance and adult growth rate, seedling competitive ability, and life form, respectively, showed an 'S-shaped' pattern with significant negative correlation coefficients for excessive water availability scenarios, significant positive correlation coefficients for insufficient water availability scenarios and correlation coefficients close to zero for the base model.

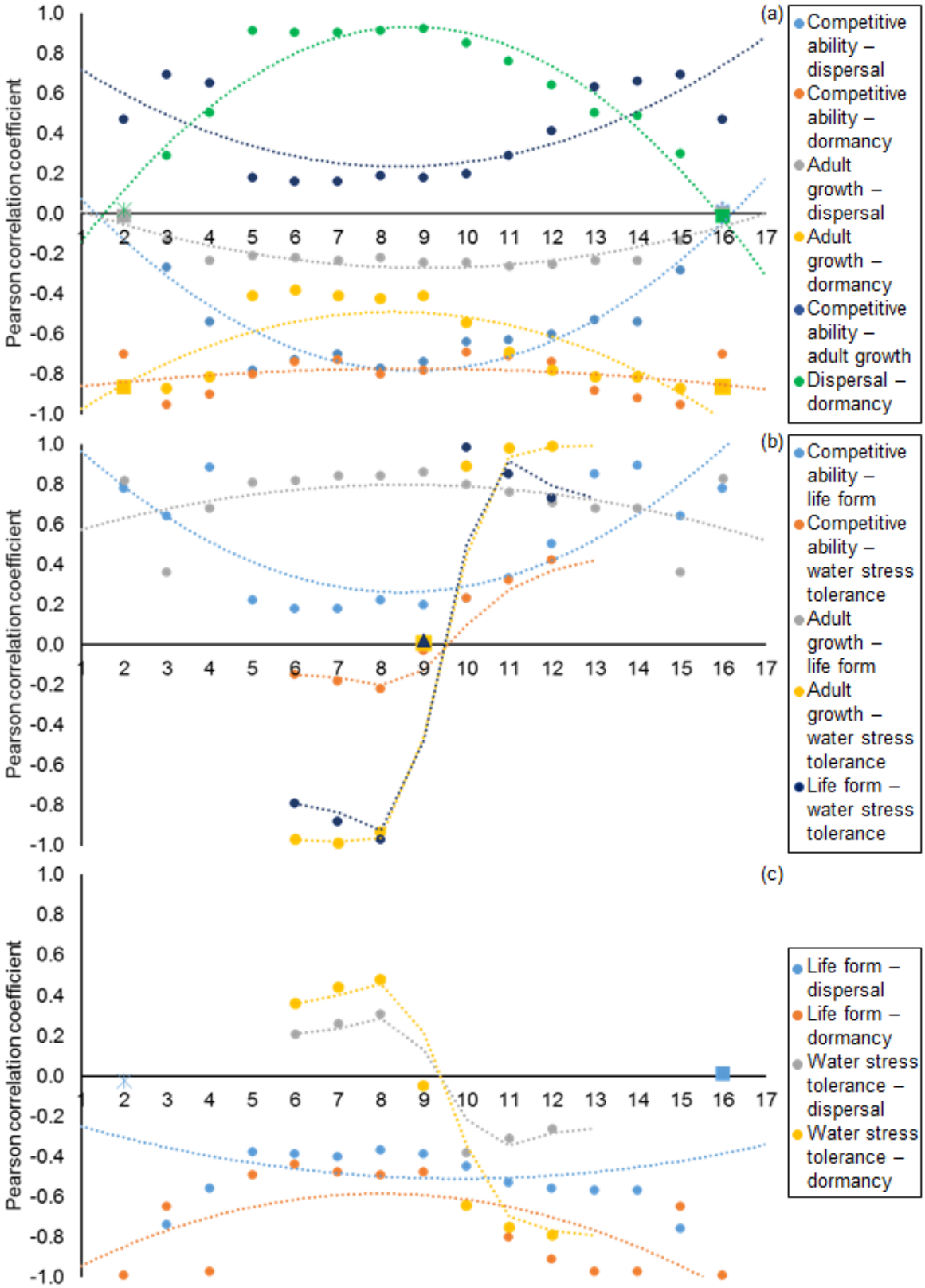

Fig. 3.4. Pearson correlation coefficients of trait pairs successful under seventeen levels of soil water potential. (1) Ψ = 0, (2) Ψ = -3.7 mm, (3) Ψ = -5.5, (4) Ψ = -7.3, (5) Ψ = -150, (6) Ψ = -195, (7) Ψ = -225, (8) Ψ = -255, (9) Ψ = -1900, (10) Ψ = -25400, (11) Ψ = -41000, (12) Ψ = -56000, (13) Ψ = -79000, (14) Ψ = -80001, (15) Ψ = -125000, (16) Ψ = -171000, (17) Ψ = -300000. Note that the fit lines are intended as a visual support for the reader and do not indicate mathematical relationships between the correlation coefficients and soil water potentials. (a) Trait pairs associated with a competition-colonization trade-off. (b) Trait pairs associated with a competition-longevity trade-off. (c) Trait pairs associated with a longevity–colonization trade-off. □ $P > 0.05$, Δ $P < 0.05$, * $P < 0.01$, ○ $P < 0.001$.

The last group of trait correlations might be classified as a longevity–colonization trade-off (Fig. 3.4c). The correlation between water stress tolerance and seed dispersal distance or seed dormancy was significantly negative for scenarios with insufficient water availability, significantly positive for scenarios with excessive water availability and close to zero under the base model. Life form and seed dispersal distance were significantly negatively correlated under all soil water potentials except Ψ = -3.7 mm and Ψ = -171000 mm. I also found a significant negative correlation between life form and seed dormancy which increased with increasing water stress intensity for both excessive and insufficient soil water availability except Ψ = -5.5 mm and Ψ = -125000 mm.

3.3.3. Self-thinning

The simulated thinning slopes were similar to the slope predicted by the self-thinning rule and only marginally but significantly shallower (one-sample $t(9) = 19.21$, $p < 0.001$) with a mean of -1.446 and 95% CI [-1.452 to -1.440].

3.4. Discussion

The overall results show that soil water potential was a main driver of functional trait composition and diversity. Conversely, plant functional traits and their specific combination (PFT) were key to explaining the response of plant individuals to different soil water potentials. Two main results strengthen this conclusion. First, plant functional traits and PFTs were restricted to a specific range of soil water potentials. Second, the strength and significance of functional trait correlations changed with water stress intensity. In the following, I discuss these main results with respect to the initial questions and the ability of PLANTHeR to reproduce the self-thinning rule.

3.4.1. Functional trait and plant functional type segregation

I found segregation along water stress gradients on two organizational levels. On the one hand, the two functional trait strategies for water stress tolerance high(T)/low(t) clearly segregated along soil water potential gradients, with coexistence only possible if soil water potentials were optimal for both (base model). On the other hand, plant functional types resulting from the combination of the six studied functional traits were restricted to specific water stress intensities. These findings strongly

support hydrological niche segregation as an important determinant of the abundance and distribution of plant species (Adler et al. 2006; Verhulst et al. 2008; Silvertown et al. 2015).

A crucial step to predict species response to changes in soil water is to detect the specific functional traits which underlie the hydrological niche segregation (Laughlin & Laughlin 2013). However, until now only a few descriptive field studies have examined functional traits linked to hydrological niche segregation (Oddershede et al. 2015; Silvertown et al. 2015). These studies resulted in site-specific functional trait composition and were often biased by confounding habitat factors such as management or local species pool (Oddershede et al. 2015). In contrast to such field studies, PLANTHeR predicts a generic functional trait composition of plant communities solely as a function of the soil water potential and individual behavior, i.e. without any confounding factors.

Many functional trait patterns emerging from PLANTHeR supported previous studies. First, I interpret the segregation and selection of functional traits and PFTs to be a result of competitive exclusion (Gause 1934). The theory of competitive exclusion predicts that the best competitor for a single limiting resource should displace all other species from a habitat independent from their initial densities (Tilman 1982). This is in line with my result that even though all 64 PFTs had similar initial density, a maximum of only two PFTs were able to coexist in the long run. Second, PLANTHeR predicted that perennials with high competitive ability, low dormancy and high adult growth rates had the highest success in all scenarios (Wilson & Tilman 1991; Schippers et al. 2001). Similar to my results, Schippers et al. (2001) found that non-dormant perennials dominated in spatially and temporally homogenous habitats. Likewise, Bauer et al. (2002) showed that annuals are generally excluded in homogenous habitats due to the monopolization of establishment sites by perennials. Third, the segregation along soil water potential gradients of the two functional trait strategies for water stress tolerance was most likely driven by a trade-off between adaptations to shortage of water and adaptations to excessive water. This trade-off was indirectly implemented in PLANTHeR in the water competition module via the choice of four critical values Ψ_1 - Ψ_{PWP}. When the soil water potential was within the range where this trade-off was inoperative (base model), the two functional trait strategies for water stress tolerance did not segregate. Previous field studies reported this trade-off as a major

constraint that underlies hydrological niche segregation in various environments and phylogenetic groups (Silvertown et al. 1999; 2015). Fourth, only in the two scenarios with the highest water stress intensity were individuals with long maximum seed dispersal distance (D) successful. This is in line with the theory that predicts that greater dispersal is favored in stressful environments (Teller et al. 2014). In summary, PFT segregation as well as the selection of the two functional traits water stress tolerance and seed dispersal distance were determined by soil water, while PFT diversity and selection of the functional traits life form, seed dormancy, seedling competitive ability, and maximum adult growth rate were driven by community-internal processes, namely competition for the single resource soil water. Hence, the presented functional trait composition and diversity of the plant communities was unique to soil water and cannot be directly transferred to abiotic factors which are not a resource such as soil pH.

3.4.2. Trade-offs and positive correlations

The most intriguing finding of my study was the absence of universal trade-offs; rather, the correlation strength was by itself a function of water stress intensity. This is a direct result of my trade-off unrestricted approach and highlights the urgent need for more such studies and the limitations of models based on trade-offs defined *a priori*.

Among others, I found significant trade-offs between all traits representing competitive ability (seedling competitive ability and adult growth rate) and all traits promoting colonization ability in time and space (seed dormancy and seed dispersal distance). These results indicate that the classical competition-colonization trade-off did play an important role for hydrological niche segregation, which is in line with most theories on niche evolution (e.g., Tilman 1994; Chesson 2000; Körner & Jeltsch 2008).

In contrast to theoretical predictions, however, the strength of these trade-offs was not constant but changed consistently with water stress intensities in a unimodal fashion. Increasing water stress intensity weakened the trade-off competitive ability and seed dispersal while the trade-off between competitive ability and seed dormancy was consistently strengthened.

A weak or missing competition-dispersal trade-off is a typical syndrome of habitats in which microsite availability has a low importance as a selective force (Seifan et al. 2012). In my study, an increase in water stress intensity increased individual mortality, which in turn led to a higher availability of relatively heterogeneously distributed microsites. Thus, availability of microsites at a given point in time became less important as a selective force, which hence decreased the need for a competition-dispersal trade-off (Yu & Wilson 2001; Seifan et al. 2012). On the other hand, with increasing water stress intensity, the importance of the temporal availability of a given site gained in importance as a selective force, which increased the need for a dormancy-competition trade-off (Snyder 2006).

Further evidence for the increased importance of temporal site availability with increasing stress is the weakened positive correlation between seed dormancy and seed dispersal distance (Seifan et al. 2012). Both dormancy and dispersal may allow species to exploit rare gap openings as recruitment sites, especially within competitive communities (Milton et al. 1997; Holmes & Wilson 1998). Therefore, these two traits are considered as alternative traits, and theory predicts a trade-off, rather than a positive correlation, between them (Venable & Brown). However, Snyder (2006) showed that high temporal predictability of the environment reduces the need for a trade-off between dispersal and dormancy and may even promote a positive relationship. My results show that despite the long temporal predictability of abiotic conditions, the predictability of the biotic environment (microsite availability) changed with increasing water stress intensity, which consistently weakened the positive correlation between dormancy and dispersal.

Another trade-off associated with species coexistence is between species longevity and competitive ability (Tilman 1994). Again, I did not reproduce this well-known trade off but found a positive correlation between life form (annuals *vs.* perennials) and both traits related to competitive ability. However, the need for a longevity-competition trade-off might have been reduced, since the differentiation between traits associated with the competition-colonization trade-off was sufficient to generate coexistence (Tilman 1994).

In summary, several of the emergent trait correlations supported previous findings. For example, the classical competition-colonization trade-off played a major role in maintaining PFT diversity and niche

segregation under different water stress intensities. However, rather unexpectedly, the strength of these (and other) trait correlations changed consistently in a unimodal fashion across water stress intensities. This unimodal change resulted from the dual effect of soil water on plant performances. The implications of this result are twofold. First, a dichotomous trait space with a singular pre-defined trade-off was insufficient to model hydrological niche segregation. Secondly, soil water had a strong impact on the functional structure of plant communities and could even alter postulated classical trade-offs.

This suggests that neither positive nor negative trait correlations should be considered universal and used as a basis to choose PFTs for modelling studies, as is done in many geo-biosphere models (Bonan et al. 2002; Verant et al. 2004; Lapola et al. 2008). Instead, the trade-off unrestricted approach based on multiple traits used in PLANTHeR proved highly useful for studying species response to soil water as well as to disturbance (Seifan et al. 2012).

3.4.3. Self-thinning

Even though PLANTHeR includes several submodels which are inconsistent with the basic assumptions of the self-thinning rule (seed production, size-symmetric competition, mixed communities, etc.), it was able to reproduce thinning slopes surprisingly close to the expected -3/2.

The slight deviance towards shallower thinning slopes in PLANTHeR might be a result of the mode of competition for water. Due to the non-pre-emptable uniform distribution of water, water competition is generally assumed to be size-symmetric (Schulte et al. 2013). Previous studies showed that size-symmetric competition generally flattens the thinning slopes in theoretical plant populations (Chu et al. 2010; Lin et al. 2014). For example, Lin et al. (2014) found thinning slopes equal to -1.1, whereas Chu et al. (2010) reported thinning slopes as high as -0.8 if competition was size-symmetric. In comparison to these studies, the predicted thinning slopes by PLANTHeR are relatively steep.

One possible explanation for this might be that neither study included recruitment, i.e. both were even-aged. Recruitment as such does not prevent populations from following the general principles of the self-thinning rule, especially if the biomass of the recruitment is negligible (Westoby 1984; Schulze et al. 2005; Luyssaert et al. 2008). However, it has been shown that in uneven-aged and/or mixed-

species populations the thinning slope tends to be steeper (Schulze et al. 2005), which might explain the results predicted by PLANTHeR.

I conclude that each of the submodels in PLANTHeR that is inconsistent with the self-thinning rule offsets the thinning slope in another direction, which in combination resulted in thinning slopes relatively close the classical -3/2.

Existing models which investigate the thinning slope under environmental stress or different competition modes do not include recruitment (Chu et al. 2010; Lin et al. 2014). However, most natural plant populations do recruit and, depending on the pattern and periodicity of this recruitment, may vary in age (Van Wagner 1978; Splechtna & Gratzer 2005). Considering the expected changes in soil water availability due to climate change, future studies should investigate the combined effect of water stress, size-symmetric competition, and recruitment.

Conclusions

Given that the terrestrial water cycle is prone to anthropogenic alteration and expected to be strongly influenced by climate change (Vörösmarty & Sahagian 2000), it is important to understand the relationship between plant functional traits, community structure and hydrological niche segregation. Classical niche concepts are unable to provide a general explanation for species' relative abundance and community structure due to underlying simplistic assumptions. In particular, many concepts focus on a limited number of trade-offs, including the competition-colonization trade-off. I used a highly flexible approach that models functional traits without defining trade-offs *a priori*. Instead all trade-offs and trait correlations emerge from individual behavior and soil water availability. Another important innovation of PLANTHeR is that it represents highly resolved, spatially explicit, long-term vegetation dynamics applicable to both forests and grasslands.

The model behavior of PLANTHeR was plausible in that it reproduced some well accepted patterns such as the theory of competitive exclusion and the self-thinning rule (Gause 1934; Yoda et al. 1963). PLANTHeR also confirmed accumulating evidence from field observations for hydrological niche segregation (Silvertown 2004). However, some of the resulting patterns were rather surprising. First, the strength of trait correlations, among those several associated with the well-known competition-

colonization trade-off (Tilman 1994), were a function of water stress intensities. Second, a dichotomous trait space with a singular pre-defined trade-off was insufficient to model hydrological niche segregation.

In summary, PLANTHeR was able to reproduce and explain classical plant community patterns while highlighting important research gaps. Especially the result that the intensity of trait correlations is a function of environmental factors is new and deserves further attention. With this in mind, a future study will examine how spatiotemporal variability of environmental factors, specifically of soil water, affect the intensity of trait correlations and the thereof resulting consequences for species coexistence with special regards to the storage effect as suggested by Silvertown et al. 2015.

Chapter 4

Density-dependent dynamics in plant communities deviate from simple rules due to age structure, multiple species and abiotic stress

The self-thinning rule which relates changes in mean plant biomass to density through time is a well-studied concept in plant ecology. A pertinent debate centers around the generality of the values of the thinning intercept and slope. For example, intercept and slope may vary along abiotic stress gradients. However, variations in the biomass-density relationship due to abiotic stress have been studied only in highly simplified settings such as in even-aged monospecific populations without recruitment, short stress gradients, or *a posteriori* selected data points for fitting the self-thinning line.

Here, I simulate changes in the entire biomass-density relationship over time of uneven-aged multi-species communities using a complete water stress gradient from excessive to insufficient soil water availability.

I show that both excessive and insufficient water availability strongly and consistently modified the entire biomass-density trajectory including the values of the slope of the classical self-thinning line. Namely, with increasing stress the slope decreased in communities with high density and increased in communities with low density. Additionally, also under moderate conditions the fact that I allowed recruitment and the coexistence of several plant functional types modified the biomass-density trajectory, too. Most interestingly, I detected four sections characterizing the biomass-density relationship instead of the classical three-sectioned biomass-density trajectories. Furthermore, early mortality was density-independent mainly as a result of annual plant mortality. Finally, the inclusion of recruitment could fill gaps created by mortality which consistently decreased the slope of thinning sections. I conclude that there is no generally applicable biomass-density relationship. Classical even-aged monospecific studies do not capture processes in realistic plant populations and communities

such as the occurrence of recruitment or the coexistence of multiple species and thus, fail to predict variations in the biomass-density relationship due to abiotic stress.

4.1. Introduction

One of the most important principles in plant ecology is the self-thinning rule which relates changes in mean plant biomass to density through time. The rule predicts that this relationship in even-aged monospecific plant populations undergoing density-dependent mortality forms a straight self-thinning line with a slope of - 3/2 when the logarithm of mean surviving plant biomass *w* is plotted against the logarithm of plant density *N*. The rule is usually expressed as a power law $w = kN^{-a}$, where *k* and *a* are the self-thinning intercept and slope, respectively (Yoda et al. 1963; Westoby 1984; Weiner & Freckleton 2010). Although there is broad consensus about the general process of self-thinning, there has been much debate about the fundamental validity of the specifics of the self-thinning rule, especially with respect to the values of the intercept and slope (Weller 1991; Lonsdale 1990; White et al. 2007). For example, it has been shown that these values may vary in populations subjected to abiotic stress such as resource deficit (Morris 2003; Chu et al. 2010; Lin et al. 2014). Specifically, based on the review of Morris (2003) six patterns of possible responses of the intercept *k* and slope *a* to resource deficit have been observed: (1) both *k* and *a* stay constant; (2) both *k* and *a* decrease; (3) *k* decreases but *a* stays constant; (4) *k* increases but *a* stays constant; (5) *k* increases but *a* decreases; or (6) *k* decreases but *a* increases. The first pattern is also referred to as the 'common line' pattern, whereas the other patterns are 'different line' patterns (Morris 2003). However, the intensity and direction of variation in *k* and *a* seem to be completely unpredictable and no general pattern as to why and under which conditions the values are modified when resource availability changes has been established to date. Plant physiological response curves along below- and aboveground resource gradients usually follow a unimodal relationship, i.e. both a deficiency as well as a surplus of resources hamper plant performance (Austin 1990). Soil water is an ideal resource for addressing the above questions in detail. Namely, it is a key resource for plants and essential to numerous physiological functions (Silvertown et al. 2015). In contrast to other resources, water simultaneously acts as a disturbance agent (flooding and drought) and can lead to the partial or total destruction of a plant

individual (Grime 1977). Furthermore, water is associated with other soil conditions that regulate oxygen concentration and nutrient availability (Yang & Jong 1971; Mustroph et al. 2016). Thus, both insufficient and excessive water availability reduce plant performance (Feddes et al. 1978; Moeslund et al. 2013; Silvertown et al. 2015), and studies of 'complete' water gradients can yield important insights about possible changes in the intercept and slope of the self-thinning line under abiotic stress. A previous experiment indicated that there was no significant change in both the intercept and slope under moderate water deficit in comparison to well-watered conditions (Liu et al 2006). However, there is no study which examines changes in the intercept and slope along a complete stress gradient, e.g. from excessive to insufficient water availability.

Competition for water is generally assumed to be size-symmetric due to its non-pre-emptable uniform distribution (Schwinning & Weiner 1998; Schulte et al. 2013). Previous studies showed that size-symmetric competition generally increase α (Stoll et al. 2002; Chu et al. 2010; Lin et al. 2014). However, these studies are based on monospecific populations without recruitment, i.e. of even-age. Yet, ignoring recruitment, species coexistence, and changes in species composition along stress gradients appear a large simplification of the processes occurring in nature which hampers our ability to understand the complexity and spatiotemporal variability of multi-species natural ecosystems. This is especially true for water stress gradients where the dual effect of water as a resource and a disturbance modifies the functional and structural composition of plant communities in a very complex manner (Silvertown et al. 2015; Herberich et al. 2017).

Another shortcoming of previous studies regarding changes in density-dependent effects due to abiotic stress is that they focused only on changes in the self-thinning section (Morris 2003; Chu et al. 2010; Lin et al. 2014). However, the self-thinning section is only part of the entire biomass-density trajectory (hereinafter abbreviated as 'bdt') (Begon et al. 1991; Berger & Hildenbrandt 2003). Classical bdts additionally include a fast growing section and a post-thinning section (Begon et al. 1991; Berger & Hildenbrandt 2003). A previous experiment indicated that even moderate water deficit can delay the onset of the self-thinning process in comparison to well-watered conditions (Liu et al 2006), and thus likely alter the duration of all bdt sections.

This is the first attempt to comprehensively investigate changes in the entire biomass-density trajectory along a complete stress gradient within an uneven-aged, multi-species plant community. Using a spatially explicit individual-based model, I investigated occurrence, duration and characteristics of the different sections of the biomass-density trajectory as well as the values of *k* and *a* along a soil water gradient.

4.2. Materials and methods

To answer the above research question I performed a set of simulation experiment with the individual-based model PLANTHeR. A complete model description following the ODD (Overview, Design concepts, Details, (Grimm et al. 2006, 2010)) protocol can be found in chapter 2. Here, I only specify the 'Diversity and functional composition of simulated plant communities', 'Soil water scenarios', 'Spatial and temporal scales' and 'Statistical analysis' simulated in this chapter.

4.2.1. Diversity and functional composition of plant communities

A detailed analysis of the diversity, functional composition and functional trait trade-offs of the simulated plant communities can be found in chapter 3. Here, I only give a brief overview over the main points of the functional composition which affect the biomass-density relationship.

In PLANTHeR, each individual is characterized by six general, composite functional traits which can represent several alternative traits depending on the specific ecosystem. Two traits are related to competitive ability (seedling competitive ability, maximum adult growth rate), two traits represent spatiotemporal colonization abilities (seed dormancy, seed dispersal distance), one trait affects longevity (life form), and one trait affects the response to abiotic stress (water stress tolerance). Each functional trait is represented by two opposing strategies: perennial(P)/annual(a) life form, high(T)/low(t) water stress tolerance, long(D)/short(d) seed dispersal distance, long-(S)/short-term(s) seed dormancy, strong(C)/weak(c) seedling competitive ability, and high(G)/low(g) maximum adult growth rate (Seifan et al. 2012, 2013). Except for the functional traits 'life form' and 'water stress tolerance' (Sect. 4.2.1), the functional trait strategy indicated by the capital letter stands for 80% of the maximum trait value whereas the strategy indicated by the lowercase letter stands for 20%, respectively. Seed dormancy, seedling competitive ability, and maximum adult growth rate are

probabilistic traits with a maximum of 100%. Maximum seed dispersal distance is 20 m (Nathan & Muller-Landau 2000). The exact trait values are drawn for each individual separately from a normal distribution with the PFT strategy as mean and 10% of the maximum trait value as standard deviation (SD).

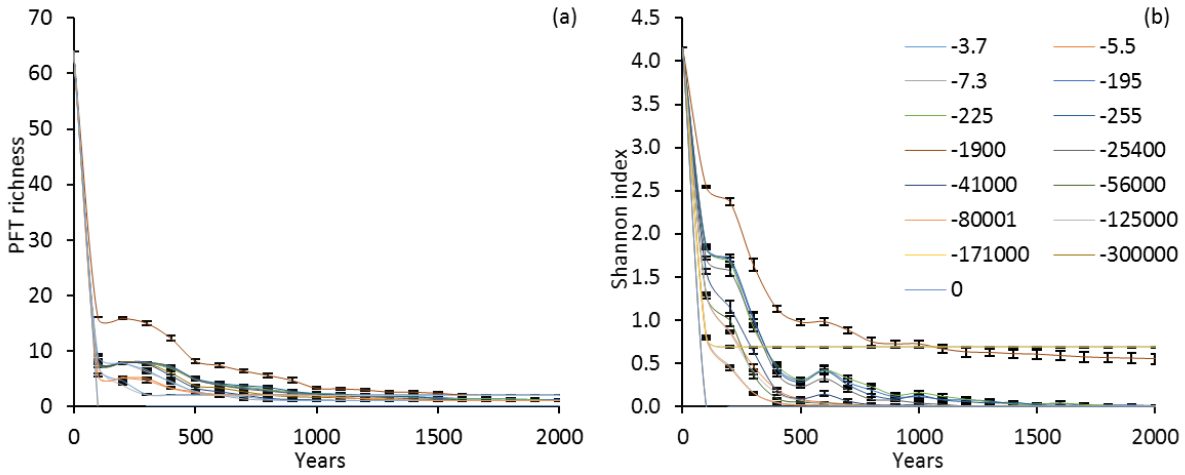

Fig. 4.1. Adapted from chapter 3. Change in mean ± SD PFT richness (a) and Shannon diversity index (b) of ten repetitions over time for seventeen soil water potentials [mm]. PFT richness and Shannon diversity index were generally consistent in their trend in time, however, these two measures did not stabilize at the exact point in time for all soil water potentials. PFT richness stabilized latest after 1500 years, meaning that I did not find any significant differences ($p > 0.05$) in PFT richness for all soil water potentials after 1500 years. On the other hand, the values of the Shannon diversity index stabilized latest after 1100 years for all soil water potentials.

PLANTHeR models diverse communities comprising up to 64 PFTs resulting from the full factorial combinations of the functional trait strategies (Seifan et al. 2012, 2013; Herberich et al. 2017). In each of the 15 simulated soil potential scenarios, communities were initialized with the highest diversity, i.e. all 64 PFTs had similar initial densities (Fig. 4.1). Diversity decreased over time due to competitive exclusion and a maximum of two PFTs were able to coexist in the long run (Fig. 3.3, Fig. 4.1).

4.2.2. Soil water scenarios

Similar to the soil water scenarios of chapter 3, I defined two different reduction functions for high water stress tolerant ($f_T(\Psi)$) and low water stress tolerant PFTs ($f_t(\Psi)$) (Table 4.1) (Herberich et al. 2017). The critical potentials Ψ_i [mm] were chosen as to maximize differences between the two opposing PFT strategies. High water stress tolerance signifies high tolerance to droughty conditions

but low tolerance to wet conditions and *vice-versa* for low water stress tolerance (Silvertown et al. 1999).

Table 4.1.
Critical potentials Ψ_i [mm] of water uptake governing the reduction function for PFTs with high water stress tolerance ($f_T(\Psi)$) and low water stress tolerance ($f_t(\Psi)$).

Ψ_i	Water stress tolerance high	Water stress tolerance low
Ψ_1	-150	-1
Ψ_2	-300	-10
Ψ_3	-10000	-2000
Ψ_{PWP}	-240000	-80000

Soil water scenarios were chosen based on the reduction functions $f(\Psi)$ to represent gradients of water stress intensities for high water stress tolerant and low water stress tolerant PFTs. Here, only cases with negligible seasonal and inter-annual soil water potential variability are considered. The growing season is thus assumed to be statistically homogenous and modelled in 15 soil water potential scenarios Ψ [mm] (Table 4.2). At soil water potentials between -300 and -2000 mm, the values of both reduction functions, $f_T(\Psi)$ for high water stress tolerance and $f_t(\Psi)$ for low water stress tolerance, equal one, i.e. no PFT experiences stress. Therefore, Ψ = -1900 mm was chosen to represent a 'base model'. Each of the 15 soil water potential scenarios was repeated ten times.

Table 4.2.
15 simulated soil water potential scenarios Ψ [mm] representing different stress intensities, i.e. f(Ψ), for high water stress tolerant (T) and low water stress tolerant (t) PFTs.

Ψ	$f_T(\Psi)$	$f_t(\Psi)$	Stress and target PFT
-30.0 E+4	**0.00**	0.00	Insufficient water availability T
-17.1 E+4	**0.30**	0.00	Insufficient water availability T
-12.5 E+4	**0.50**	0.00	Insufficient water availability T
-80.0 E+3	**0.70**	0.00	Insufficient water availability T
-56.0 E+3	0.80	**0.30**	Insufficient water availability t
-41.0 E+3	0.90	**0.50**	Insufficient water availability t
-25.4 E+3	0.93	**0.70**	Insufficient water availability t
-1.9 E+3	**1.00**	**1.00**	Sufficient water availability T & t
-255	**0.70**	1.00	Excessive water availability T
-225	**0.50**	1.00	Excessive water availability T
-195	**0.30**	1.00	Excessive water availability T
-7.3	0.00	**0.70**	Excessive water availability t
-5.5	0.00	**0.50**	Excessive water availability t
-3.7	0.00	**0.30**	Excessive water availability t
0	0.00	**0.00**	Excessive water availability t

4.2.3. Initialization

Similar to previous self-thinning simulation studies (e.g. Chu et al. 2010; Lin et al. 2014), the model is

initialized with a random spatial distribution of adult plants. Each grid cell has a 50% chance of being occupied by an adult, resulting in initial densities of approximately $10^{2.3}$ individuals/m² similar to typical densities of temperate herbaceous communities (Schippers et al. 2001). The specific individual identity is then determined randomly such that each of the 64 PFTs has the same probability to occupy the cell (Seifan et al. 2012, 2013; Sect. 2.16). Irrespective of the PFT, initial biomass of an adult plant is set to 125 mg.

4.2.4. Spatial and temporal scales

PFT richness and Shannon diversity index reached a stable state after 1500 years for all soil water potentials (Fig. 4.1). I therefore chose 2000 years as simulation time. The model landscape consisted of a grid of 800 × 800 cells with periodic boundaries to avoid boundary effects.

4.2.5. Statistical analysis

The bdt can be subdivided into different sections by means of the skewness (third moment) of the biomass distribution (Berger et al. 2002). Thereby, bdt sections during which communities underwent self-thinning are indicated by a characteristic decay of positive skewness (Berger et al. 2002). For each self-thinning section identified by that approach, regression lines were fitted to the $\log_{10}$-transformed mean biomass *w* and density *N* using a reduced major axis analysis (RMA) (sensu Warton et al. 2006). I tested with a one-sample t-test whether the slopes were equal to -3/2 and whether the slopes and intercepts of each soil water scenario differed from those of the base model.

All statistical analyses were performed in R 3.1.2.

4.3. Results

The biomass-density trajectories, bdts, could be subdivided into different sections of community structure indicated by the skewness of the biomass distribution for all soil water scenarios (Fig. 4.2, Appendix B).

When Ψ was within the range where $f_T(\Psi)$ and $f_t(\Psi)$ differed, the duration and existence of bdt sections and values of *k* and *a* of self-thinning sections were dominated by the PFT strategy for water stress tolerance with the higher f(Ψ) value, from now on called dominant reduction function $f_d(\Psi)$ (Fig. 4.3,

Appendix B). That is because independent of similar initial densities, the best competitor for soil water dominated the model landscape (see also Herberich et al. 2017).

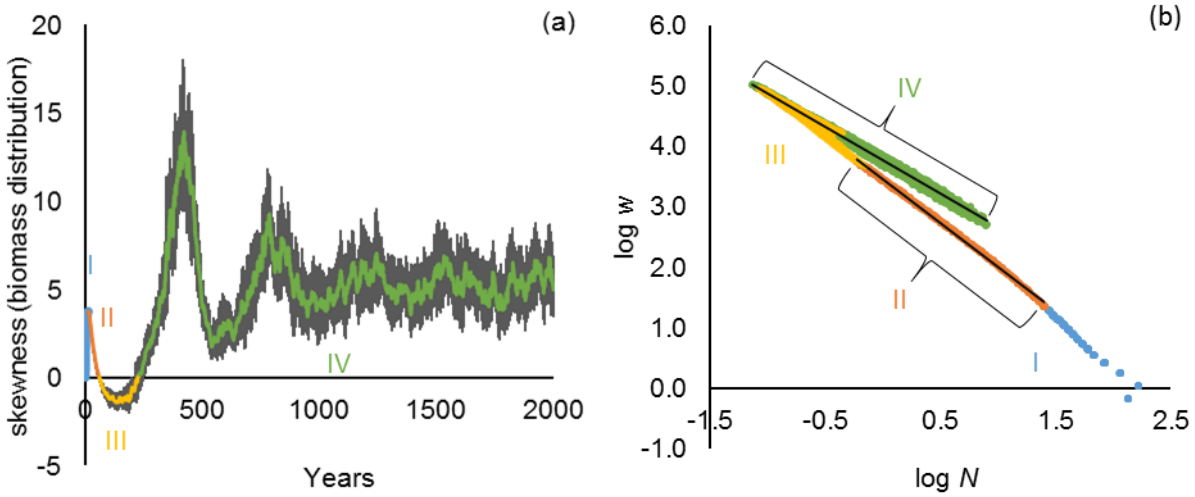

Fig. 4.2. (a) Change in mean ± SD (in grey) skewness of the biomass distribution of the base model across ten replicates over 2000 years. The two x-intercepts and the first maximum defined four distinct sections which are highlighted using a color code. (b) Entire biomass-density trajectory of the base model; i.e. relationship between the logarithm of mean plant biomass of survivors *w* (mg/m²) and the logarithm of plant density *N* (individuals/m²) for all ten replicates over 2000 years. Colors show the four sections of community structure indicated by skewness of the biomass distribution in Fig. 4.2a. Black lines represent the fitted regression lines to the self-thinning sections using a reduced major axis analysis (RMA). Fitted slopes had a mean of -1.446 (95% CI [-1.452 to -1.440]) in section II and a mean of -1.100 (95% CI [-1.104 to -1.096]) in section IV.

When the soil water potential was within the range where $f_d(\Psi) = 1.0$, i.e. the dominant PFT strategy did not experience any stress, the duration of bdt sections as well as the values of *k* and *a* of the self-thinning sections were not significantly different from the base model (Fig. 4.2, Fig. 4.3, Appendix B Fig. B8 – B11). In these scenarios, the first maximum and both x-intercepts of the skewness subdivided the bdts into four distinct sections which will be explained in the following. Section I was characterized by an increase of positive skewness and ended with the first maximum of skewness. In this section bdts showed a non-linear relation between *w* and *N*. Section II was characterized by a constant decay of positive skewness between the first maximum and the first x-intercept. In this section bdts had a linear relation between log *w* increase and log *N* decrease which corresponded to the classical self-thinning line. All regression lines between log *w* and log *N* were significant. The fitted slopes were marginally but significantly shallower than the slope predicted by the self-thinning rule (Fig. 4.3). Section III showed a negative skewness between the two x-intercepts. In this section the bdts deviated

from the linear self-thinning line because the growth rate of the initial cohort reached zero. Section IV started at the second x-intercept with a positively increasing skewness and was characterized by periodic changes in skewness. Over time, this periodicity was less pronounced and less synchronized among simulation replicates. Bdts in this section had a linear relationship between log w and log N. An increase in density and a decrease in mean biomass was accompanied by an increase in skewness and *vice-versa*. All regression lines between log *w* and log *N* were significant. The slopes were significantly shallower than -3/2 (Fig. 4.3). The transition between section III and IV corresponded approximately to the point in time of maximum yield (base model 235 ± 25 years) (Appendix C).

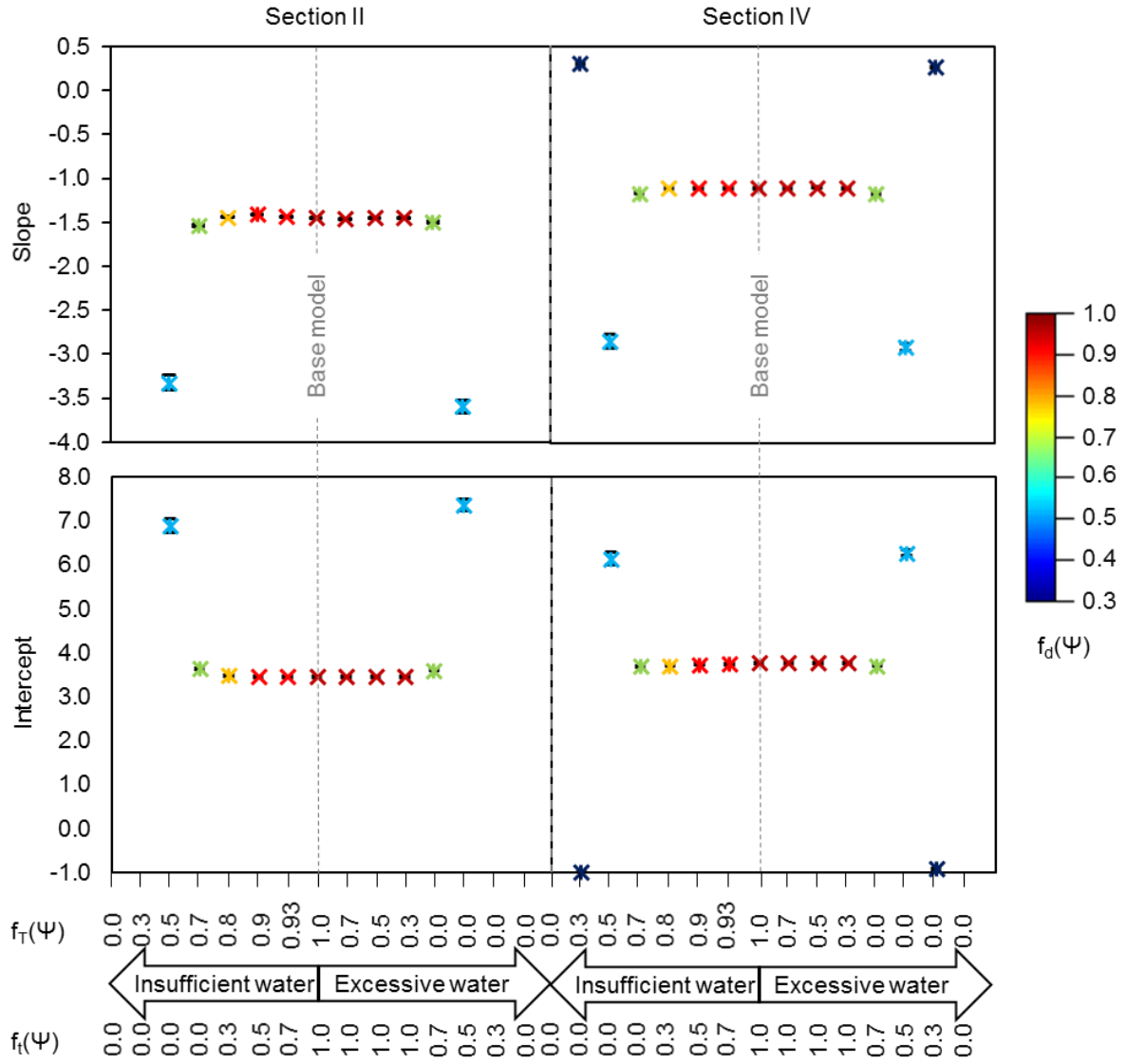

Fig. 4.3. Changes in slope and intercept of two observed self-thinning sections (section II and IV) within the entire biomass-density trajectory with increasing water stress for both excessive and insufficient water availability, i.e. decreasing $f_d(\Psi)$. P values refer to significant differences from the values of the base model: × P > 0.01. ✱P ≤ 0.001 (one-sample t-test).

With increasing water stress intensity for both excessive and insufficient water availability; i.e. decreasing $f_d(\Psi)$, the duration and presence of bdt sections as well as the values of *k* and *a* of the self-thinning sections changed in a consistent manner (Fig. 4.3, Appendix B). The duration of section I (except $f_d(\Psi) = 0.3$), II (except $f_d(\Psi) = 0.3$), and IV (except $f_d(\Psi) = 0.5$) increased with decreasing $f_d(\Psi)$. In contrast, the duration of section III decreased with decreasing $f_d(\Psi)$ and below $f_d(\Psi) < 0.9$ this section disappeared (Appendix B). The values of *k* and *a* of the self-thinning section II were not significantly different from the base model if $f_d(\Psi) > 0.8$ (common line pattern) but were significantly different from the base model if $f_d(\Psi) \leq 0.8$ (different line pattern). The different line patterns were: (1) *k* kept constant and *a* increased if $f_d(\Psi) = 0.8$, and (2) *k* increased and *a* decreased if $f_d(\Psi) < 0.8$ (Fig. 4.3). In the self-thinning section IV, the values of *k* and *a* showed different line patterns: (1) *k* decreased and *a* was constant if $1.0 > f_d(\Psi) < 0.7$, (2) both *k* and *a* decreased if $f_d(\Psi) = 0.7$, (3) *k* increased and *a* decreased if $f_d(\Psi) = 0.5$, and (4) *k* decreased and *a* increased if $f_d(\Psi) = 0.3$ (Fig. 4.3).

4.4. Discussion

My overall results indicate that there is no generally applicable biomass-density trajectory bdt. Instead the entire bdt, including the intercept and slope of the classical self-thinning line, were a function of the water stress intensity. Specifically, there is 'no slope that fits them all', i.e. a general valid self-thinning slope cannot be specified. This does not mean that previous attempts to assign such a universal value to the slope of the self-thinning line are not valid. However, the inclusion of a few important characteristics of natural populations and communities such as the occurrence of recruitment or the coexistence of multiple PFTs into my model allowed for a deeper understanding of the mechanisms underlying density-dependent processes in natural communities under abiotic stress. In the following, I first briefly highlight the similarities between my model results and that of previous studies and then discuss the deviations and their reasons.

First, I found that the bdts could be subdivided into several distinct sections of community structure which were indicated by changes in skewness of the biomass distribution over time (Berger et al. 2002). Second, consistent with previous studies, my results showed that the growth reduction in stressed communities delayed the onset of self-thinning (increase duration of section I) as well as retarded the

process itself (increase duration of section II) (Liu et al. 2006; Zhang et al. 2017). Third, under minor water stress, the entire bdt including values of *k* and *a* of self-thinning sections was only marginally (if at all) different from the one under optimal water conditions, i.e. the base model. This means in these scenarios the common line pattern emerged (Morris 2003). However, with increasing stress intensity both by excessive and insufficient soil water availability different line patterns appeared. In line with my findings, previous studies on changes in the values of *k* and *a* due to resource deficit found the common line pattern when the deficit was minor (Kays & Happer 1974; Lonsdale & Watkinson 1982; Liu et al. 2006) whereas different line patterns have been observed when the deficit was serious (Morris 2003). Interestingly, this shift in pattern of the direction and magnitude of variations in *k* and *a* is not restricted to gradients of resource availability as in previous studies, but I could show that it also holds for other types of abiotic stress, such as excessive water availability.

Remarkably, the strong deviation of the values of *k* and *a* from the base model when abiotic stress was serious were the same at both ends of the gradients, a pattern that has not been observed before. Namely, the studies that addressed abiotic stress gradients, either focused on unidirectional stress gradients, e.g. resource deficit (e.g. Morris 2003; Liu et al. 2006; Lin et al. 2014), or did not specify the stress type (Chu et al. 2010). The observed jumps in *k* and *a* can be explained with a decrease of the density range ($\log_{10}(N_{min}/N_{max})$), i.e. less change in density over time. Similar to studies on plant populations, communities with a low density range but a relatively high mean density had the lowest thinning slopes ($f_d(\Psi) = 0.5$) while communities with a low density and a relatively low mean density had the highest thinning slopes ($f_d(\Psi) = 0.3$) (Westoby 1984; Lonsdale 1990; Zhang et al. 2005). Lonsdale (1990) stated that populations with a small density range lack sufficiently long growth periods, and can thus be considered in an early stage of self-thinning. My findings suggest that growth reduction due to abiotic stress can cause a similarly small density range in plant communities with the corresponding effects for the values of the thinning slope even over long growth periods.

In addition to the prominent effects of stress, the addition of a few important processes of realistic communities into PLANTHeR caused several interesting deviances from classical bdts even when only considering the minor stressed communities. Namely, rather unexpectedly, PLANTHeR predicted that

under minor water stress the bdts included four sections in contrast to the classical three-sectioned bdts (Lonsdale 1990; Begon et al. 1991; Berger & Hildenbrandt 2003). However, the predicted four sections can be plausibly explained with the additional submodels included in PLANTHeR which are inconsistent with the basic assumptions of the self-thinning rule (recruitment, size-symmetric competition, diverse communities, etc.). Section I and II delineated the beginning and the end of the self-thinning process of the initial cohort which was indicated by a characteristic rise and decay of positive skewness (Berger et al. 2002). In section I, the bdts showed an immediate onset of mortality which contradicts classical bdts in which the first section indicates fast growth without or little mortality (Lonsdale 1990; Begon et al. 1991; Berger & Hildenbrandt 2003). This inconsistency was directly related to the fact that my model simulated different coexisting PFTs. Specifically, early mortality was mainly due to annual life form and stochasticity in perennial survival, and thus density independent. Despite this density independent mortality, the skewness in the first section of the self-thinning process increased. This size diversification originated in PFT specific differences in individual growth rates due to variance in the functional traits maximum adult growth rate and life form. Section II corresponded to the classical self-thinning section with values corresponding closely to the expected -3/2. This is striking given that several of my submodels were inconsistent with the basic assumptions of the self-thinning rule. I interpret this as the outcome of an averaging process similar to Herberich et al. (2017) who reported that under optimal water conditions, submodels with opposing effects on the thinning slope, i.e. size-symmetric competition increases whereas recruitment decreases the slope, can balance each other, and thus result in thinning slopes typically observed in natural populations (Lonsdale 1990). In section III, the bdts deviated from the linear self-thinning line because individuals of the initial cohort almost attained their maximum size. Therefore, mortality probability due to senescence increased and subsequently, increased the formation of gaps into which new individuals could recruit. Previous studies mostly ignored recruitment and thus, the gaps formed in section III could not be filled so that the bdt bends below the self-thinning line and eventually run parallel to the x-axis (Berger et al. 2002; Monserud et al. 2004). In PLANTHeR, gaps were filled via recruitment which straightened the bdt (Kohyama 1992; Zeide 1995). Section IV represented the self-thinning process of

new generations as a sequence of alternating phases of size diversification and homogenization. Over time, these phases desynchronized between simulation runs and decreased in amplitude and period. This was caused by a shift from the initial even-aged cohort to an increasingly uneven-aged mosaic of large individuals and aggregated patches of recruitment (Moeur 1997). Consequently, density-dependent mortality occurred locally within patches of recruitment resulting in a spatially desynchronized the self-thinning process (Moeur 1997). This had twofold consequences for the community structure. First, after a constant increase since initialization, the community yield reached a maximum at a point in time approximately corresponding to the transition between section III and IV. The yield then dropped and settled to a quasi-equilibrium. Interestingly, these observed yield dynamics resemble biomass dynamics in a forest landscape comprising of tree species with relatively similar longevities and sizes following a large-scale disturbance (Bormann & Likens 1979; Shugart 2014). Second, the values of the thinning slope shifted to -1.1. Theory predicts that even-aged monospecific populations thinning along slopes of -3/2 eventually reach a maximum yield which then stays constant over time. At maximum yield, any increase in mean biomass is accompanied by a corresponding decrease in plant density (Lonsdale 1990). This leads to a shift in the thinning slope to -1 (Lonsdale & Watkinson 1982; Westoby 1984). Interestingly, my results indicate that in uneven-aged diverse communities a corresponding shift in the thinning slope to -1.1 occurs at maximum yield even though their yield is not constant over time but at quasi-equilibrium.

Conclusions

Historically, the self-thinning rule was designed and validated for even-aged monospecific populations (Yoda et al. 1963; Westoby 1984). Since then, it has been suggested that the principles of the self-thinning rule also hold for uneven-aged multi-species communities (Kohyama 1992; Schulze et al. 2005; Vospernik & Sterba 2015). However, the validity of the specifics of the self-thinning rule have been studied less in this context. Nevertheless, the specifics, especially the -3/2 thinning slope, are often used for management decisions, productivity assessments, and carbon budgeting of more natural uneven-aged multi-species communities (Cao 1994; Pretzsch & Biber 2005; Stankova & Shibuya 2007; Newton 2012; Luyssaert et al. 2008). My work aims to broaden the applicability of self-thinning

study to a community level and presents a tool to simulate more natural ecosystems (functionally diverse communities).

My results indicate that there is no generally applicable biomass-density trajectory (bdt). Instead the presence and duration of all bdt sections, as well as values of the intercept and slope of the classical self-thinning line, changed across an abiotic stress gradient. Consequently, to predict variations in the biomass-density relationships across abiotic stress gradients the entire bdt should be considered rather than excluding data points or entire sections of the bdt (e.g., Liu et al. 2006; Chu et al. 2010; Lin et al. 2014). Remarkably, at both ends of the stress gradient the values of the intercept and slope differed similar in direction and intensity from benign conditions, a pattern that has not been observed before. However, also under benign conditions the representation of more natural uneven-aged multi-species communities, i.e. the simulation of recruitment and the inclusion of multiple PFTs, caused several interesting deviations of the bdt. Namely, recruitment consistently steepened the slope of thinning sections and enabled an additional fourth bdt section in contrast to classical three-sectioned bdts (Begon et al. 1991; Berger & Hildenbrandt 2003). Further, early mortality was density independent due to the coexistence of different PFTs of various sizes and longevities.

This study shows that rather than trying to pinpoint fundamentally valid values to the thinning intercept and slope, studies on the self-thinning rule should focus on mechanism and patterns behind possible variations. The fact that the values of the thinning intercept and slope, as well as other measures within the entire bdts, changed in a consistent manner across a gradient of water stress intensity from excessive to insufficient soil water availability does neither generalize nor dissipate the rule but instead increases its applicability. I thus advocate an explicit focus on predictable deviations from the classical self-thinning line in future studies in order to better understand the mechanisms behind density-dependence in natural populations and communities.

Chapter 5

Temporal storage effect explains hydrological niche segregation and coexistence in plant communities across the full range of soil water availability

Climate change will modify not only the means of climatic variables but also their variance, with more extreme events predicted by most models. However, despite the well-known importance of temporally-varying environments in determining population and community dynamics, the consequences of the changes in temporal variance of precipitation patterns on plant communities are one of the least understood aspects of global climate change. Based on theory, it has been suggested that the temporal storage effect may explain diversity and functional composition of plant communities under temporally-varying soil water conditions. However, this idea has only been tested for arid communities.

In this chapter, I used PLANTHeR to investigate the hypothesis that temporal variation in soil water will promote species coexistence via the temporal storage effect as well in humid climates. Furthermore, I investigated which plant functional traits are key in explaining coexistence in various temporal patterns of soil water availability across different spatial soil water gradients ranging from excessive to insufficient soil water availability.

My results confirmed that the temporal storage effect promotes diversity if individuals differ in their hydrological niche. Furthermore, coexistence was boosted by simulating functionally diverse communities which include various traits to buffer against the different temporal patterns of soil water availability. Specifically, at high levels of temporal variation the functional traits flood stress tolerance and life form were the most important functional traits in determining the individual's response, while surprisingly under minor temporal variation long-distance seed dispersal boosted coexistence through spatial refuges. Strikingly, the predicted plant community patterns of diversity and functional composition remained similar over different gradients of excessive and insufficient soil water

availability in space.

In general, my results suggested that the diversity and functional composition of plant communities is largely determined by the patterns of temporal soil water variability not only in highly water limited ecosystems such as in arid and semi-arid climates but even in humid climates. This highlights that classical ecological climate impact research which mainly focuses on the effects of changes in mean water availability on plant growth may fall short in capturing the main effects of climate change.

5.1. Introduction

Scientific evidence is concurrent in that the anthropogenic-induced climate change will continuously alter means of temperature and precipitation globally. In addition, climate change is expected to increase temporal climate variability as well as the occurrence of extreme climatic events such as droughts, floods or hurricanes (Allan & Soden 2008; Easterling et al. 2000). Despite this prediction, most ecological climate impact studies have focused on how changes in climatic means will affect the structure and functioning of ecological systems and communities. However, the structural and functional composition of plant communities is suggested to be more susceptible to a decrease in predictability, especially of precipitation patterns, than to a change in climatic means (Reyer et al. 2013). This lack of studies addressing the impact of increased climate variability is further surprising since plant ecological theory on how temporal environmental variation affects individual performance (Novoplansky & Goldberg 2001; Picotte et al. 2007), population or community dynamics (Pfister 1998; Chesson 2000a; Morris & Doak 2004; Snyder & Tartowski 2006; Li & Ramula 2015) is abundant and can provide testable predictions for the response of plants to increasing climate variability.

A prominent ecological theory relating temporal environmental variation to community diversity is the temporal storage effect (Chesson 1994; Chesson 2000a; Chesson 2000b). The temporal storage effect allows environmental niche differences of a set of species to promote competitive coexistence in temporally-varying environments. A basic assumption of the temporal storage effect is that the members of that set of species need to have reciprocal negative interactions. This set of species could possibly coexist depending on the characteristics and interaction of three main contributing elements: (1) species-specific responses to the environment, (2) covariance between the environment and

competition and (3) buffered population growth rate (Chesson 1994; Chesson 2000a; Chesson 2000b). Buffered population growth may result from various plant traits, such as traits related to species' growth rate strategies or longevity, which decrease the sensitivity of specific life-history stages to temporal environmental variation (Chesson 2000a; Májeková et al. 2014). Functional traits can be a direct link between species response and environmental factors (Cornelissen et al. 2003). These traits relate environmental factors to individual fitness via their effects on growth, reproduction, and survival (Laughlin & Laughlin 2013).

Most interesting in the context of climate change is the suggestion that the temporal storage effect may promote plant species coexistence under temporally-varying soil water availabilities (Silvertown et al. 2015). Soil water has a dual effect on plant communities meaning that soil water is a key resource for plants while it simultaneously acts as a disturbance agent (Silvertown et al. 2015; Grime 1977). Furthermore, water is associated with other soil conditions that regulate oxygen concentration and nutrient availability (Mustroph et al. 2016). Hence, both excessive and insufficient soil water availability hamper plant performance and may consequently determine the coexistence of plant species (Feddes et al. 1978; Moeslund et al. 2013; Herberich et al. 2017). Accordingly, it has been shown that the functional composition, diversity and distribution of plant communities is highly sensitive to changes in soil water availability (Silvertown et al. 2015; Herberich et al. 2017). Therefore, the relationship between soil water and plant community dynamics should be key to studying vegetation response to climate change.

The influence of soil water on the composition and distribution of local vegetation is especially evident in the increasing number of field observations related to the so-called hydrological niche segregation (Silvertown et al. 2015). Plant species can be defined by species-specific ranges of soil water conditions, i.e. their hydrological niche, such that the species' presence and location in the landscape can be described using functions of soil water (Silvertown et al. 1999).

However, the mere description of distribution patterns is not sufficient to predict species' response to changes in mean and variance of soil water; one also needs to investigate the actual consequences of hydrological niche segregation for plant communities (Silvertown et al. 2015). Few studies showed that

hydrological niche segregation is responsible for coexistence (e.g. Adler et al. 2006; Verhulst et al. 2008; Herberich et al. 2017; for a review see Silvertown et al. 2015), whereas a larger number showed that hydrological niche segregation influences the community assembly (Beatty 1987, Reynolds et al. 1997).

However, little is known about the mechanisms linking hydrological niche segregation and coexistence (Silvertown et al. 2015). Soil water is an ideal environmental factor to allow for the temporal storage effect because it is highly variable in both time and space on a fine scale, so that hydrologically heterogeneous habitats such as wet heathlands or temporarily flooded meadows may even exhibit opposing types of water stress in the course of a growing season (Oddershede et al. 2015). Still, this insufficient state of knowledge also holds for the temporal storage effect; i.e. the few studies which did indicate the temporal storage effect as a possible coexistence mechanism underlying hydrological niche segregation were confined to arid climates (Adler et al. 2006; Cheng et al. 2006; Verhulst et al. 2008; Angert et al. 2009; Kowaljow & Fernandez 2011; for a review see Silvertown et al. 2015). This is regrettable because understanding coexistence mechanisms and their relationship to temporal climatic variation will be key to predicting vegetation response to climate change.

It is a challenge to predict the functional traits that will be important in determining species response to temporally-varying soil water conditions, i.e. the traits that might buffer the population growth rate against temporally-varying soil water. One reason for this is that the predictive power of a given functional trait for species response patterns can change across different environmental conditions (de Bello et al. 2005). For example, Herberich et al. (2017) showed that functional trait trade-offs associated to coexistence and hydrological niche segregation changed in a unimodal fashion along a gradient of spatially and temporally homogenous soil water. Thus, any study to investigate the temporal storage effect as a possible coexistence mechanism underlying hydrological niche segregation should not include any *a priori* defined trade-off and investigate whether the predicted traits are consistent across different soil water conditions.

In this chapter, I used the generic individual-based model PLANTHeR (PLAnt fuNctional Traits Hydrological Regimes) which describes plant functional trait abundance as a function solely of the soil

water potentials and individual behavior (Herberich et al. 2017). PLANTHeR includes general, composite functional traits from the whole-plant economic spectrum (Reich 2014) which can represent several alternative functional traits depending on the specific ecosystem. An important innovation of the model is that it does not assume any *a priori* trade-offs and therefore is naïve with respect to the selection of functional traits. Consequently, PLANTHeR allows to test whether functional traits remain consistent as determinants of temporal response patterns under different soil water conditions.

Specifically, I ask:

1) Do temporally-varying soil water potentials promote coexistence via the temporal storage effect in humid climates?
2) Which plant functional traits are key to explaining the response of plant individuals to temporal variation of soil water potentials?
3) Are the plant functional traits which predict the plant individual's response to temporal variation stable over different spatial gradients of excessive and insufficient soil water availability?

5.2. Materials and methods

PLANTHeR is a generic spatially explicit individual-based model designed to evaluate the relative importance of soil water for the functional and structural composition of plant communities. Thus, as opposed to existing state variable models testing the storage effect (e.g. Chesson 1985; Chesson 2000b), PLANTHeR includes variability, local interactions (immediate competition), and complete life-cycles as well as an explicit representation of space. In spite of this, PLANTHeR is in general consistent with the basic assumptions of the temporal storage effect. PLANTHeR simulates two kinds of mutually negative interactions between individuals: (1) seedling competition for vacant positions (Chapter 2 Sect. 2.17.3) and (2) competition for soil water (Chapter 2 Sect. 2.17.7). Both competitive interactions are explicit functions of the environment, i.e. the environment and competition covary. Depending on the specific parametrization of the plant functional type (PFT), the simulated populations can buffer their population growth against unfavorable soil water conditions via seed dormancy, adult growth, adult longevity and/or spatial refuges.

A complete model description of PLANTHeR following the ODD (Overview, Design concepts, Details, (Grimm et al. 2006, 2010)) protocol can found in chapter 2. Here, I only give the most important points regarding the setup of the simulation experiments used in this chapter: 'Functional traits and PFT parameterization', 'Soil water scenarios' and 'Spatial and temporal scales'.

5.2.1. Functional traits and PFT parameterization

PLANTHeR models diverse communities comprising up to 64 PFTs. These PFTs result from the full factorial combinations of six functional traits (Seifan et al. 2012, 2013; Herberich et al. 2017).

Differences between species strategies to buffer their population growth rate against temporal variation in their environment have been associated with a functional trade-off, the so-called whole plant economic spectrum (Reich 2014). The whole plant-economic spectrum includes relevant key functional traits known to be related to species life history, reproduction and growth rate strategies (Reich 2014). I selected general, composite functional traits from the whole plant economic spectrum to represent various possible strategies to buffer against temporal variation in soil water potentials. In the previous chapters, I already showed that these plant functional traits and their specific combination (PFT) were key to explaining the response of plant individuals to different spatiotemporal homogeneous soil water scenarios.

Two traits were related to the individual's competitive ability (seedling competitive ability and maximum adult growth rate). Two traits represented colonization abilities in time and space (seed dormancy and seed dispersal distance) and two traits affected the individual's longevity (life form and flood stress tolerance). Each functional trait is represented by two opposing strategies: perennial(P)/annual(a) life form, low(T)/high(t) flood stress tolerance, long(D)/short(d) seed dispersal distance, long-(S)/short-term(s) seed dormancy, strong(C)/weak(c) seedling competitive ability, and high(G)/low(g) maximum adult growth rate (Seifan et al. 2012, 2013). Except for the functional trait 'life form' and 'flood stress tolerance', the functional trait strategy indicated by the capital letter stands for 80% of the maximum trait value whereas the strategy indicated by the lowercase letter stands for 20%, respectively. Seed dormancy, seedling competitive ability, and maximum adult growth rate are probabilistic traits with 100% being the maximum. Maximum seed dispersal distance is 20 m (Nathan

& Muller-Landau 2000). The exact functional trait values are drawn for each individual separately from a normal distribution with the PFT strategy as mean and 10% of the maximum trait value as standard-deviation.

Differences between PFT strategies for low(T)/high(t) flood stress tolerance are simulated by means of a reduction function f(Ψ), a dimensionless prescribed function of the soil water potential Ψ [cm] based on four critical values Ψ_1 - Ψ_{PWP} (Feddes et al. 1978). The critical potentials Ψ_i [cm] of both flood stress tolerance strategies were chosen based on field measurements in mixed riparian vegetation of humid climates (De Silva et al. 2008; Lowry & Loheide 2010; Loheide & Booth 2011) (Table 5.1). Thereby, low flood stress tolerance represents riparian vegetation of humid subtropical climates (Köppen Cfa) with a higher tolerance to dry conditions but lower tolerance to wet conditions and *vice-versa* for high flood stress tolerance which represents riparian vegetation of humid continental climates (Köppen Dwa) (De Silva et al. 2008; Lowry & Loheide 2010; Loheide & Booth 2011).

Table 5.1
Critical potentials Ψ_i [cm] of water uptake governing the reduction function f(Ψ) for plant functional types with low flood stress tolerance (T) and high flood stress tolerance (t).

Ψ_i	Low flood stress tolerance (T)	High flood stress tolerance (t)
Ψ_1	-10	0
Ψ_2	-25	-3
Ψ_3	-2000	-300
Ψ_{PWP}	-8000	-2000

5.2.2. Soil water scenarios

Soil water scenarios were designed as two soil water potential gradients in space perturbed by spatially homogenous extreme events with three perturbation frequencies 0.5 (approx. biennial return interval), 0.1 (approx. 10 year return interval), or 0.01 (approx. 100 year return interval) (Fig. 5.1). I additionally simulated control scenarios for each spatial gradient without any perturbation.

The specific soil water potentials Ψ of each spatial gradient were chosen based on the reduction functions of low($f_T(\Psi)$)/high($f_t(\Psi)$) flood stress tolerant PFTs to represent gradients of excessive and insufficient soil water availability (Fig. 5.1; Table 5.2). To implement the spatial gradients, I divided the model landscape into three subplots: (i) Ψ was within the range where f(Ψ) of the target PFT strategy

equals zero, i.e. maximum water stress intensity for the target, (ii) Ψ was within the range where f(Ψ) of the target PFT strategy equals one, i.e. no water stress for the target, and (iii) Ψ ranged linearly from subplot (i) to subplot (ii) creating a gradient of water stress intensity for the target PFT strategy. By randomly changing length of subplots (i) and (ii) between years, using a normal distribution (10 m ± 5 %), the creation of a fixed border within the spatial gradients was prevented, while the highly predictable nature of the spatial gradient was kept.

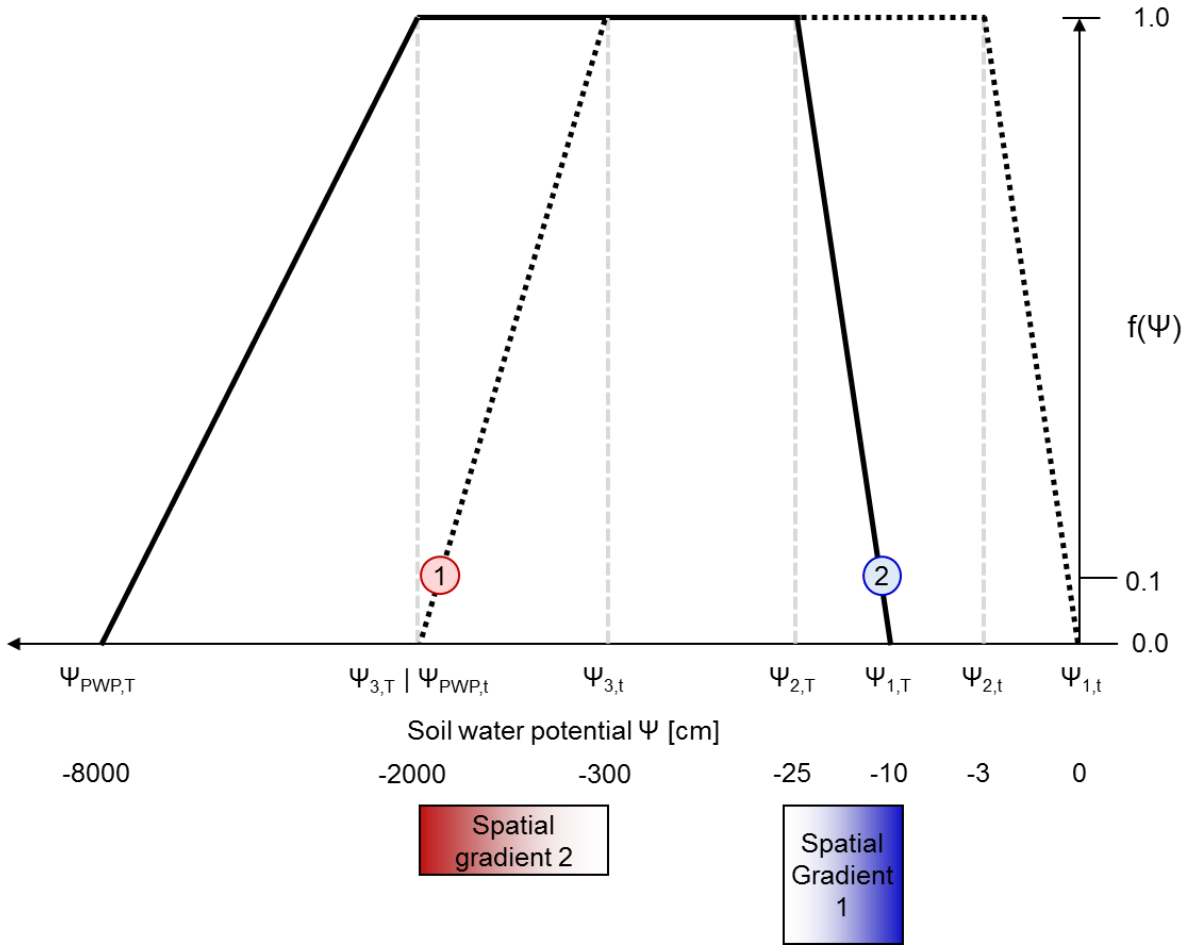

Fig. 5.1. Choice of soil water potentials Ψ [cm] based on the reduction function low flood stress tolerant PFTs ($f_T(\Psi)$; solid black line) and high flood stress tolerant PFTs ($f_t(\Psi)$; dotted black line) to represent two spatial gradients of water stress intensities. Circled numbers indicate the soil water potential during a spatially homogenous extreme event which perturbs the associated spatial gradient with frequency 0.5, 0.1, or 0.01.

I designed the extreme events so that one of the flood stress tolerance strategies was perturbed to arbitrarily low density (Chesson 2000b). Note that sensu Chesson (2000b), the perturbed strategy will be termed invader and is denoted by the label *i*. The other strategy, which was not perturbed to low

densities, is called resident (label *r*). Note that *r* is the disturbance indicator. The specific Ψ in case of a perturbation was set so that $f_i(\Psi) = 0.1$ and $f_r(\Psi) = 1.0$ (Fig. 5.1; Table 5.2).

Each of the 8 soil water scenarios was repeated ten times.

Table 5.2.
Design of eight soil water scenarios based on two soil water potential gradients Ψ [cm] in space; i.e. gradients of water stress intensities for low flood stress tolerant PFTs ($f_T(\Psi)$) and high flood stress tolerant PFTs ($f_t(\Psi)$ for both excessive and insufficient water availability. Spatial gradients are perturbed by extreme events, designed as spatially homogenous soil water potentials, with three perturbation frequencies 0.5, 0.1, or 0.01.

Spatial gradient	1	2
Stress	excessive water	insufficient water
Target	T	t
$f_T(\Psi)$	0 to 1	1
$f_t(\Psi)$	1	0 to 1
Ψ	-10 to -25	-2000 to -300
Extreme event	1	2
Stress	insufficient water	excessive water
Invader	t	T
$f(\Psi)_T$	1	0.1
$f(\Psi)_t$	0.1	1
Ψ	-1830	-11.5

5.2.3. Spatial and temporal scales

The goal of this study was to explain the relationship between functional traits, trade-offs and soil water potentials. To ensure that the resulting functional traits, PFTs and trait correlations were not just a representation of a single moment in time, I compared PFT richness and Shannon diversity index every 25 years along the simulation runs (Seifan et al. 2012) (Fig. 5.2). PFT richness and Shannon diversity index were generally consistent in their trend in time, however, these two measures did not stabilize at the exact point in time for all soil water potentials. PFT richness stabilized latest after 500 years, i.e. no significant differences ($p > 0.05$) in PFT richness for all soil water potentials after 500 years. On the other hand, the values of the Shannon diversity index stabilized latest after 375 years for all soil water potentials. I therefore chose 600 years as the simulation time.

The model landscape was designed as a transect of a grid of 200 × 2000 cells with periodic boundaries to avoid boundary effects.

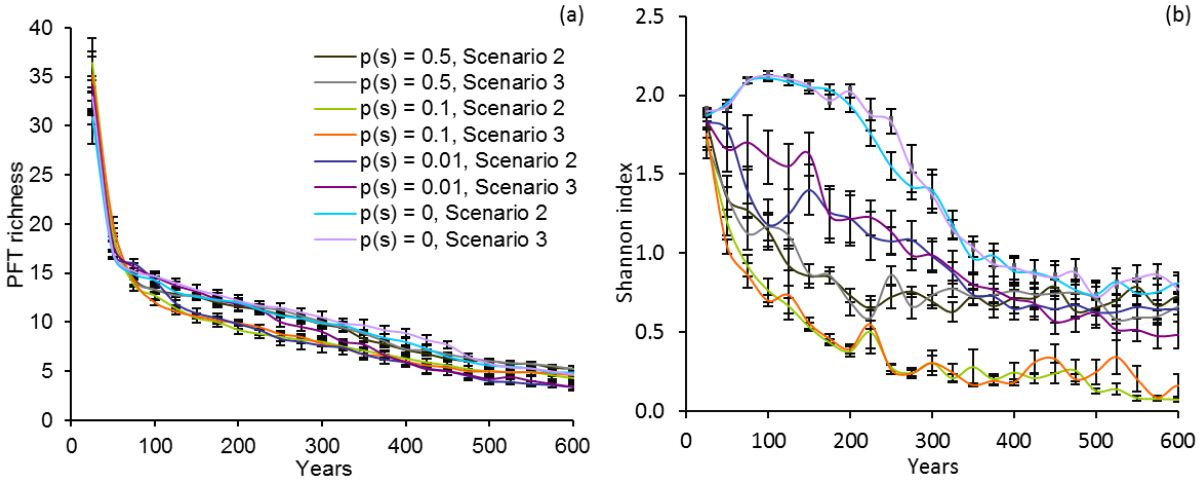

Fig. 5.2. Change in mean ± SD PFT richness (a) and Shannon diversity index (b) of ten repetitions over time for eight soil water scenarios. Soil water scenarios were designed as two spatial gradients of water stress intensities perturbed by spatially homogenous extreme events with four different perturbation frequencies p(s).

5.2.4. Statistical analysis

To quantify coexistence between low and high flood stress tolerant PFTs, I calculated the mean rate of increase for the respective resident population, mean ln λ_r(t), and invader population, mean ln λ_i(t), over the last 100 years of the simulation time (Chesson 2000b):

$$N_x(t+1) = \lambda_x(t)\ N_x(t)$$

where N_x is the number of individuals in population x, and λ_x is the rate of increase of population x. According to a classical invasibility analysis the coexistence is stable if both mean ln λ_r(t) and mean ln λ_i(t) are higher than one (Chesson 2000b). Thus, I tested with a two-sided one-sample t-test whether mean ln λ_r(t) and/or mean ln λ_i(t) were equal to one. Furthermore, I evaluated spatial coexistence by comparing the invader and resident populations' yield which is allometrically related to the ZOI area covered by the respective populations.

5.3. Results

For both soil water potential gradients in space, the mean rate of increase of the invader population, mean ln λ_i(t), and of the resident population, mean ln λ_r(t), increased with increasing perturbation frequency (Fig. 5.3). At perturbation frequency ≥ 0.1 both mean ln λ_i(t) and mean ln λ_r(t) were significantly higher than one.

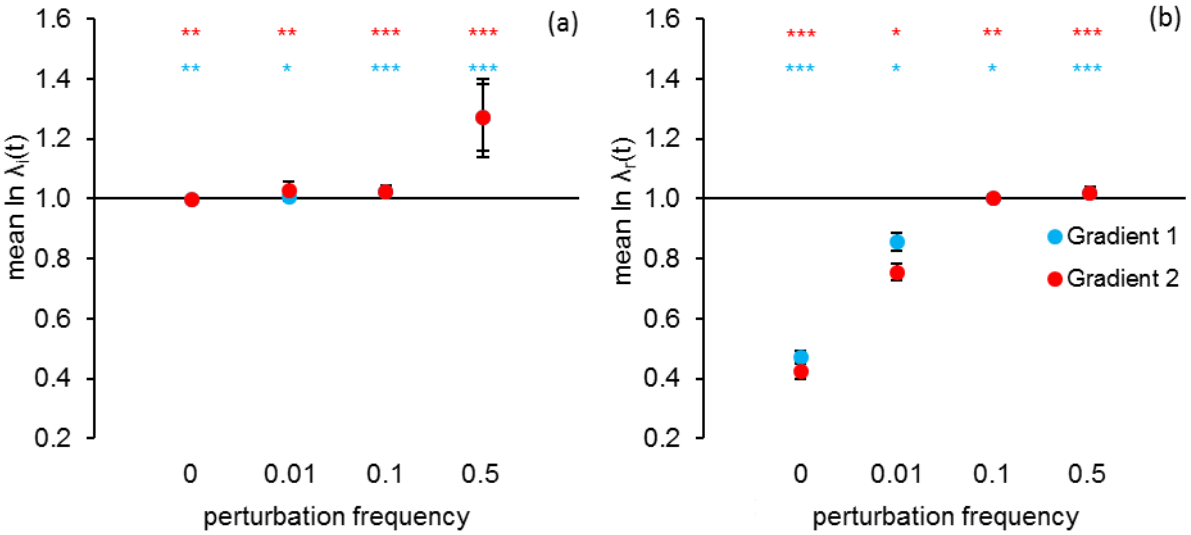

Fig. 5.3. Mean ± SE rate of increase of (a) the invader, mean ln λ_i(t), and (b) the resident population, mean ln λ_r(t), across ten repetitions for two soil water potential gradients in space as a response to four different perturbation frequencies. Mean ln λ(t) of each single repetition was averaged over the last 100 years of simulation time. Stars indicate whether the mean rates of increase were significantly different from one (two-sided one-sample t-test). *** $p < 0.005$, ** $p < 0.05$, * $p < 0.5$.

Likewise for both spatial gradients, the yield of resident population increased while the yield of the invader population decreased with increasing perturbation frequency (Fig. 5.4).

In all eight soil water scenarios after 600 years, individuals with a short-term seed dormancy, strong seedling competitive ability, and high maximum adult growth rate dominated the model landscape (Fig. 5.5). On the other hand, the relative abundance of the functional traits seed dispersal distance, life form and flood stress tolerance varied depending on perturbation frequency in a similar fashion for both spatial gradients. In soil water scenarios without perturbation, i.e. control scenarios, perennials with a short distance dispersal and with the perturbed flood stress tolerance strategy (invaders) dominated the model landscape. As a response to minor temporal variation of soil water potentials (perturbation frequency 0.01) the relative abundance of long distance dispersal increased (Fig. 5.5c, red arrow), while the relative abundance of perennial life form and invaders stayed constant.

Increasing the temporal variation to perturbation frequency 0.5 led to an increase of the relative abundance of annual life form and residents (Fig. 5.5 a & b, red arrows), while the relative abundance of long distance dispersal decreased.

All observed changes in the relative abundance of functional traits were consistently similar across both soil water potential gradients in space, i.e. excessive and insufficient soil water availability yielded the same response patterns in functional trait importance and abundance for explaining the temporal variation of PFT density.

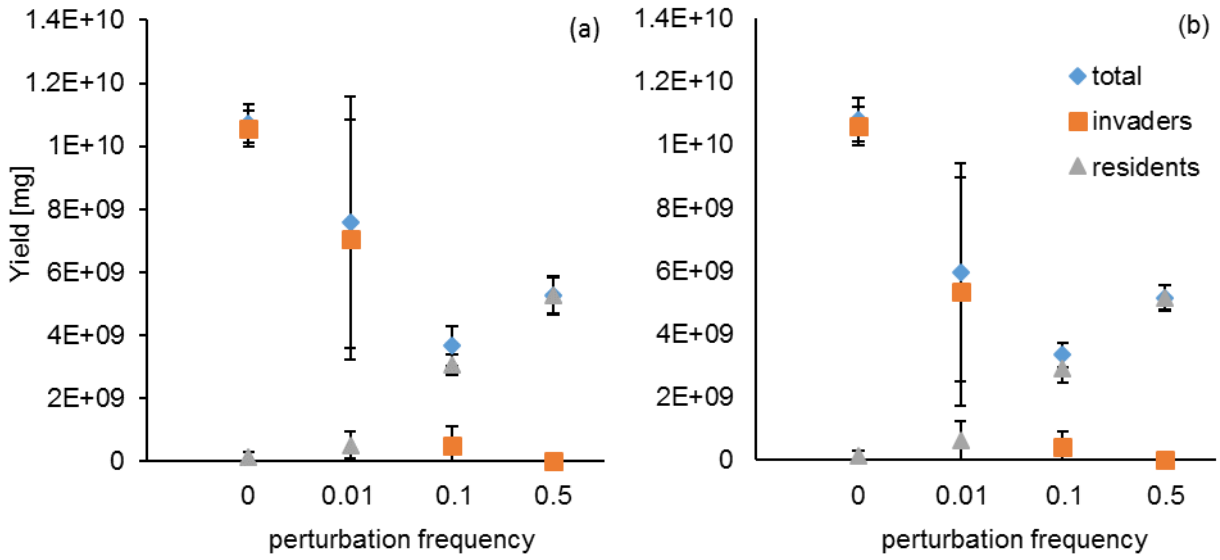

Fig. 5.4. Mean ± SD yield [mg] of the total community, the invader, and the resident population across ten repetitions as a response to four different perturbation frequencies for two soil water potential gradients in space. (a) excessive soil water availability (spatial gradient 1). (b) insufficient soil water availability (spatial gradient 2).

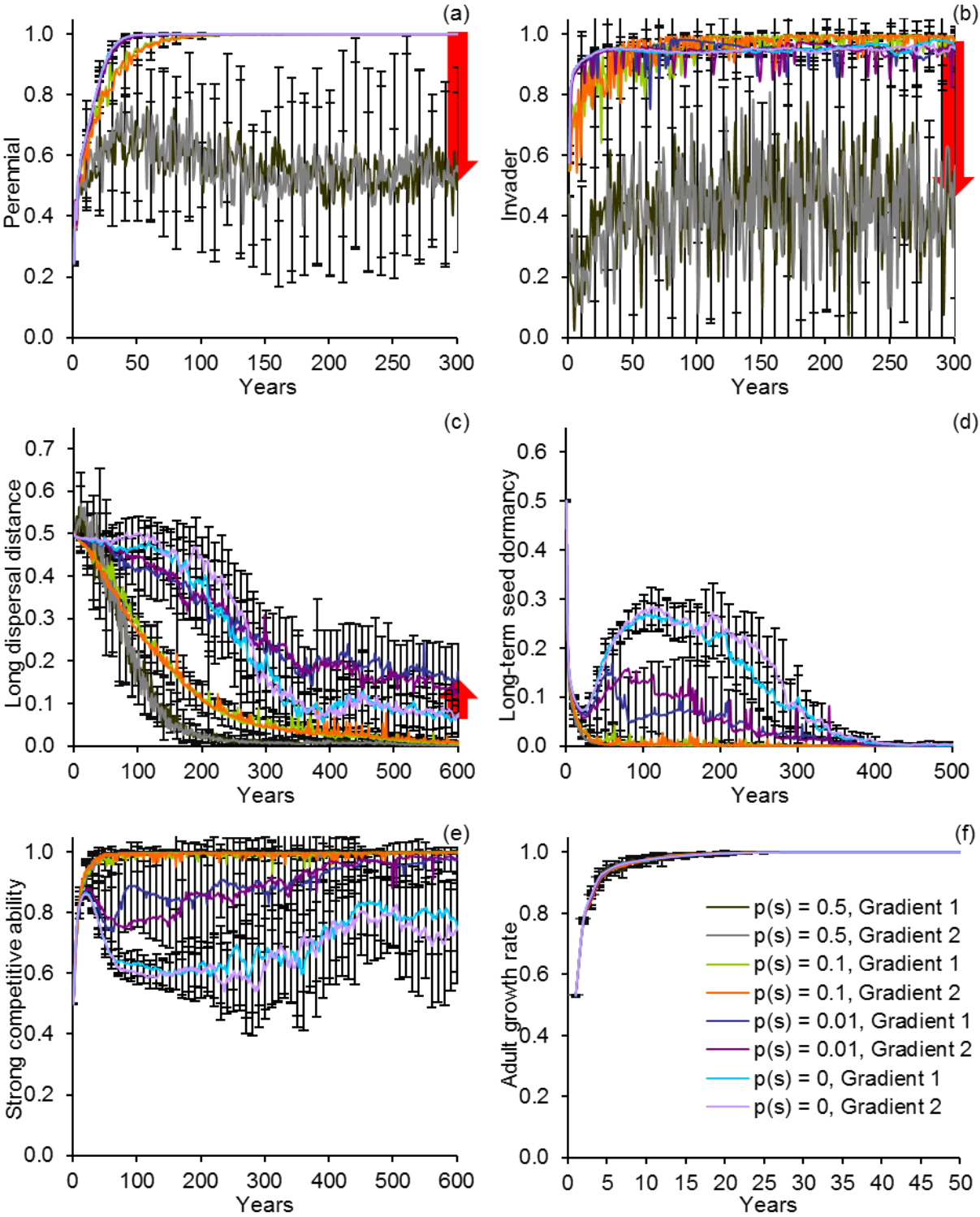

Fig. 5.5. Change in mean ± SD relative abundance of the capital letter PFT strategy (fraction of PFT strategy among all coexisting individuals) over time across eight soil water scenarios. Soil water scenarios were designed as two soil water potential gradients in space to represent gradients of both excessive (spatial gradient 1) and insufficient soil water availability (spatial gradient 2). Gradients were perturbed by spatially homogenous extreme events with four different perturbation frequencies p(s). (a) Fraction of perennials. (b) Fraction of the perturbed flood stress tolerance strategy (invader), i.e. in scenarios with gradient 1 fraction of high flood stress tolerance and in scenarios with gradient 2 fraction of low flood stress tolerance. (c) Fraction of long maximum dispersal distance. (d) Fraction of long-term seed dormancy. (e) Fraction of strong competitive ability. (f) Fraction of high maximum adult growth rate.

5.4. Discussion

My overall results highlight temporal variation of soil water as a main driver of coexistence and functional composition in plant communities. Strikingly, the following discussed patterns of coexistence and of the functional traits, which determined the response to temporally-varying soil water conditions, remained stable over different soil water gradients in space, i.e. excessive and insufficient soil water availability.

The simulation results show that high and low flood stress tolerant PFTs, i.e. conditional on the soil water scenario residents and invaders, could coexist over a wide range of temporal variation of the soil water. Following a classical invasibility analysis there was a stable coexistence at perturbation frequencies ≥ 0.1, i.e. the mean rate of increase over time of both residents and invaders were higher than one (Chesson 2000b). Thus, temporal variation of soil water promoted stable coexistence between high and low flood stress tolerant PFTs if the extreme event occurred at least every ten years. These results are the first to show that hydrological niche differences in plant communities can promote stable coexistence in habitats with temporally-varying soil water via the temporal storage effect. Thus, I could confirm the suggestion by Silvertown et al. (2015) that the temporal storage effect can act as a coexistence mechanisms underlying hydrological niche segregation.

Strikingly, against the assumptions of an invasibility analysis (and classical population growth models (Akçakaya et al. 1999)) even when mean ln λ_r(t) was significantly less than 1.0, the resident population did not become extinct. Instead after 600 years, residents were still present at very low densities. This inconsistency was a direct results my individual-based modelling approach which allowed for the inclusion of variability and local interactions of individuals. Consequently, the actual individual behavior showed contingency leading to demographic stochasticity, and thus enabling coexistence. On the contrary, existing state-variable models testing the storage effect, e.g. the lottery model and derivatives (Chesson 1985; Chesson 2000b), are based on the mean rate of increase over time. This rate does not include intraspecific variation but defines the mean for an individual experiencing certain environmental conditions (Chesson 2000b).

Another component in PLANTHeR which boosted the coexistence of invaders and residents are the numerous functional traits which could possibly buffer the population growth rates. These traits are not restricted by *a priori* defined trade-offs to specific combinations so that the emerging trait combinations reflected the best adaptation to the specific temporal pattern of soil water conditions. With regards to the anthropogenic climate change, this result implies that functionally diverse communities may have the potential to adapt to an increased frequency of extreme events (Tielbörger et al. 2014). However, my results imply that an increased frequency of extreme events may lead to a shift in abundance of functional traits. Specifically, my results show that the functional traits seed dispersal distance, life form and flood stress tolerance were key to explaining the response of plant individuals to temporal variation of soil water potentials. Intriguingly, irrespective of the soil water scenario, individuals with a short-term seed dormancy, strong competitive ability, and high maximum adult growth rate dominated the model landscape, i.e. these functional traits were irrelevant to ensure temporal stability of the population growth rate over time. This is in contrast to previous findings which suggest that differences in species' growth rates and competitive ability may reflect different ability of species' populations to buffer against unfavorable conditions (Chesson 2000a; Majeková et al. 2014; Reich 2014). Furthermore, seed dormancy is the classical bet-hedging mechanism to buffer against detrimental effects of temporal soil water variation on population growth (Harel et al. 2011; Tielbörger et al. 2014). However, the need to buffer the population growth rate via the functional traits seed dormancy, competitive ability, and adult growth might have been reduced, since the differentiation of the functional traits seed dispersal distance, life form, and flood stress tolerance was sufficient to generate coexistence.

Specifically, with an increase in perturbation frequency, the simulation results predict a general sequence of the relative density of the functional traits seed dispersal distance, followed by flood stress tolerance and life form. As a response to minor temporal variation of soil water potentials the abundance of individuals with long distance dispersal increased. At higher perturbation frequencies, long-distance dispersal was not sufficient to compensate the impediment of individual plant performances, so that PFTs with the resident water stress strategy (disturbance indicators) and annual

life form emerged (McIntyre et al. 1995; Schippers et al. 2001; Seifan et al. 2012). Similar to my results, Schippers et al. (2001) found a sequence of dominance of non-dormant perennials, dormant perennial, non-dormant annuals and dormant annuals with an increase in spatial disturbance intensity, i.e. proportion of random cells affected every year. Both seed dormancy and seed dispersal distance are bet-hedging mechanisms which promote colonization abilities in time and space (Milton et al. 1997; Holmes & Wilson 1998). Therefore, these two traits are considered as alternative traits (Venable & Brown 1988). I interpret the emergence of long distance dispersal as a response to minor temporal variation, rather than long-term seed dormancy, to be a side effect of the specific definition soil water scenarios, i.e. a continuous soil water gradient in space perturbed by a spatially homogenous extreme event. Due to the spatial predictability of the soil water gradient, the probability for new gap creation differed depending on the location within the model landscape. Since the chances to find available colonization microsites changed continuously with the distance from the mother plant, surviving plants required investment in seed dispersal in space, which translated into an increase in seed dispersal distances (Svensson et al. 2009; Seifan et al. 2012). In line with my results, previous studies showed that when the environment is spatially variable buffering may occur by dispersal between localities in different environmental states (Chesson 2000a), i.e. traits associated with spatial distribution can boost the temporal storage effect through spatial refuges (Kortessis & Chesson 2014). Specifically, temporal environmental variation in space can lead to coexistence when individuals are concentrated in locations where they are strongly sensitive to the environment and weakly sensitive to competition (Kortessis & Chesson 2014). My results suggest that increasing seed dispersal distance, a functional trait which links spatial environmental variation to competitive interactions in time, might be sufficient to compensate the detrimental effects of minor temporal variation of a spatial soil water gradient on the population growth rate and thus, can ensure coexistence. I expect that soil water scenarios in which a spatially heterogeneous, unpredictable model landscape is perturbed by a spatially heterogeneous, unpredictable extreme event, i.e. similar to the disturbance scenarios of Schippers et al. (2001), would select for PFTs with long-term seed dormancy. However, the interpretation and

applicability of such soil water scenarios is questionable since in natural ecosystems soil water tends to change gradually in space (Silvertown et al. 2015).

In line with classical disturbance theory, the community yield decreased with increasing perturbation frequency (Grime 1977). Unexpectedly, the simulation results at intermediate frequency (0.1) did not follow this general trend, instead these simulations showed the lowest overall yield. Furthermore, these simulations were not in line with the general sequence of the relative density of functional traits and had the lowest Shannon diversity. Therefore, I suggest that this frequency might indicate a tipping point where the frequency was too high to ensure coexistence via bet-hedging mechanisms but too low to prevent the monopolization of establishment sites by perennials, i.e. too low to allow for the emergence of annual life form. The low yield could possibly be an effect of niche complementarity (Tilman et al. 2006; Tilman et al. 2014). The complementarity hypothesis states that biomass production may be higher in diverse communities since the various constituent species may use resources in complementary ways and thus, utilize a greater proportion of resources (Tilman et al. 2006; Tilman et al. 2014). However, to confirm the complementarity hypothesis further simulations (e.g. based on single-PFT communities) would be required to properly test for overyielding and avoid sampling effects.

Most interestingly in the context of climate change is that the above described patterns of coexistence and functional traits were similar across different spatial gradients of excessive and insufficient soil water availability. This resulted from the dual effect of soil water on plant performances and is in line with previous studies on gradients of spatiotemporal homogenous soil water availability which showed consistent changes in the function and structure of plant community as a response to excessive and insufficient soil water availability (chapter 3; chapter 4). This finding has twofold implications. First, not only in highly water limited ecosystems such as in arid and semi-arid climates (Snyder & Tartowski 2006) but even in humid climates, temporal variation in soil water availability is an important factor influencing the diversity and functional composition of plant communities. Second, the diversity and functional composition of plant communities were determined by the pattern of temporal variability of soil water and the PFT-specific water stress intensity. This finding supports plant ecological theory

on the importance of temporal environmental variation on individual performance (Novoplansky & Goldberg 2001; Picotte et al. 2007), population and community dynamics (Pfister 1998; Chesson 2000a; Morris & Doak 2004; Snyder & Tartowski 2006; Li & Ramula 2015). However, this is in contrast to the massive body of ecological climate impact studies which has primarily focused on how changes in climatic means affect plant communities.

Conclusions

Climate change models predict for many regions a change in both the mean and temporal variability of precipitation with an increasing number of extreme events, and corresponding consequences for plant soil water availability (Easterling et al. 2000). In this chapter, I confirmed previous suggestions that temporal variability of soil water can promote diversity, i.e. lead to coexistence, due to the temporal storage effect in humid climates if individuals differ in their hydrological niche. Specifically, coexistence over a wide range of temporal-varying soil water conditions was ensured by simulating an initial functionally diverse community which could buffer its population growth rate via various functional traits. In line with previous studies, high frequencies of temporal perturbation by an extreme event selected for annual plants and the disturbance indicator (residents). However, rather unexpectedly at minor frequencies long distance dispersal ensured coexistence of PFTs through spatial refuges instead of seed dormancy which is considered as the classical bet-hedging mechanism to buffer against temporally-varying soil water conditions (Harel et al. 2011; Tielbörger et al. 2014). This was a direct result of the simulation scenarios designed as soil water gradients in space, similar to natural ecosystems. Another surprising result was the emergence of a tipping point community indicated by the lowest productivity and Shannon diversity at intermediate levels of temporal variability of soil water. These results facilitate important research questions: First, can the temporal storage effect related to hydrological niche segregation promote diversity sufficiently to allow for niche complementary effects? Second, are the observed patterns of coexistence and functional composition stable over further perturbation frequencies with special regards to the tipping point scenario?

In general, given that the frequency and intensity of extreme events is predicted to increase beyond the range of natural variability (Field et al. 2014), this chapter highlights the urgent need of further studies investigating the effects of changes in climatic temporal variation.

Chapter 6

Conclusions

Water is of fundamental importance for most plant individual performances and, even more interesting in the scope of climate change, crucial in determining distribution and abundance of plant species in time and space (Feddes et al. 1978; Moeslund et al. 2013; Silvertown et al. 2015). The influence of water on the distribution and composition of plant communities is especially evident in the increasing number of field observations related to hydrological niche segregation (Silvertown et al. 2015). However, as outlined in chapter 1, the mechanisms and consequences underlying hydrological niche segregation are still uncertain. Some of this uncertainty has been resolved in this dissertation by answering the research questions put forward in chapter 1.

First, I studied the specific plant characteristics, i.e. functional traits, which were key in explaining the distribution patterns of plant functional types segregating along a gradient of excessive to insufficient soil water (chapter 3). In line with most theories on niche evolution (e.g., Tilman 1994; Chesson 2000; Körner & Jeltsch 2008), the classical competition-colonization trade-off played a major role in determining functional diversity and niche segregation. However, rather unexpectedly, the strength of this (and other) trait correlation changed consistently in a unimodal fashion along the soil water gradient. This unimodal change resulted from the dual effect of soil water on plant performances, i.e. both excessive and insufficient water availability impede individual plant performances (Feddes et al. 1978; Moeslund et al. 2013). Particularly noteworthy is that the absence of universal trade-offs resulted directly from my trade-off unrestricted modelling approach. This highlights the urgent need for more trade-off unrestricted studies to test whether similar conclusions can be generated with different environmental factors.

Second, I investigated the consequences for the biomass-density relationship of plant communities subjected to this gradient of excessive to insufficient soil water (chapter 4). Interestingly, the entire biomass-density trajectory, including the values of the slope of the classical self-thinning line, changed

in a consistent manner across the soil water gradient. Specifically, in line with previous studies on gradients of resource availability (Liu et al. 2006), the growth reduction in seriously stressed communities decreased the potential for density-dependent mortality. Consequently, the thinning slope in communities with high density decreased while the thinning slope in communities with low density increased (Westoby 1984; Lonsdale 1990; Zhang et al. 2005). Remarkably, these observed differences in the values of the thinning slope were similar in direction and intensity at both ends of the stress gradient, a pattern that has not been observed before. Classical three-sectioned biomass-density trajectories were originally validated for even-aged, monospecific populations (Begon et al. 1991; Berger & Hildenbrandt 2003). The simulation of more natural uneven-aged multi-species communities caused several interesting deviations of the biomass-density trajectories from the classical biomass-density trajectories even under minor water stress. Namely, recruitment consistently steepened the slope of thinning sections and enabled an additional fourth section in the biomass-density trajectories. Furthermore, early mortality was density independent due to the coexistence of different plant functional types of various sizes and longevities. These findings have important implications for the management, productivity assessment and carbon budgets of natural uneven-aged multi-species communities where often 'eyes-closed' the specifics of the self-thinning line, especially the value of the classical thinning slope -3/2, are applied (e.g., Pretzsch & Biber 2005; Luyssaert et al. 2008; Newton 2012).

Third, I showed that temporal variability of soil water can promote coexistence through the temporal storage effect even in humid climates, if individuals differ in their hydrological niche (in chapter 5). Coexistence was further boosted by the functional diversity of the plant community by that the constituent PFTs could buffer their growth rate via various functional traits. With regards to the ongoing climate change, this implies that functionally diverse communities may have the potential to adapt to an increased frequency of extreme events, however, the functional composition of plant communities may change. Specifically, in line with previous studies, high frequencies of temporal perturbation by an extreme event selected for annual plants and the disturbance indicator (resident). However, rather unexpectedly at minor frequencies long distance seed dispersal ensured coexistence

of plant functional types through spatial refuges, instead of seed dormancy which is the classical bet-hedging mechanism to buffer against temporally-varying soil water conditions (Harel et al. 2011; Tielbörger et al. 2014). This was a direct result of the simulation scenarios designed as soil water gradients in space, similar to natural ecosystems.

Remarkably, many of the above described community patterns changed in a comparable way at both ends of the soil water range, i.e. excessive and insufficient water availability selected for a similar function and structure of plant communities, a result that has not been reported before. However, this finding is highly plausible given the implemented stress reduction modelling approach for soil water uptake which assumes both excessive and insufficient soil water availability as non-optimal water conditions (Feddes et al. 1978). This stress reduction modelling approach is frequently used in hydrosystem modelling (e.g. Feddes & Raats 2004; Skaggs et al. 2006; Šimůnek & Hopmans 2009) which makes it highly desirable for a coupled vegetation-hydrology model. However, to the best of my knowledge, there is no other study which implemented this reduction function in a dynamic individual-based vegetation model.

The simulation results presented in chapter 3 to 5 of this dissertation enhanced our understanding of changes in community dynamics as well as the abundance of plant functional traits and their specific combinations (PFTs) in response to the hydrological regime while highlighting important research gaps. For example, the here presented individual-based model PLANTHeR (PLAnt fuNctional Traits Hydrological Regimes) is generally able to represent a continuous variation in functional traits, however, in the simulation experiments used in this dissertation each functional trait was represented by two opposing functional trait strategies. Thus, future studies should investigate functional diversity patterns and optimal functional traits values along soil water gradients in a continuous trait-space. Furthermore, there is a need to test the ability of PLANTHeR to represent specific natural ecosystems based on data sets. An ongoing project couples PLANTHeR to a complex, highly resolved hydro(geo)logical model (Li et al. work in progress) so that both vegetation and hydrology can be simulated truly dynamic.

In summary in this dissertation, I showed that plant community dynamics and functional trait abundance vary significantly with soil water availability. These variations will inevitably affect hydrological processes such as interception, infiltration, or runoff (Manfreda et al. 2010). Thus, to predict changes in the interrelation of the dynamics of vegetation and hydrology due to climate change or other anthropogenic alteration calls for truly dynamic representation of vegetation which should not be approximated as a static homogenous 'green layer' (e.g. Therrien et al. 2006). Dynamic vegetation models can be powerful tools to study vegetation response to an environmental factor and are thus essential to predict species' response to climate change. Still, existing dynamic vegetation models are weakened by simplistic representations of biotic interactions and by modelling few plant functional types or life forms defined *a priori* based on a small set of postulated characteristics (e.g. Bonan et al. 2002; Verant et al. 2004; Lapola et al. 2008). In this dissertation, I addressed these simplifications with the development of PLANTHeR which simulates highly resolved, spatially explicit, long-term vegetation dynamics applicable to both forests and grasslands. The individual-based modelling approach of PLANTHeR enabled an explicit representation of local interaction and individual variability, and thus allowed the emergence of several important new findings. Furthermore, PLANTHeR challenges some widely accepted assumptions about dichotomous trade-offs and subjective PFT classifications. Thus, I suggest that PLANTHeR is a flexible tool that can be easily adapted for further ecological-modelling questions which could not be answered by existing dynamic vegetation models.

References

Adler, P. B., HilleRisLambers, J., Kyriakidis, P. C., Guan, Q., Levine, J. M., 2006. Climate variability has a stabilizing effect on the coexistence of prairie grasses. *Proc. Natl. Acad. Sci. U.S.A. 103*, 12793-12798.

Akçakaya, R., Burgman, H., Ginzburg, M. A., Akcakaya, L. R. R., Burgman, M. A., Ginzburg, L. R., 1999. *Applied population ecology: principles and computer exercises using RAMAS EcoLab 2.0*. Applied Biomathematics.

Allan, R. P., Soden, B. J., 2008. Atmospheric warming and the amplification of precipitation extremes. *Science 321*, 1481–1484.

Angert, A. L., Huxman, T. E., Chesson, P., Venable, D. L., 2009. Functional tradeoffs determine species coexistence via the storage effect. *Proc. Natl. Acad. Sci. U.S.A. 106*, 11641-11645.

Austin, M. P., 1990. Community theory and competition in vegetation. In: Grace, J. B. (Eds.), Tilman, D. (Eds.), *Perspectives on Plant Competition*. Academic Press, Inc., 215-238.

Bakker, J. P., Poschlod, P., Strykstra, R. J., Bekker, R. M., Thompson, K., 1996. Seed banks and seed dispersal: important topics in restoration ecology. *Acta Bot. Neerl. 45*, 461-490.

Bauer, S., Berger, U., Hildenbrandt, H., Grimm, V., 2002. Cyclic dynamics in simulated plant populations. *Proc. R. Soc. London, Ser. B 269*, 2443-2450.

Beatty, S. W., 1987. Spatial distributions of Adenostoma species in southern California chaparral: An analysis of niche separation. *Ann. Assoc. American Geo. 77*(2), 255-264.

Begon, M., Harper, J. L., Townsend, C. R., 1991. Ökologie: Individuen, Populationen und Lebensgemeinschaften. *Birkhäuser Verlag*, Basel.

Berger, U., Hildenbrandt, H., 2003. The strength of competition among individual trees and the biomass-density trajectories of the cohort. *Plant Ecol. 167*(1), 89-96.

Berger, U., Hildenbrandt, H., Grimm, V., 2002. Towards a standard for the individual-based modeling of plant populations: self-thinning and the field-of-neighborhood approach. *Nat. Res. Model. 15*, 39-54.

Bittner, S., Talkner, U., Krämer, I., Beese, F., Hölscher, D., Priesack, E., 2010. Modeling stand water budgets of mixed temperate broad-leaved forest stands by considering variations in species specific drought response. *Agric. For. Meteorol. 150*, 1347-1357.

Bonan, G. B., Levis, S., Kergoat, L., Oleson, K. W., 2002. Landscapes as patches of plant functional types: An integrating concept for climate and ecosystem models. *Global Biogeochem. Cycles 16*.

Borgogno, F., D'Odorico, P., Laio, F., Ridolfi, L., 2010. A stochastic model for vegetation water stress. *Ecohydrol. 3*, 177-188.

Bormann, F. H., Likens, G. E., 1979. Catastrophic disturbance and the steady state in northern hardwood forests. *American Sci. 67*, 660–669.

Cao, Q. V., 1994. A tree survival equation and diameter growth model for Loblolly Pine based on the self-thinning rule. *J. Appl. Ecol. 4*, 693-698.

Caplat, P., Anand, M., 2009. Effects of disturbance frequency, species traits and resprouting on directional succession in an individual-based model of forest dynamics. *J. Ecol. 97*, 1028-1036.

Caplat, P., Anand, M., Bauch, C., 2008. Symmetric competition causes population oscillations in an individual-based model of forest dynamics. *Ecol. Model. 211*, 491-500.

Cheng, X., An, S., Li, B., Chen, J., Lin, G., Liu, Y., Luo, Y., Liu, S., 2006. Summer rain pulse size and rainwater uptake by three dominant desert plants in a desertified grassland ecosystem in northwestern China. *Plant Ecol. 184*, 1-12.

Chesson, P. L., 1985. Coexistence of competitors in spatially and temporally varying environments: a look at the combined effects of different sorts of variability. *Theor. Popul. Biol. 28*, 263-287.

Chesson, P., 1994. Multispecies competition in variable environments. *Theor. Popul. Biol. 45*, 227–276.

Chesson, P., 2000a. Mechanisms of maintenance of species diversity. *Ann. Rev. Ecol. Syst. 31*, 343-366.

Chesson, P., 2000b. General theory of competitive coexistence in spatially varying environments. *Theor. Popul. Biol. 58*, 211-237

Chu, C. J., Weiner, J., Maestre, F. T., Wang, Y. S., Morris, C., Xiao, S., Yuan, J. L., Du, G. Z., Wang, G., 2010. Effects of positive interactions, size symmetry of competition and abiotic stress on self-thinning in simulated plant populations. *Ann. Bot. 106*, 647-652.

Cornelissen, J. H. C., Lavorel, S., Garnier, E., Diaz, S., Buchmann, N., Gurvich, D. E., Reich, P. B., ter Steege, H., Morgan, H. D., van der Heijden, M. G. A., Pausas, J. G., 2003. A handbook of protocols for standardised and easy measurement of plant functional traits worldwide. *Aust. J. Bot. 51*, 335-380.

Crawley, M. J., May, R. M., 1987. Population dynamics and plant community structure: competition between annuals and perennials*. J. Theor. Biol. 125*, 475–489.

Czárán, T., 1998. *Spatiotemporal Models of Population and Community Dynamics*. Chapman and Hall, London Population And Community Biology Series 21.

Dawson, T. E., 1993. Hydraulic lift and water use by plants: implications for water balance, performance and plant-plant interactions. *Oecologia 95*(4), 565-574.

de Bello, F., Lepš, J., Sebastià, M. T., 2005. Predictive value of plant traits to grazing along a climatic gradient in the Mediterranean. *J. Appl. Ecol. 42*, 824–833.

de Silva, M. S., Nachabe, M. H., Šimůnek, J., Carnahan, R., 2008. Simulating root water uptake from a heterogeneous vegetative cover. *J. Irrig. Drain. Eng. 134*(2), 167-174.

DiVittorio, C. T., Corbin, J. D., D'Antonio, C. M., 2007. Spatial and temporal patterns of seed dispersal: an important determinant of grassland invasion. *Ecol. Appl. 17*, 311-316.

Easterling, D. R., Meehl, G. A., Parmesan, C., Changnon, S. A., Karl, T. R., Mearns, L. O., 2000. Climate extremes: observations, modeling, and impacts. *Science 289*(5487), 2068-2074.

Esther, A., Groeneveld, J., Enright, N. J., Miller, B. P., Lamont, B. B., Perry, G. L., Schurr, F. M., Jeltsch, F., 2008. Assessing the importance of seed immigration on coexistence of plant functional types in a species-rich ecosystem. *Ecol. Model. 213*(3), 402-416.

Feddes, R. A., Kowalik, P. J., Zaradny, H., 1978. Simulation of Field Water Use and Crop Yield: Simulation Monograph. *Pudoc Wageningen*, Netherlands, pp. 9–30.

Feddes, R. A., Raats, P. A. C., 2004. Parameterizing the soil–water–plant root system. *Unsaturated-zone Modeling: Progress, Challenges, Applications 6*, 95-141.

Field, C. B., Barros, V. R., Dokken, D. J., Mach, K. J., Mastrandrea, M. D., Bilir, T. E., Chatterjee, M., Ebi, K. L., Estrada, Y. O., Genova, R. C., Girma, B., Kissel, E. S., Levy, A. N., MacCracken, S., Mastrandrea, P. R., White, L. L., 2014. Climate Change 2014: Impacts, Adaptation, and Vulnerability. Part A: Global and Sectoral Aspects. Contribution of Working Group II to the Fifth Assessment Report of the Intergovernmental Panel on Climate Change. *Cambridge University Press*, Cambridge, United Kingdom and New York, NY, USA.

Fischer, R., Armstrong, A., Shugart, H. H., Huth, A., 2014. Simulating the impacts of reduced rainfall on carbon stocks and net ecosystem exchange in a tropical forest. *Environ. Modell. Softw. 52*, 200-206.

Gause, G. F., 1934. Experimental analysis of Vito Volterra's mathematical theory of the struggle for existence. *Science 79*, 16-17.

Gitay, H., Noble, I. R., 1997. What are functional types and how should we seek them?, in: Smith, T. M., Shugart, H. H., Woodward, F. I. (Eds.), *Plant Functional Types—Their Relevance to Ecosystem Properties and Global Change*. Cambridge University Press, Cambridge, pp. 3–43.

Grier, C. C., Elliott, K. J., McCullough, D. G., 1992. Biomass distribution and productivity of Pinus edulis-Juniperus monosperma woodlands of north-central Arizona. *For. Ecol. Manage. 50*, 331-350.

Grime, J. P., 1977. Evidence for the existence of three primary strategies in plants and its relevance to ecological and evolutionary theory. *American Naturalist*, 1169-1194.

Grimm, V., 1999. Ten years of individual-based modelling in ecology: what have we learned and what could we learn in the future?. *Ecol. Model. 115*, 129-148.

Grimm, V., Berger, U., Bastiansen, F., Eliassen, S., Ginot, V., Giske, J., Goss-Custard, J., Grand, T., Heinz, S., Huse, G., Huth, A., Jepsen, J. U., Jørgensen, C., Mooij, W. M., Müller, B., Pe'er, G., Piou, C., Railsback, S. F., Robbins, A. M., Robbins, M. M., Rossmanith, E., Rüger, N., Strand, E., Souissi, S., Stillman, R. A., Vabø, R., Visser, U., DeAngelis, D. L., 2006. A standard protocol for describing individual-based and agent-based models. *Ecol. Model. 198*, 115–126.

Grimm, V., Berger, U., DeAngelis, D. L., Polhill, J. G., Giske, J., Railsback, S. F., 2010. The ODD protocol: a review and first update. *Ecol. Model. 221*, 2760-2768.

Harel, D., Holzapfel, C., Sternberg, M., 2011. Seed mass and dormancy of annual plant populations and communities decreases with aridity and rainfall predictability. *Basic Appl. Ecol. 12*, 674–684.

Herberich, M. M., Gayler, S., Anand, M., Tielbörger, K., 2017. Hydrological niche segregation of plant functional traits in an individual-based model. *Ecol. Model. 356*, 14-24.

Hodgson, J. G., Wilson, P. J., Hunt, R., Grime, J. P., Thompson, K., 1999. Allocating C-S-R plant functional types: a soft approach to a hard problem. *Oikos 85*, 282-294.

Holmes, E. E., Wilson, H. B., 1998. Running from trouble: long-distance dispersal and the competitive coexistence of inferior species. *American Naturalist 151*, 578-586.

Huffman, D. W., Crouse, J. E., Chancellor, W. W., Fulé, P. Z., 2012. Influence of time since fire on pinyon–juniper woodland structure. *For. Ecol. Manage. 274*, 29-37.

Kaiser, H., 1979. The dynamics of populations as result of the properties of individual animals. *Fortschritte der Zoologie 25*, 109-136.

Kattge, J., Diaz, S., Lavorel, S., Prentice, I. C., Leadley, P., Bönisch, G., Garnier, E., Westoby, M., Reich, P. B., Wright, I. J., Cornelissen, J.H.C., 2011. TRY–a global database of plant traits. *Glob. Chang. Biol. 17*(9), 2905-2935.

Kays, S., Harper, J. L., 1974. The regulation of plant and tiller density in a grass sward. *J. Ecol.* 62, 97–105.

Kohyama, T., 1992. Density-size dynamics of trees simulated by a one-sided competition multi-species model of rain forest stands. *Ann. Bot. 70*(5), 451-460.

Körner, K., Jeltsch, F., 2008. Detecting general plant functional type responses in fragmented landscapes using spatially-explicit simulations. *Ecol. Model. 210*, 287-300.

Kortessis, N., Chesson, P., 2014. Spatial variation can boost temporal storage through spatial refuges. *Paper presented at 99th ESA Annual Convention 2014*.

Kowaljow, E., Fernandez, R. J., 2011. Differential utilization of a shallow water pulse by six shrub species in the Patagonian steppe. *J. Arid Environ. 75*(2), 211–214.

Kukowski, K. R., Schwinning, S., Schwartz, B. F., 2013. Hydraulic responses to extreme drought conditions in three co-dominant tree species in shallow soil over bedrock. *Oecologia 171*, 819-830.

Lapola, D. M., Oyama, M. D., Nobre, C. A., Sampaio, G., 2008. A new world natural vegetation map for global change studies. *Anais da Academia Brasileira de Ciências 80*, 397-408.

Laughlin, D. C., Laughlin, D. E., 2013. Advances in modeling trait-based plant community assembly. *Trends Plant Sci. 18*, 584-593.

Lehsten, V., Kleyer, M., 2007. Turnover of plant trait hierarchies in simulated community assembly in response to fertility and disturbance. *Ecol. Model. 203*, 270-278.

Levitt, J., 1980. Responses of plants to environmental stresses. Academic Press, New York, NY.

Li, S. L., Ramula, S., 2015. Demographic strategies of plant invaders in temporally varying environments. *Popul. Ecol. 57*(2), 373-380.

Li, S., Gayler,S., Basu, N., Tielbörger, K., Vegetation-Hydrology Feedbacks. *Work in progress*.

Lin, Y., Huth, F., Berger, U., Grimm, V., 2014. The role of belowground competition and plastic biomass allocation in altering plant mass–density relationships. *Oikos 123*, 248-256.

Liu, J., Wei, L., Wang, C.-M., Wangl, G.-X., Wei, X.-P., 2006. Effect of water deficit on self-thinning line in Spring Wheat (Triticum aestivum L.) populations. *J. Integ. Plant Biol. 48*, 415–419.

Loheide, S. P., Booth, E. G., 2011. Effects of changing channel morphology on vegetation, groundwater, and soil moisture regimes in groundwater-dependent ecosystems. *Geomorphology 126*(3), 364-376.

Lonsdale, W. M., 1990. The Self-Thinning Rule: Dead or Alive?. *Ecol. 71*, 1373-1388.

Lonsdale, W. M., Watkinson, A. R., 1982. Light and self-thinning. *New Phytologist 90*(3), 431-445.

Lowry, C. S., Loheide, S. P., 2010. Groundwater-dependent vegetation: Quantifying the groundwater subsidy. *Water Resourc. Res. 46*(6).

Luyssaert, S., Schulze, E. D., Börner, A., Knohl, A., Hessenmöller, D., Law, B. E., Ciais, P., Grace, J., 2008. Old-growth forests as global carbon sinks. *Nature 455*, 213-215.

Majeková, M., de Bello, F., Doležal, J., Lepš, J., 2014. Plant functional traits as determinants of population stability. *Ecol. 95*(9), 2369-2374.

Manfreda, S., Smettem, K., Iacobellis, V., Montaldo, N., Sivapalan, M., 2010. Coupled ecological–hydrological processes. *Ecohydrol. 3*, 131-132.

Mauchamp, A., Rambal, S., Lepart, J., 1994. Simulating the dynamics of a vegetation mosaic: a spatialized functional model. *Ecol. Model. 71*(1), 107-130.

Mayer, A. M., Poljakoff-Mayber, A., 1982. *The Germination of Seeds: Pergamon International Library of Science, Technology, Engineering and Social Studies*. Elsevier.

McIntyre, S., Lavorel, S., Tremont, R. M., 1995. Plant life-history attributes: their relationship to disturbance response in herbaceous vegetation. *J. Ecol. 83*, 31–44.

Milton, S. J., Dean, W. R. J., Klotz, S., 1997. Effects of small-scale animal disturbances on plant assemblages of set-aside land in Central Germany. *J. Veg. Sci. 8*, 45-54.

Moeslund, J. E., Arge, L., Bøcher, P. K., Dalgaard, T., Ejrnæs, R., Odgaard, M. V., Svenning, J. C., 2013. Topographically controlled soil moisture drives plant diversity patterns within grasslands. *Biodivers. Conserv. 22*, 2151-2166.

Moeur, M., 1997. Spatial models of competition and gap dynamics in old-growth Tsuga heterophylla/Thuja plicata forests. *For. Ecol. Manage. 94*(1-3), 175-186.

Monserud, R. A., Ledermann, T., Sterba, H., 2004. Are self-thinning constraints needed in a tree-specific mortality model?. *For. Sci. 50*(6), 848-858.

Morris, E. C., 2003. How does fertility of the substrate affect intraspecific competition? Evidence and synthesis from self-thinning. *Ecol. Res. 18*(3), 287-305.

Morris, W. F., Doak, D. F., 2004. Buffering of life histories against environmental stochasticity: accounting for a spurious correlation between the variabilities of vital rates and their contributions to fitness. *American Naturalist 163*(4), 579-590.

Mustroph, A., Sauter, M., Geigenberger, P. van Dongen, J., 2016. (Über)leben ohne Sauerstoff. *Biologie in unserer Zeit 46*, 32–40.

Nathan, R., Muller-Landau, H. C., 2000. Spatial patterns of seed dispersal, their determinants and consequences for recruitment. *Trends Ecol. Evol. 15*(7), 278-28

Newton, P.F., 2012. A decision-support system for forest density management within upland black spruce stand-types. Environ. *Model. Softw. 35*, 171–187.

Novoplansky, A., Goldberg, D. E., 2001. Effects of water pulsing on individual performance and competitive hierarchies in plants. *J. Veg. Sci. 12*(2), 199-208.

Oddershede, A., Svenning, J. C., Damgaard, C., 2015. Topographically determined water availability shapes functional patterns of plant communities within and across habitat types. *Plant Ecol. 216*, 1231-1242.

Orellana, F., Verma, P., Loheide, S. P., Daly, E., 2012. Monitoring and modeling water-vegetation interactions in groundwater-dependent ecosystems. *Rev. Geophys. 50*(3).

Pfister, C. A., 1998. Patterns of variance in stage-structured populations: evolutionary predictions and ecological implications. *Proc. Natl. Acad. Sci. USA 95*(1), 213-218.

Picotte, J. J., Rosenthal, D. M., Rhode, J. M., Cruzan, M. B., 2007. Plastic responses to temporal variation in moisture availability: consequences for water use efficiency and plant performance. *Oecologia 153*(4), 821-832.

Pretzsch, H., Biber, P., 2005. A re-evaluation of Reineke's rule and stand density index. *For Sci. 51*, 304–320.

Reich, P. B., Tjoelker, M. G., Machado, J. L., Oleksyn, J., 2006. Universal scaling of respiratory metabolism, size and nitrogen in plants. *Nature 439*(7075), 457-461.

Reyer, C. P., Leuzinger, S., Rammig, A., Wolf, A., Bartholomeus, R. P., Bonfante, A., de Lorenzi, F., Dury, M., Gloning, P., Abou Jaoudé, R., Klein, T., 2013. A plant's perspective of extremes: terrestrial plant responses to changing climatic variability. *Glob. Chang. Biol. 19*, 75–89.

Reynolds, H. L., Hungate, B. A., Chapin III, F. S., D'Antonio, C. M., 1997. Soil heterogeneity and plant competition in annual grassland. *Ecol. 78*(7), 2076-2090.

Roberts, E. H., 1972. Storage environment and the control of viability. in: Roberts, E. H. (Eds.), *Viability of Seeds*. Chapman and Hall, London, pp. 14-58.

Scheiter, S., Langan, L., Higgins, S. I., 2013. Next-generation dynamic global vegetation models: learning from community ecology. *New Phytologist 198*(3), 957-969.

Schippers, P., Van Groenendael, J. M., Vleeshouwers, L. M., Hunt, R., 2001. Herbaceous plant strategies in disturbed habitats. *Oikos 95*, 198–210.

Schulte, M. J. D., Matyssek, R., Gayler, S., Priesack, E., Grams, T. E., 2013. Mode of competition for light and water amongst juvenile beech and spruce trees under ambient and elevated levels of O3 and CO2. *Trees 27*, 1763-1773.

Schulze, E. D., Beck, E., Müller-Hohenstein, K., 2005. Self-Thinning. in: Schulze, E. D., Beck, E., Müller-Hohenstein, K., Czeschlik, D. (Eds.), *Plant Ecology*. Springer, Berlin, pp. 403-406.

Schwinning, S., Weiner, J., 1998. Mechanisms determining the degree of size asymmetry in competition among plants. *Oecologia 113*, 447-455.

Seifan, M., Seifan, T., Jeltsch, F., Tielbörger, K., 2012. Combined disturbances and the role of their spatial and temporal properties in shaping community structure. *Perspect. Plant Ecol. Evol. Syst. 14*, 217-229.

Seifan, M., Seifan, T., Schiffers, K., Jeltsch, F., Tielbörger, K., 2013. Beyond the Competition-Colonization Trade-Off: Linking Multiple Trait Response to Disturbance Characteristics. *American Naturalist 181*, 151-160.

Shugart, H. H., 2014. Models of the Dynamics of Mosaic Landscapes. *Bull. Ecol. Soc. America 95*(2), 117-120.

Silvertown, J., 2004. Plant coexistence and the niche. *Trends Ecol. Evol. 19*, 605-611.

Silvertown, J., Araya, Y., Gowing, D., 2015. Hydrological niches in terrestrial plant communities: a review. *J. Ecol. 103*, 93-108.

Silvertown, J., Dodd, M. E., Gowing, D. J., Mountford, J. O., 1999. Hydrologically defined niches reveal a basis for species richness in plant communities. *Nature 400*, 61-63.

Šimůnek, J., Hopmans, J. W., 2009. Modeling compensated root water and nutrient uptake. *Ecol. Model. 220*(4), 505-521.

Skaggs, T. H., van Genuchten, M. T., Shouse, P. J., Poss, J. A., 2006. Macroscopic approaches to root water uptake as a function of water and salinity stress. *Agric. Water Manage. 86*(1), 140-149.

Snell, R. S., Huth, A., Nabel, J. E. M. S., Bocedi, G., Travis, J. M. J., Gravel, D., Bugmann, H., Gutiérrez, A. G., Hickler, T., Higgins, S. I., Reineking, B., Scherstjanoi, M., Zurbriggen, N., Lischke, H., 2014. Using dynamic vegetation models to simulate plant range shifts. *Ecography 37*(12), 1184-1197.

Snyder, K. A., Tartowski, S. L., 2006. Multi-scale temporal variation in water availability: implications for vegetation dynamics in arid and semi-arid ecosystems. *J. Arid Environ. 65*(2), 219-234.

Snyder, R. E., 2006. Multiple risk reduction mechanisms: can dormancy substitute for dispersal? *Ecol. Lett. 9*, 1106–1114.

Snyder, R. E., 2011. Leaving home ain't easy: non-local seed dispersal is only evolutionarily stable in highly unpredictable environments. *Proc. R. Soc. London, Ser. B 278*, 739-744.

Splechtna, B. E., Gratzer, G., 2005. Natural disturbances in Central European forests: approaches and preliminary results from Rothwald, Austria. *For. Snow Landsc. Res. 79*, 57-67.

Stankova, T.V., Shibuya, M., 2007. Stand density control diagrams for Scots pine and Austrian black pine plantations in Bulgaria. *New For. 34*, 123–141.

Stoll, P., Weiner, J., Muller-Landau, H., Müller, E., Hara, T., 2002. Size symmetry of competition alters biomass–density relationships. *Proc. R. Soc. London, Ser. B, 269*(1506), 2191-2195.

Stoyan, D., Wagner, S., 2001. Estimating the fruit dispersion of anemochorous forest trees. *Ecol. Model. 145*, 35-47.

Svensson, J. R., Lindegarth, M., Pavia, H., 2009. Equal rates of disturbance cause different patterns of diversity. *Ecol. 90*, 496–505.

Teller, B. J., Campbell, C., Shea, K., 2014. Dispersal under duress: Can stress enhance the performance of a passively dispersed species?. *Ecol. 95*, 2694-2698.

Therrien, R., McLaren, R. G., Sudicky, E. A., Panday, S. M., 2006. HydroGeoSphere: A three-dimensional numerical model describing fully-integrated subsurface and surface flow and solute transport. *Groundwater Simul. Group, Waterloo, Ontario, Canada*.

Tielbörger, K., Bilton, M. C., Metz, J., Kigel, J., Holzapfel, C., Lebrija-Trejos, E., Konsens, I., Parag, H. A., Sternberg, M., 2014. Middle-Eastern plant communities tolerate 9 years of drought in a multi-site climate manipulation experiment. *Nature Communications 5*, 5102-5111.

Tilman, D., 1994. Competition and biodiversity in spatially structured habitats. *Ecol. 75*, 2–16.

Tilman, D., 2004. Niche tradeoffs, neutrality, and community structure: a stochastic theory of resource competition, invasion, and community assembly. *Proc. Natl. Acad. Sci. U.S.A. 101*, 10854-10861.

Tilman, D., Isbell, F., Cowles, J. M., 2014. Biodiversity and ecosystem functioning. *Ann. Rev. Ecol. Syst. 45*, 471-493.

Tilman, D., Reich, P. B., Knops, J. M., 2006. Biodiversity and ecosystem stability in a decade-long grassland experiment. *Nature 441*, 629-632.

Van Wagner, C. E., 1978. Age-class distribution and the forest fire cycle. *Can. J. For. Res. 8*, 220-227.

Venable, D. L., Brown, J. S., 1988. The selective interactions of dispersal, dormancy, and seed size as adaptations for reducing risk in variable environments. *American Naturalist 131*, 360-384.

Verant, S., Laval, K., Polcher, J., De Castro, M., 2004. Sensitivity of the continental hydrological cycle to the spatial resolution over the Iberian Peninsula. *J. Hydrometeorol. 5*, 267-285.

Verhulst, J., Montaña, C., Mandujano, M. C., Franco, M., 2008. Demographic mechanisms in the coexistence of two closely related perennials in a fluctuating environment. *Oecologia 156*, 95-105.

Violle, C., Bonis, A., Plantegenest, M., Cudennec, C., Damgaard, C., Marion, B., Le Cœur, D., Bouzillé, J. B., 2011. Plant functional traits capture species richness variations along a flooding gradient. *Oikos 120*, 389-398.

Vörösmarty, C. J., Sahagian, D., 2000. Anthropogenic disturbance of the terrestrial water cycle. *BioScience 50*, 753-765.

Vospernik, S., Sterba, H., 2015. Do competition-density rule and self-thinning rule agree?. *Ann. For. Sci. 72*(3), 379-390.

Warton, D. I., Wright, I. J., Falster, D. S., Westoby, M., 2006. Bivariate line-fitting methods for allometry. *Biol. Rev. 81*, 259-291.

Watts, S. M., 2010. Pocket gophers and the invasion and restoration of native bunchgrass communities. *Restor. Ecol. 18*, 34-40.

Weiner, J., Freckleton, R. P., 2010. Constant final yield. *Ann. Rev. Ecol. Syst. 41*, 173-92.

Weiner, J., Stoll, P., Muller-Landau, H., Jasentuliyana, A., 2001. The effects of density, spatial pattern, and competitive symmetry on size variation in simulated plant populations. *American Naturalist 158*, 438-450.

Weller, D. E., 1991. The Self-Thinning Rule: Dead or Unsupported?--A Reply to Lonsdale. *Ecol. 72*(2), 747-750.

Wesseling, J. G., 1991. Meerjarige simulatie van grondwaterstroming voor verschillende bodemprofielen, grondwatertrappen en gewassen met het model SWATRE. *Wageningen, DLO-Staring Centrum, Rapport 152*, 63.

West, G. B., Brown, J. H., Enquist, B. J., 1999. A general model for the structure and allometry of plant vascular systems. *Nature 400*, 664-667.

Westoby, M., 1984. The self-thinning rule. *Adv. Ecol. Res. 14*, 167-226.

White, C. R., Cassey, P., Blackburn, T. M., 2007. Allometric exponents do not support a universal metabolic allometry. *Ecol. 88*(2), 315-323.

Wilensky, U., 1999. NetLogo. http://ccl.northwestern.edu/netlogo/. Center for Connected Learning and Computer-Based Modeling, Northwestern University. Evanston, IL.

Wilson, S. D., Tilman, D., 1991. Component of plant competition along an experimental gradient of nitrogen availability. *Ecol. 72*, 1050-1065.

Wright, I. J., Reich, P. B., Westoby, M., Ackerly, D. D., 2004. The worldwide leaf economics spectrum. *Nature 428*(6985), 821-827.

Yang, S. J., Jong, E. D., 1971. Effect of soil water potential and bulk density on water uptake patterns and resistance to flow of water in wheat plants. *Can. J. Soil Sci. 51*, 211-220.

Yoda, K., Kira, T., Ogawa, H. Hozumi, K., 1963. Intraspecific competition among higher plants. XI. Self-thinning in overcrowded pure stands under cultivated and natural conditions. *J. Biol. Osaka City University 14*, 107–129.

Zeide, B., 1995. A relationship between size of trees and their number. *For. Ecol. Manage. 72*, 265-272.

Zhang, L., Bi, H., Gove, J. H., Heath, L. S., 2005. A comparison of alternative methods for estimating the self-thinning boundary line. *Can. J. For. Res. 35*(6), 1507-1514.

Zhang, W. P., Jia, X., Wang, G. X., 2017. Facilitation among plants can accelerate density-dependent mortality and steepen self-thinning lines in stressful environments. *Oikos*.

Appendix

Appendix A: Supplementary information on modelled PFTs

Table A1: 64 modelled PFTs in the plant community which resulted from full factorial combinations of twelve functional trait strategies. Functional trait strategies were: perennial(P)/annual(a) life form, high(T)/low(t) water stress tolerance, long(D)/short(d) seed dispersal distance, long-(S)/short-term(s) seed dormancy, strong(C)/weak(c) seedling competitive ability, and high(G)/low(g) maximum adult growth rate (Seifan et al. 2012, 2013).

Plant Functional Type	Life form Perennial (P) / annual (a)	Water stress tolerance high (T) / low (t)	Maximum seed dispersal distance Long (D) / short (d)	Seed dormancy Long- (S) / short-term (s)	Competitive ability Strong (C) / weak (c)	Maximum growth rate High (G) / low (g)
PFT1	P	T	D	S	C	g
PFT2	P	T	D	S	c	G
PFT3	P	T	D	S	c	g
PFT4	P	T	D	s	C	G
PFT5	P	T	D	s	C	g
PFT6	P	T	D	s	c	G
PFT7	P	T	D	s	c	g
PFT8	P	T	d	S	C	G
PFT9	P	T	d	S	C	g
PFT10	P	T	d	S	c	G
PFT11	P	T	d	S	c	g
PFT12	P	T	d	s	C	G
PFT13	P	T	d	s	C	g
PFT14	P	T	d	s	c	G
PFT15	P	T	d	s	c	g
PFT16	P	t	D	S	C	G
PFT17	P	t	D	S	C	g
PFT18	P	t	D	S	c	G
PFT19	P	t	D	S	c	g
PFT20	P	t	D	s	C	G
PFT21	P	t	D	s	C	g
PFT22	P	t	D	s	c	G
PFT23	P	t	D	s	c	g
PFT24	P	t	d	S	C	G
PFT25	P	t	d	S	C	g
PFT26	P	t	d	S	c	G
PFT27	P	t	d	S	c	g
PFT28	P	t	d	s	C	G
PFT29	P	t	d	s	C	g
PFT30	P	t	d	s	c	G
PFT31	P	t	d	s	c	g
PFT32	a	T	D	S	C	G

PFT33	a	T	D	S	C	g
PFT34	a	T	D	S	c	G
PFT35	a	T	D	S	c	g
PFT36	a	T	D	s	C	G
PFT37	a	T	D	s	C	g
PFT38	a	T	D	s	c	G
PFT39	a	T	D	s	c	g
PFT40	a	T	d	S	C	G
PFT41	a	T	d	S	C	g
PFT42	a	T	d	S	c	G
PFT43	a	T	d	S	c	g
PFT44	a	T	d	s	C	G
PFT45	a	T	d	s	C	g
PFT46	a	T	d	s	c	G
PFT47	a	T	d	s	c	g
PFT48	a	t	D	S	C	G
PFT49	a	t	D	S	C	g
PFT50	a	t	D	S	c	G
PFT51	a	t	D	S	c	g
PFT52	a	t	D	s	C	G
PFT53	a	t	D	s	C	g
PFT54	a	t	D	s	c	G
PFT55	a	t	D	s	c	g
PFT56	a	t	d	S	C	G
PFT57	a	t	d	S	C	g
PFT58	a	t	d	S	c	G
PFT59	a	t	d	S	c	g
PFT60	a	t	d	s	C	G
PFT61	a	t	d	s	C	g
PFT62	a	t	d	s	c	G
PFT63	P	T	D	S	C	G
PFT64	a	t	d	s	c	g

Appendix B: Biomass-density trajectories and skewness of the biomass distribution for all 15 soil water scenarios.

Changes in the biomass-density trajectory, bdt, over time could be tracked by means of skewness of the biomass distribution. Section I (blue) was characterized by an increase of positive skewness and ended with the first maximum of skewness. Section II (orange) was characterized by a constant decay of positive skewness between the first maximum and the first x-intercept. Section III (yellow) was characterized by a negative skewness between the two x-intercepts. Section IV (green) started at the second x-intercept with a positive increasing skewness and was characterized by alternating phases of increasing and decreasing skewness.

Figure B1 to B15 show for all fifteen soil water scenarios: (a) Entire biomass-density trajectory, i.e. relationship between the logarithm of mean plant biomass of survivors *w* (mg/m²) and the logarithm of plant density *N* (individuals/m²) for all ten replicates over 2000 years. Colors show the four sections of community structure indicated by skewness of the biomass distribution in Fig. b. The steeper dotted line has a slope of - 3/2 and the flat dashed line has a slope of -1.1. (b) Change in mean ± SD skewness of biomass distribution across ten replicates over 2000 years. The x-intercepts and first maximum define distinct sections of community structure which are highlighted using a color code. Standard deviation of the ten replicates is shown in grey.

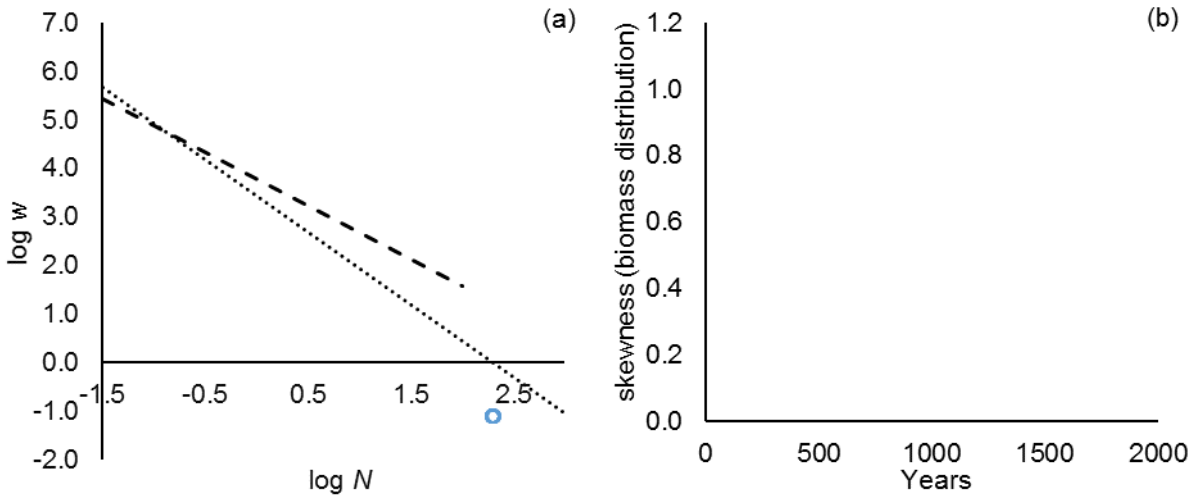

Fig. B1. Soil water potential -300000, $f_d(\Psi)$ = 0.00.

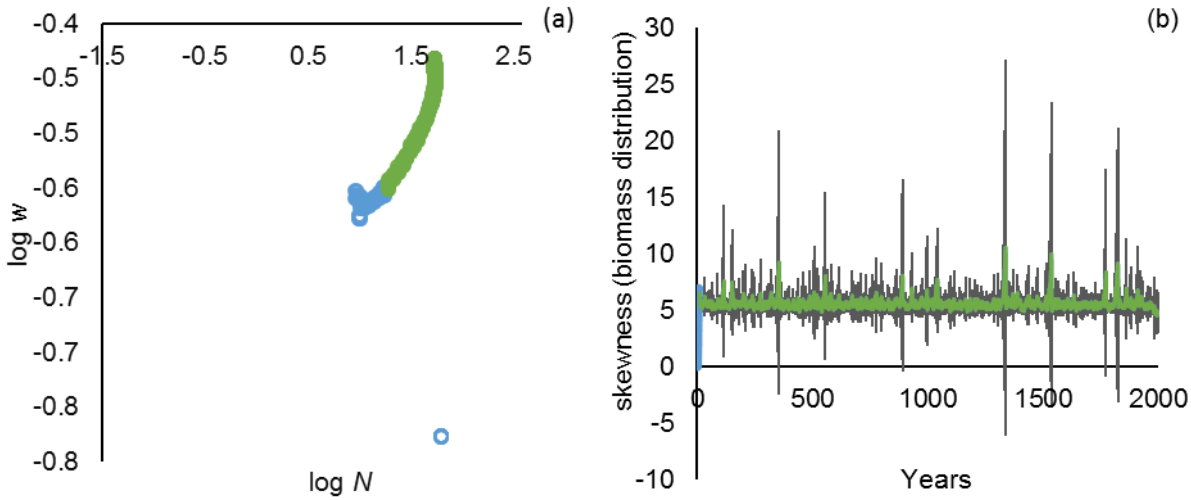

Fig. B2. Soil water potential -171000, $f_d(\Psi)$ = 0.30.

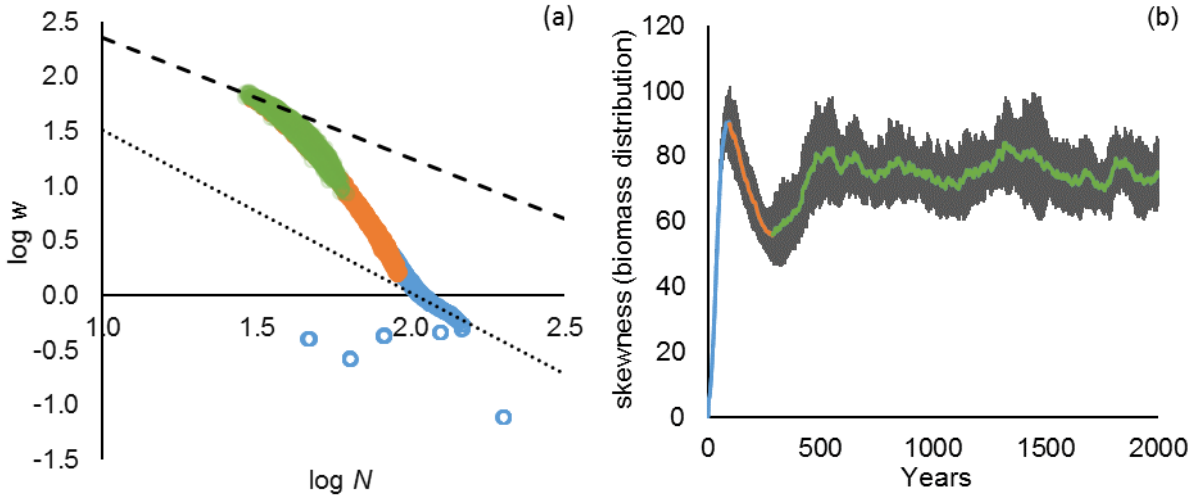

Fig. B3. Soil water potential -125000, $f_d(\Psi)$ = 0.50.

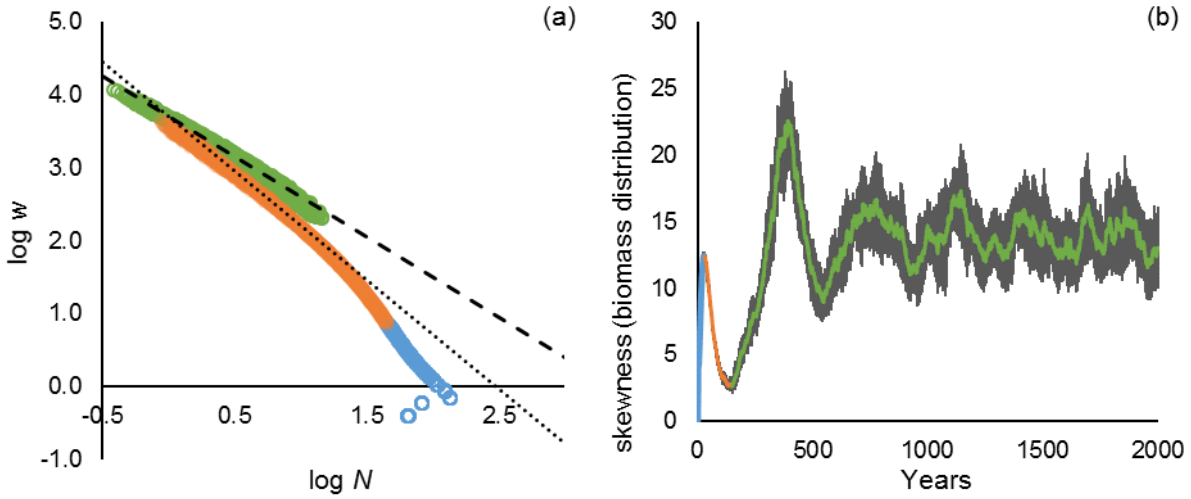

Fig. B4. Soil water potential -80001, $f_d(\Psi)$ = 0.70.

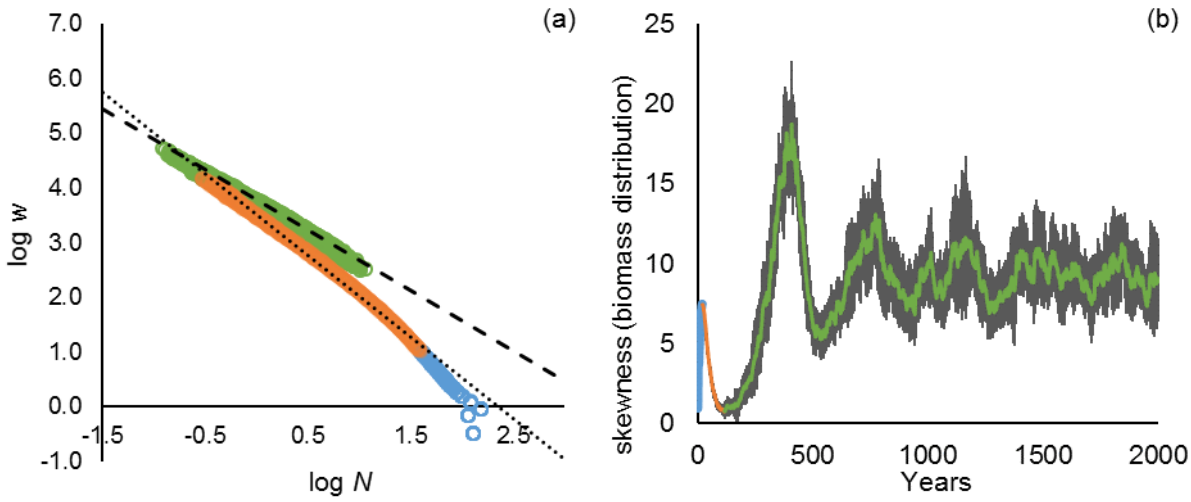

Fig. B5. Soil water potential -56000, $f_d(\Psi) = 0.80$.

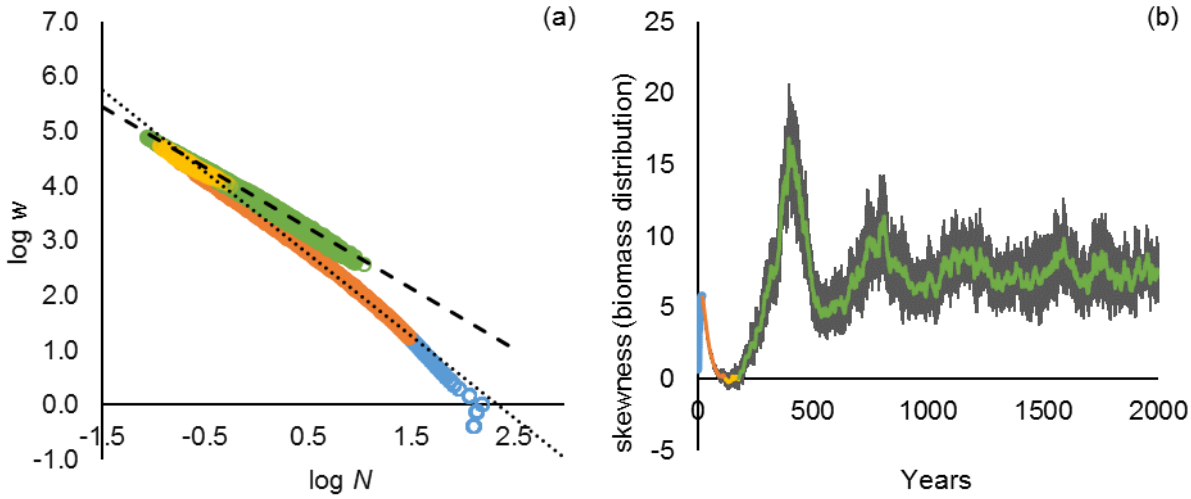

Fig. B6. Soil water potential -41000, $f_d(\Psi) = 0.90$.

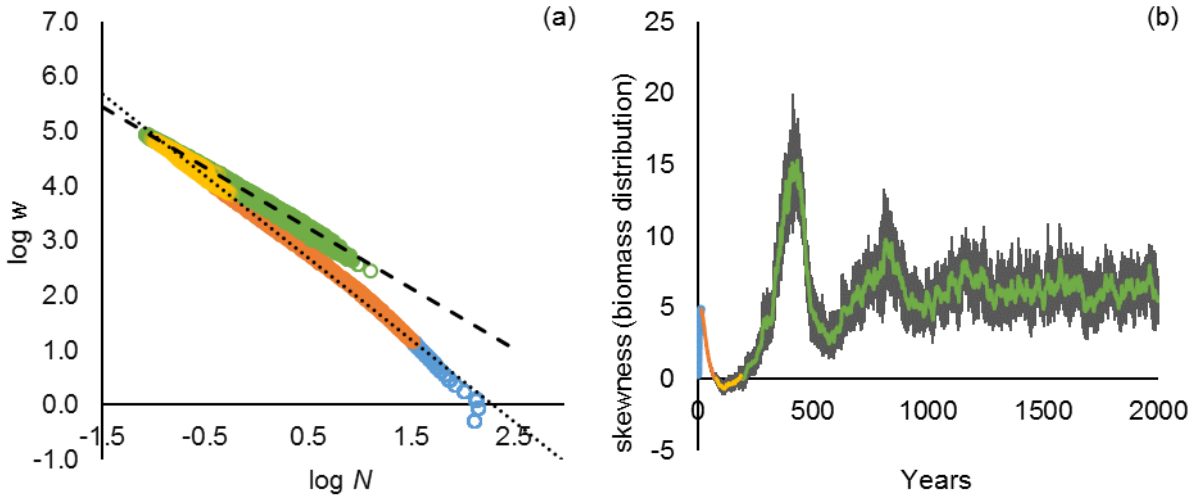

Fig. B7. Soil water potential -25400, $f_d(\Psi) = 0.93$.

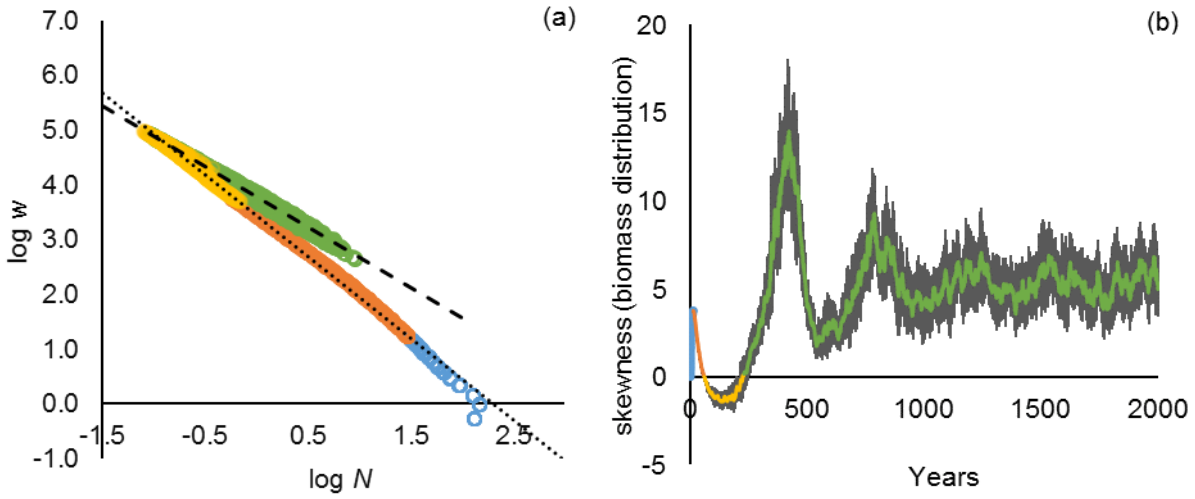

Fig. B8. Soil water potential -1900, $f_d(\Psi) = 1.00$.

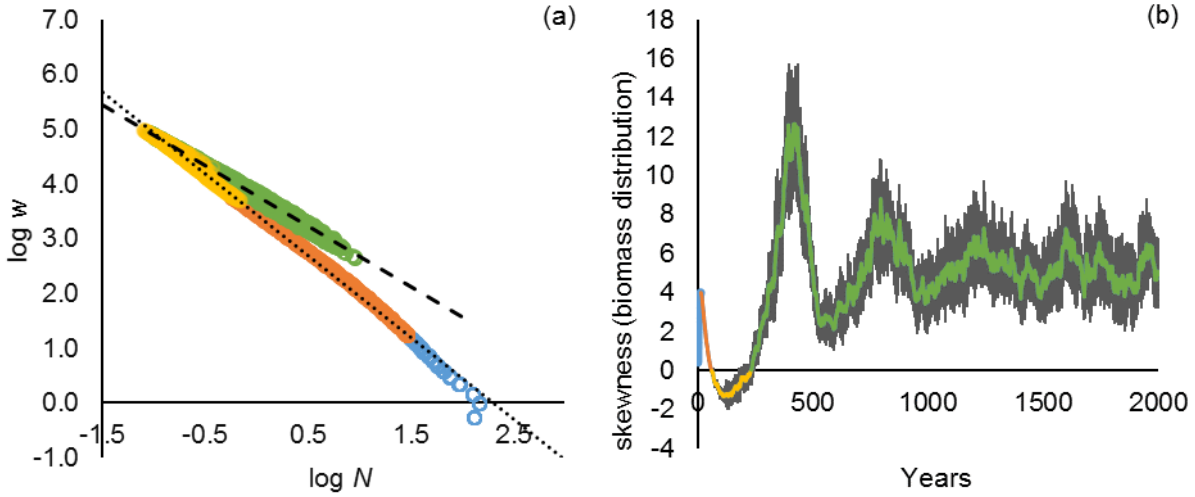

Fig. B9. Soil water potential -255, $f_d(\Psi) = 1.00$.

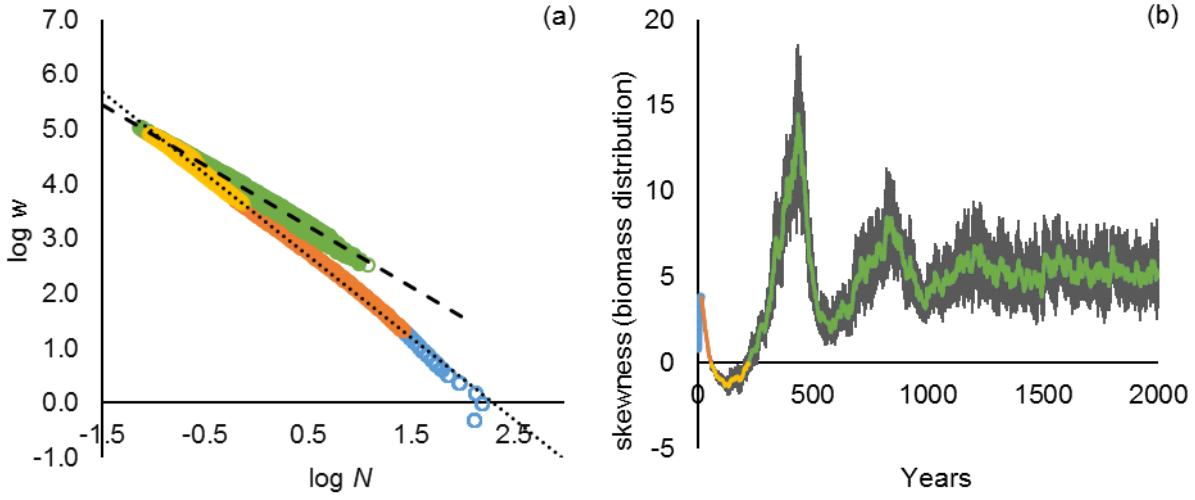

Fig. B10. Soil water potential -225, $f_d(\Psi) = 1.00$.

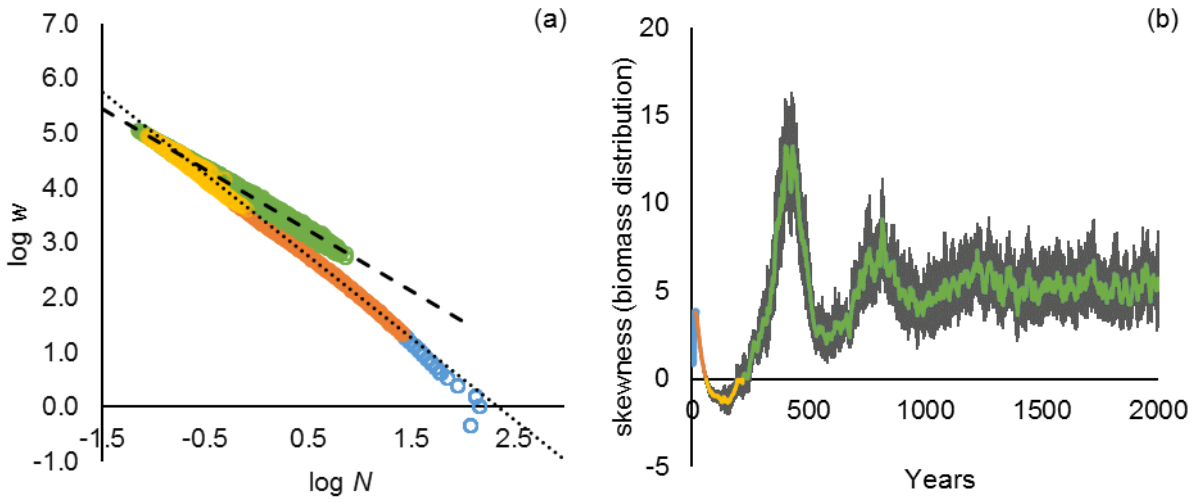

Fig. B11. Soil water potential -195, $f_d(\Psi)$ = 1.00.

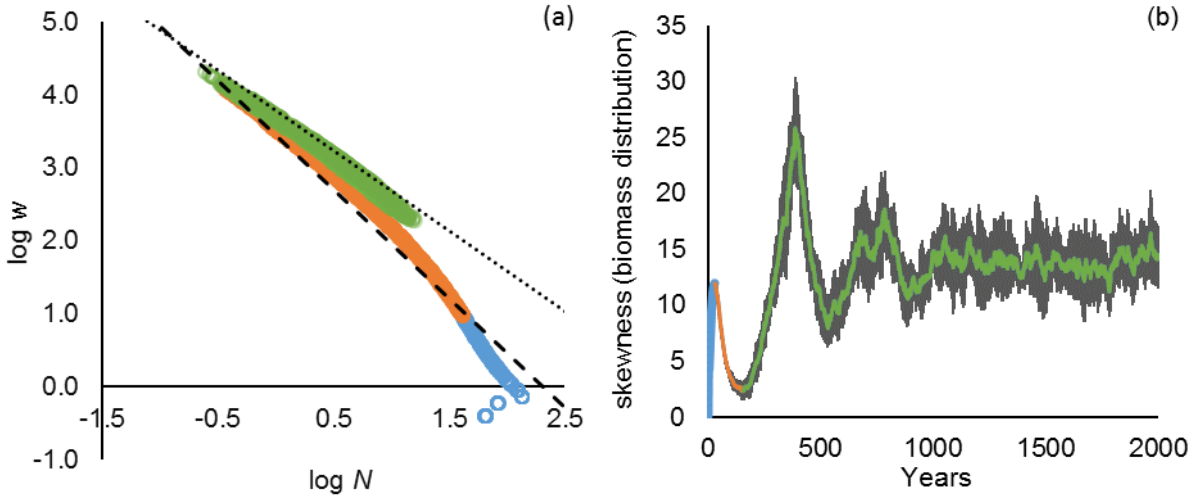

Fig. B12. Soil water potential -7.3, $f_d(\Psi)$ = 0.70.

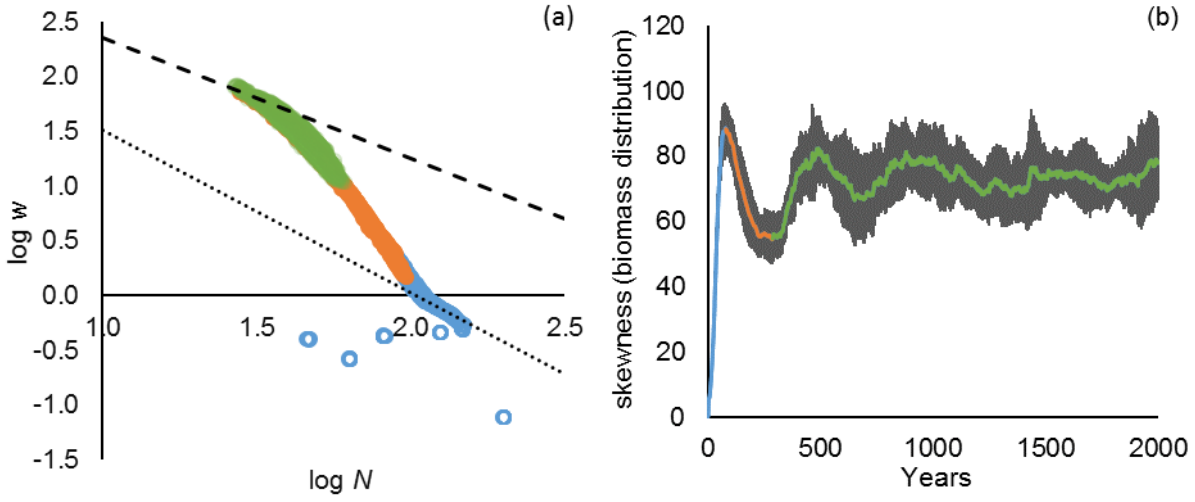

Fig. B13. Soil water potential -5.5, $f_d(\Psi)$ = 0.50.

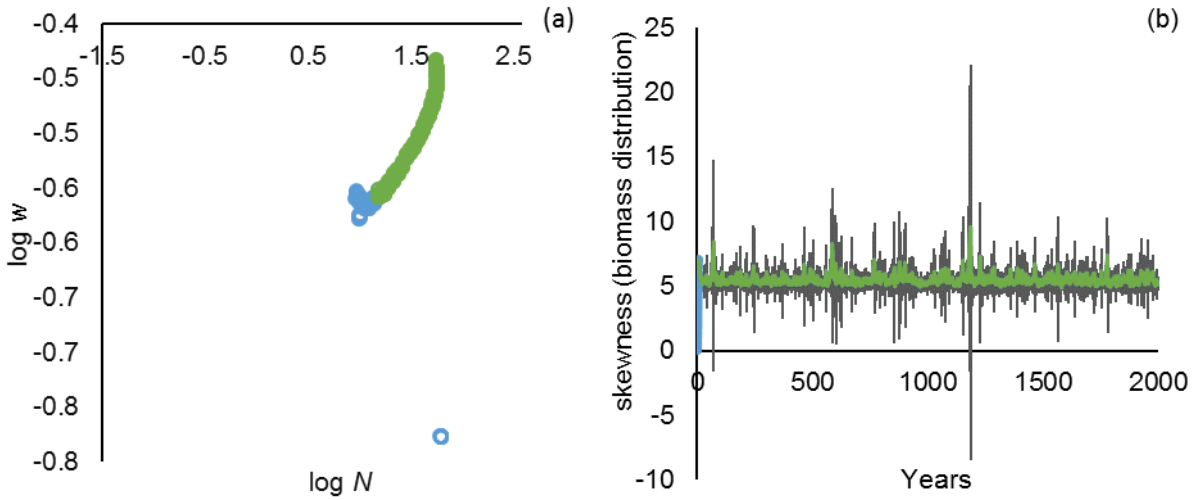

Fig. B14. Soil water potential -3.7, $f_d(\Psi)$ = 0.30.

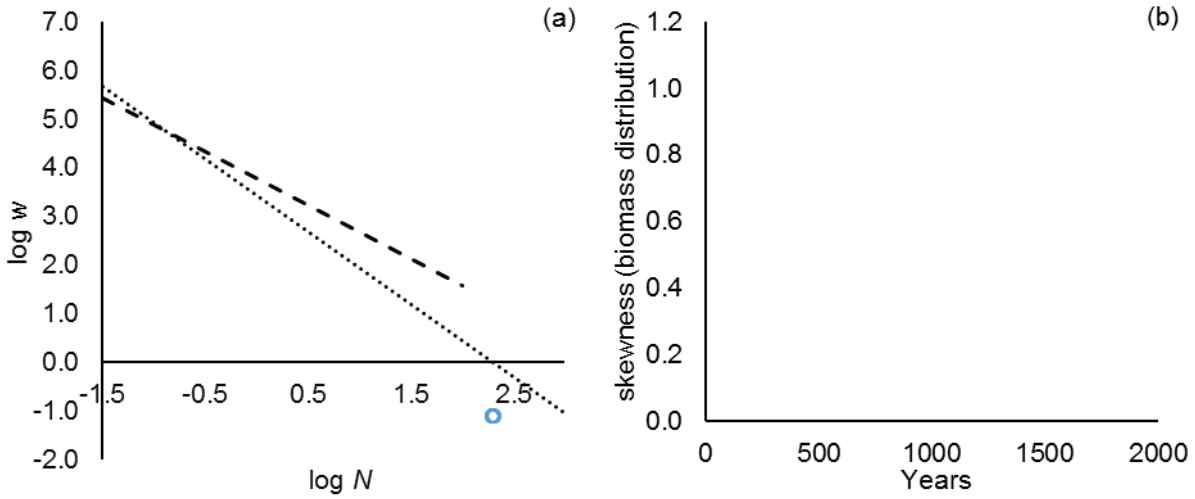

Fig. B15. Soil water potential 0, $f_d(\Psi)$ = 0.00.

Appendix C: Supplementary information on changes in community yield.

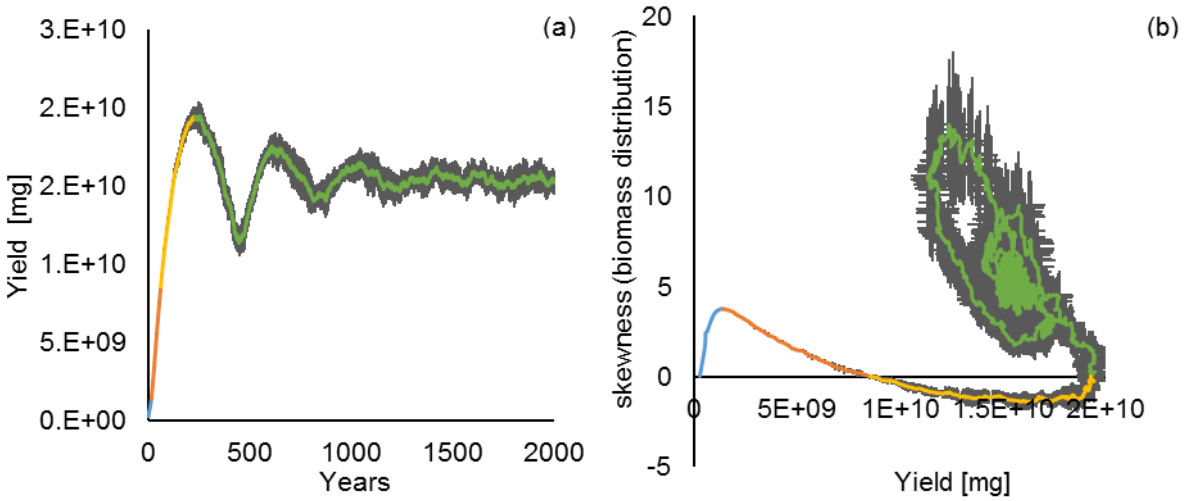

Fig. C1. Development of the community yield [mg] of the base model scenario (soil water potential -1900, $f_d(\Psi) = 1.00$). Colors show the four sections of community structure indicated by skewness of the biomass distribution in Fig. B8b. Standard deviation of the ten replicates is shown in grey. (a) Changes in mean ± SD community yield across all ten replicates over 2000 years. (b) Relationship between mean ± SD skewness of biomass distribution and mean ± SD community yield for all ten replicates over 2000 years.